Permafrost landform dynamics in high mountain environments: a multi-sensoral approach to assess rockglacier evolution

Müller, Johann Christian

Abstract: Permafrost, defined as lithospheric material whose temperature remains below 0 °C for two or more consecutive years, occurs in many high mountain regions of the European Alps. Observed and projected high rates of changes of atmospheric, earth surface and subsurface conditions in these regions will influence the state of permafrost and, therefore, inflict a strong impact on processes and landforms controlled by permafrost conditions. This may, in turn, become potentially hazardous to critical infrastructure as well as human habitat and economic sectors. Rockglaciers – common landforms in alpine periglacial regions that develop due to creeping of perennially frozen, unconsolidated material – serve as important indicators to describe the impacts of a warming climate on high mountain permafrost: Their short-term and long-term evolution represents the only feature of high mountain permafrost to be visually observable and can therefore be assessed by a variety of scientific surveying and monitoring methods. This dissertation aims to contribute to an improved understanding of rockglacier evolution combining kinematic and sediment controls by using multi-sensoral remote sensing data. The foundation of this approach are multi-temporal digital elevation models derived from airborne and terrestrial remote sensing techniques. In order to apply them reliably in high mountain environments for the assessment and quantification of landform structures and processes, this dissertation conducts a comprehensive accuracy assessment of multiple remote sensing products. These multi-temporal digital elevation models are subsequently used to quantify sediment production, transport dynamics and changes therein in high mountain periglacial systems. A cascading, systemic model is developed in order to describe and quantify sediment transfer rates and derive energy fluxes in such systems. Periglacial slopes are characterized by rockglaciers, ice-cored moraines and/or solifluction lobes and are often closely connected to glacial and gravitational landforms. All of these landforms are considered to be significant indicators for changes in climate forcing. This thesis develops a surveying strategy which is applied to quantify headwall recession, surface dynamics and rockglacier creep and facilitates the analysis of rockglacier dynamics in relation to their setting in a geomorphological process chain. Geomorphic work and sediment transfer rates are calculated to characterize and compare the potential energy of geomorphological systems and hold the opportunity to detect and quantify changes within these systems over time. The findings on backweathering rates, sediment production and rockglacier kinematics are integrated into a numerical flow model based on the conservation of mass within the debris process chain in order to assess the temporal and spatial evolution of rockglacier surfaces. The implementation of the flow model generates observed rockglacier geometries and rheologies which rely on long-term field measurements on sediment and landform dynamics.. The modeling helps to understand the driving forces of the dynamic changes of rockglaciers and demonstrates the effects of sediment supply and temperature variations on the morphological and rheological evolution of rockglaciers. Further, it elaborates to which degree these variations can account for signs of degradation and may serve as a tool to determine the state of alpine rockglaciers and their potential state of degradation which is indispensable for a comprehensive natural hazard management. This thesis presents a holistic and comprehensive approach to assess permafrost landform dynamics in high mountains. Starting with data generation and evaluation, moving to its application and quantification in the field, and resulting in an approach to model process and landform dynamics, this dissertation presents a novel, multi-sensoral approach to assess rockglacier evolution.

JOHANN CHRISTIAN MÜLLER

Permafrost Landform Dynamics in High Mountain Environments

A Multi-Sensoral Approach
to Assess Rockglacier Evolution

Mathematisch-naturwissenschaftliche Fakultät
der Universität Zürich

Dissertation
Permafrost Landform Dynamics in High Mountain Environments - A multi-sensoral approach to assess rockglacier evolution

Author
Johann Müller

Remote Sensing Laboratories
Department of Geography
University of Zurich

Winterthurerstrasse 190
CH-8057 Zurich
Switzerland
http://www.geo.uzh.ch/en/rsl

To Snllum

I. <u>Summary</u>

Permafrost, defined as lithospheric material whose temperature remains below 0 °C for two or more consecutive years, occurs in many high mountain regions of the European Alps. Observed and projected high rates of changes of atmospheric, earth surface and subsurface conditions in these regions will influence the state of permafrost and, therefore, inflict a strong impact on processes and landforms controlled by permafrost conditions. This may, in turn, become potentially hazardous to critical infrastructure as well as human habitat and economic sectors.

Rockglaciers – common landforms in alpine periglacial regions that develop due to creeping of perennially frozen, unconsolidated material – serve as important indicators to describe the impacts of a warming climate on high mountain permafrost: Their short-term and long-term evolution represents the only feature of high mountain permafrost to be visually observable and can therefore be assessed by a variety of scientific surveying and monitoring methods.

This dissertation aims to contribute to an improved understanding of rockglacier evolution combining kinematic and sediment controls by using multi-sensoral remote sensing data. The foundation of this approach are multi-temporal digital elevation models derived from airborne and terrestrial remote sensing techniques. In order to apply them reliably in high mountain environments for the assessment and quantification of landform structures and processes, this dissertation conducts a comprehensive accuracy assessment of multiple remote sensing products. These multi-temporal digital elevation models are subsequently used to quantify sediment production, transport dynamics and changes therein in high mountain periglacial systems. A cascading, systemic model is developed in order to describe and quantify sediment transfer rates and derive energy fluxes in such systems. Periglacial slopes are characterized by rockglaciers, ice-cored moraines and/or solifluction lobes and are often closely connected to glacial and gravitational landforms. All of these landforms are considered to be significant indicators for changes in climate forcing. This thesis develops a surveying strategy which is applied to quantify headwall recession, surface dynamics and rockglacier creep and facilitates the analysis of rockglacier dynamics in relation to their setting in a geomorphological process chain.

Geomorphic work and sediment transfer rates are calculated to characterize and compare the potential energy of geomorphological systems and hold the opportunity to detect and quantify changes within these systems over time.

The findings on backweathering rates, sediment production and rockglacier kinematics are

integrated into a numerical flow model based on the conservation of mass within the debris process chain in order to assess the temporal and spatial evolution of rockglacier surfaces. The implementation of the flow model generates observed rockglacier geometries and rheologies which rely on long-term field measurements on sediment and landform dynamics.. The modeling helps to understand the driving forces of the dynamic changes of rockglaciers and demonstrates the effects of sediment supply and temperature variations on the morphological and rheological evolution of rockglaciers. Further, it elaborates to which degree these variations can account for signs of degradation and may serve as a tool to determine the state of alpine rockglaciers and their potential state of degradation which is indispensable for a comprehensive natural hazard management.

This thesis presents a holistic and comprehensive approach to assess permafrost landform dynamics in high mountains. Starting with data generation and evaluation, moving to its application and quantification in the field, and resulting in an approach to model process and landform dynamics, this dissertation presents a novel, multi-sensoral approach to assess rockglacier evolution.

II. <u>Zusammenfassung</u>

Permafrost beeinflusst einen grossen Teil der europäischen Alpen. Er ist definiert als Lithosphärenmaterial, dessen Temperatur über einen Zeitraum von mindestens zwei aufeinanderfolgenden Jahren unter 0 C bleibt. Der Zustand von Permafrost wird beeinflusst von Veränderungen der Atmosphäre, der Erdoberfläche und des Untergrunds, beispielsweise durch klimatische Änderungen, welche sich auf die Permafrost-spezifischen Prozesse und Landformen auswirken.

Typische Permafrostlandformen der Hochgebirge sind Blockgletscher, die durch das kontinuierliche Kriechen eisdurchsetzter Schuttmassen entstehen. Die Messung und Beobachtung der sich hangabwärts bewegenden Landformen stellen die einzige Möglichkeit dar, Gebirgspermafrost und dessen Entwicklung indirekt und kontaktlos mit den Methoden der Fernerkundung zu untersuchen.

Diese Dissertation verfolgt das Ziel, zum Verständnis der Evolution von Blockgletschern beizutragen und damit die Auswirkungen des Klimawandels auf die Hochgebirgssysteme sowie die ablaufenden Prozesse zu verstehen. Grundlage hierfür sind multi-temporale Höhenmodelle und Kinematikdaten, die mit verschiedenen terrestrischen sowie flugzeug- und drohnengestützten Instrumenten generiert wurden.

Um die flugzeuggestützten, photogrammetrisch generierten Höhenmodelle auf ihre Anwendbarkeit im Hochgebirge zu testen, wurde eine Genauigkeitsanalyse und -prüfung anhand umfangreicher Referenzdatensätze durchgeführt,.

Die erstellten und justierten Höhenmodelle wurden weitergehend dafür verwendet, Sedimentproduktion, Transportraten und Energieflüsse in einem periglazialen Einzugsgebiet im Hochgebirge zu quantifizieren. Anhand eines kaskadierenden systemischen Modells zur Quantifizierung und Qualifizierung von Sedimentproduktion, -transport und den beteiligten Prozessen, können periglaziale Hochgebirgssysteme analysiert und der Einfluss klimatischer Veränderungen auf die Prozesse und Landformen untersucht werden. Blockgletscher, eisreiche Moränen und Solifluktionsloben sind zentrale Bestandteile jener periglazialen Hochgebirgssysteme, die oftmals in engem räumlichen Zusammenhang mit glazialen Landformen stehen. Im Zuge dieser Arbeit wird ein Ansatz entwickelt, der auf die Quantifizierung von Erosion, Sedimenttransfer und Blockgletscherbewegung angewendet wird und Aufschluss gibt über Blockgletscherdynamik im Kontext einer geomorphologischen Prozesskette.

Die errechneten Erosions-, Sedimenttransferraten sowie die beobachteten

Blockgletscherbewegungsraten wurden anschliessend in ein numerisches Fliessmodell überführt, das die zeitliche und räumliche Evolution von Blockgletschern in Abhängigkeit von Sediment-/Eiszufuhr und Temperatur modelliert. Das Modell kann dazu genutzt werden, den Einfluss von Sedimentationsdynamik, Temperaturvariationen und Blockgletschereigenschaften auf die morphologische und rheologische Evolution von Blockgletschern zu untersuchen. Degradationserscheinungen wie Kriechbeschleunigung und geometrische Veränderungen können so zum Teil auf Variationen in der Materialzufuhr und der Blockgletschertemperatur zurückgeführt werden. Als Ergebnis bietet diese Dissertation einen systemisch basierten und umfassenden Ansatz, mit dem Permafrost-bedingte Landformdynamiken im Hochgebirge untersucht werden können.

Im Rahmen der Forschungsarbeit wurden sowohl technisch-instrumentelle als auch modellbasierte Ansätze entwickelt und auf ihre Anwendbarkeit hin überprüft. Somit erweitert diese Arbeit die Permafrostforschung im Hochgebirge um einen holistischen Ansatz, der es ermöglicht, Blockgletscher und deren Evolution zu untersuchen und deren Auswirkung auf Hochgebirgssysteme besser verstehen zu können.

III. <u>Contents</u>

V

IV.   <u>Abbreviations</u>

ADS40/80	Airborne Digital Sensor 40/80
ALS	Airborne Laser Scanning
AME	Absolute Mean Error
DEM	Digital Elevation Model
FOM	Figure of Merit
GSD	Ground Sampling Distance
GW	Geomorphic Work
HRSC-A	High Resolution Stereo Camera -Airborne
IPCC	Intergovernmental Panel on Climate Change
IPY	International Polar Year
LiDAR	Light Detection and Ranging
MAAT	Mean Annual Air Temperature
MAGST	Mean Annual Ground Surface Temperature
NMAD	Normalized Median Average Deviation
PERMOS	Permafrost Monitoring Switzerland Network
RMSE	Root Mean Square Error
SD	Standard Deviation
SfM	Structure from Motion
SPCC	Sensitivity of Mountain Permafrost to Climate Change
TS	Terrestrial Survey
TEMPS	The Evolution of Mountain Permafrost in Switzerland
TLS	Terrestrial Laser Scanning
UAV	Unmanned Aerial Vehicles
WP	Work Package

PART I: Synopsis

1 Introduction

1.1 Motivation

Mountains have been identified as essential to the survival of the global ecosystem by the United Nation Conference on Environment and Development (UNCED) in Rio de Janeiro in June 1992 (UNCED, 1993). The Intergovernmental Panel on Climate Change (IPCC) stated in its fourth assessment report a "*high confidence*" that climate change will influence high alpine processes (Settele, 2014). This will alter the atmospheric, earth surface and subsurface conditions in mountain regions and will impact over 25% of the global land surface (Diaz et al., 2003), affecting approximately 26% of the world's population (Meybeck, 2001).

In view of these observed and projected high rates of environmental changes it is crucial to understand the natural processes in mountain systems in a sound manner. Sustained warming and thawing of glacial, periglacial and permafrost systems will induce vast changes on the hydrological cycle, stability of mountain slopes and climatic feedback processes in mountain regions.

Extensive areas in mountain regions are in permafrost condition, which describes lithospheric material that remains at negative ground temperatures throughout at least two consecutive years. These areas can contain considerable amounts of ice and demonstrate a high sensitivity to climatic change (Haeberli et al., 2010). Of the cryospheric components, mountain permafrost represents one of the youngest research areas. This is due to the fact that it is defined as a purely thermal phenomenon and, therefore, mostly invisible to spaceborne and airborne inspection. Systematic investigations were established in the 1980s (Etzelmüller, 2013) with the longest continuous permafrost data series in the Alps originating in 1987 (Hoelzle et al. 2002), mainly consisting of systeimatic temperature measurements. The growing scientific interest in mountain permafrost is mostly associated with the unprecedented impact of intensive warming in mountainous areas due to climate change (Nogués-Bravo et al., 2007). An increase in mean annual air temperature (MAAT) will lead to significant changes in ground thermal regimes inflicting a strong impact on processes and landforms influenced by permafrost. In turn, this may become potentially hazardous to critical infrastructure as well as human habitat and economic sectors (Kääb et al., 2005a, Gruber and Haeberli, 2007, Huggel et al., 2013).

Rockglaciers, common landforms in alpine periglacial regions that develop due to the creep of perennially frozen, ice-saturated unconsolidated material (Haeberli et al., 2006), have received particular attention in permafrost-related mountain research. In its fifth assessment

report (IPCC, 2014), the IPCC highlighted rockglaciers as important indicators to describe the impacts of a warming climate on high mountain permafrost: Their short- and long-term evolution depicts the only feature of high mountain permafrost to be visually observable and is, in consequence, accessible to a variety of scientific surveying and monitoring methods.

The application of numerous terrestrial, airborne and spaceborne remote sensing techniques to acquire data on rockglacier kinematics and surface geometries (see Haeberli et al., 2006, and Kääb, 2008, for extensive summaries) have indicated an acceleration of rockglacier velocities over the last decades (Delaloye et al., 2010, PERMOS, 2013, Bodin et al., 2015). Surface velocity measurements of rockglaciers show acceleration rates of up to 600%, which can be related to altering environmental factors such as ground surface temperature (GST) and snow cover (Wirz et al., 2015). Creep measurements at very high temporal resolutions reveal annual and seasonal velocity fluctuations mainly caused by external factors (e.g. meteorological forcing, see Wirz et al., 2016). Multi-temporal geomorphometric analyses have shown degradational processes such as subsidence features and structural disintegration of alpine rockglaciers, which can potentially become hazardous to human infrastructure and livelihoods (Kääb et al., 2007b, Roer et al., 2008, Bodin et al., 2010, Springman et al., 2013).

As a result, several monitoring, research and management strategies have been implemented in the European Alps in order to cope with changing high mountain permafrost systems with a special focus on slope movements and sediment transport. Multi-sensoral remote sensing approaches have proven to be very effective and cost-efficient to obtain data on kinematics and surface dynamics. The availability of a multi-sensoral instrumentation for several rockglacier systems in the Alps, including multi-temporal terrestrial laser scanning (TLS), airborne laser scanning (ALS), airborne photogrammetry (based on unmanned aerial vehicles UAV and airplanes) and terrestrial geodetic surveys (TS) combined with subsurface information and geomorphological mapping surveys, presents the basis for a holistic assessment of these systems, addressing sediment dynamics, rockglacier kinematics, landform characteristics and geomorphological settings.

This thesis presents the conceptual foundation, technical methodology, and application of an advanced approach to assess rockglacier dynamics and introduces a numerical modeling approach to improve the understanding of the long-term evolution and short-term dynamics of rockglacier systems.

1.2 Structure of this thesis

The subsequent thesis consists of three parts. **Part I** provides an overview of the scientific background and summarizes the main research results in a broader context. A general introduction and motivation is presented in Sect. 1, which results in the formulation of the research questions and sets out the institutional and geographical context in which these research questions are addressed. Section 2 elaborates on the scientific background and the current research needs with respect to this dissertation. A brief summary of the main research motivation, methods and findings within the three peer-reviewed publications is presented in Sect. 3. All results are discussed in a general context and in relation to the formulated research questions in Sect. 4. Concluding remarks and proposals for future research are formulated in Sect. 5.

Part II contains the full version of the peer-reviewed journal publications constituting the main research results. **Part III** provides the personal bibliography, curriculum vitae and acknowledgements of the author.

Although Part I of this thesis is written by one author, it is based mainly upon joint-authored publications (Part II). Therefore, "we" is used instead of "I" for the rest of this synopsis.

1.3 Objectives and related research questions

1.3.1 Objectives

This PhD dissertation aims to contribute to an improved understanding of rockglacier dynamics combining kinematic and sediment controls by using multi-sensoral remote sensing data. This is performed using a "backward" approach, quantifying distinct observed changes in geometry and kinematics (creep velocities) of a rockglacier that are related to changing conditions of the controlling factors (sediment and ice input and ground temperature). Many studies have reported on the acceleration of horizontal velocities of rockglaciers all over the world derived from different methods (Roer et al., 2005, Roer and Nyenhuis, 2007, Bodin et al., 2009, Delaloye et al., 2010, Delaloye et al., 2011, Lambiel, 2011, PERMOS, 2013, Bodin et al., 2015). Furthermore, the application of multi-temporal digital elevation models (DEMs) has indicated changes of rockglacier geometry, which have been considered signs of degradation, such as pronounced surface subsidence due to the melt of subsurface ice (Lambiel, 2011, Kenner et al., 2014, Bodin et al., 2015) and the development of crevasse-like features on the rockglacier (Kääb et al., 2007b, Roer et al., 2008, Springman et al., 2013). Most of these studies focus on the process of permafrost creep and surface dynamics in relation to air or ground temperature in order to assess rockglacier dynamics. However, this narrow focus only accounts for a subset of the features of a rockglacier, whereas the definition of rockglaciers as *'lobate or tongue-shaped bodies of perennially frozen unconsolidated material supersaturated with interstitial ice and ice lenses that move down slope or down valley by creep as a consequence of the deformation of ice contained in them and which are, thus, features of cohesive flow'* (Barsch, 1992, p. 176) also includes information on form, material and process. Therefore, observable rockglacier dynamics do not only result from varying temperatures but from a combination of altering sediment and ice input, permafrost creep conditions and the geomorphological setting controlling their evolution (Barsch, 1996).

Thus, this study introduces a holistic conceptual approach on rockglacier dynamics. Multi-temporal digital elevation models (DEMs) derived from several remote sensing techniques are used to quantify sediment production, transport dynamics and changes in rockglacier morphology. The proposed surveying strategy is applied to quantify headwall recession, surface dynamics and rockglacier creep and allows analyzing rockglacier dynamics in relation to their setting in a geomorphological process chain. Figure 1 presents the conceptual research approach of this dissertation. A detailed accuracy assessment of

available remote sensing data establishes the foundation for their application in process quantification, system analysis and modeling.
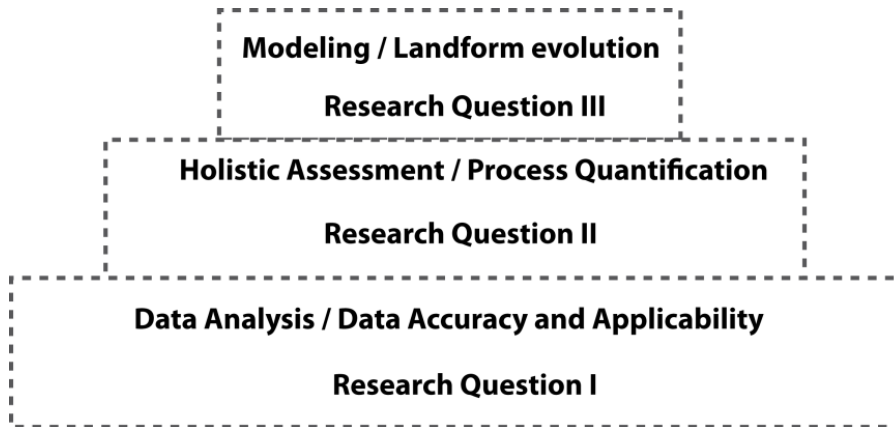

Figure 1: Conceptual approach of this dissertation.

Multi-sensoral DEMs have been repeatedly applied to quantify processes in high mountains (Roer and Nyenhuis, 2007, Tarolli et al., 2009, Abermann et al., 2010, Kenner et al., 2014; see Kääb et al. (2005a) for a thorough review of remote sensing products in high mountains in general) but their limitations according to their accuracy are rarely discussed and systematic accuracy assessments of these elevation products often remain insufficient. In order to address this shortcoming, this thesis presents the application and challenges of airborne stereophotogrammetrically-derived high-resolution DEMs and conducts a systematic accuracy assessment of several DEMs derived from different remote sensing systems (→ Research Question I, Sect. 3.1).

This assessment of the DEMs is essential for their further application to analyze and map relevant landform structures (monotemporal) and to quantify geomorphological processes (multi-temporal) such as headwall recession, creep processes and energy transfer (geomorphic work) of the talus slopes and rockglaciers. This application elaborates on the current state and systemic understanding of high mountain periglacial systems (→ Research Question II, Sect. 3.2).

The findings on backweathering rates, sediment production and rockglacier kinematics are integrated into a numerical flow model based on the conservation of mass within the debris process chain in order to calculate the temporal and spatial evolution of rockglacier surfaces. The flow model is used to generate observed rockglacier geometries and rheologies which are then subjected to variations in driving forces such as temperature and the supply of sediment and ice (→ Research Question III, Sect. 3.3).

The modeling aides to understand the driving forces of these morphological changes of rockglaciers and quantifies the influence of sediment supply and temperature variations on the morphological and rheological evolution of rockglaciers. Further, it assesses to which degree these variations can account for signs of degradation and may serve as a tool to determine the state of alpine rockglaciers and their potential state of degradation necessary for a comprehensive natural hazard management.

1.3.2   Research questions

Motivated by the addressed research objectives, the overall intention of this thesis is to contribute to an improved understanding of rockglacier evolution combining kinematic and sediment controls by using multi-sensoral remote sensing data. The concept of the PhD project consists of three distinct research questions

1. *How accurate are photogrammetrically-derived high-resolution airborne digital elevation models and what are the limitations in high mountain applications?*

2. *What are the sediment dynamics, storages and transfer rates in a coupled periglacial mountain slope system?*

3. *How do rockglaciers evolve and react to changes in environmental factors?*

which resulted in three peer-reviewed publications:

1. *Müller, J., Gärtner-Roer, I., Thee, P., Ginzler, C., 2014. Accuracy assessment of airborne photogrammetrically derived high-resolution digital elevation models in a high mountain environment. ISPRS Journal of Photogrammetry and Remote Sensing 98, 58–69.*

2. *Müller, J., Gärtner-Roer, I., Kenner R., Thee P., Morche, D., 2014. Sediment storage and transfer on a periglacial mountain slope (Corvatsch, Switzerland). Geomorphology 218, 35–44.*

3. *Müller, J., Vieli, A., Gärtner-Roer, I., 2016. Rockglaciers on the run - Understanding rockglacier landform evolution and recent changes from numerical flow modeling. The Cryosphere Discussions, (in review).*

1.4 Project context, data and study sites

This dissertation was completed within the subproject C of the SINERGIA project **T**he **E**volution of **M**ountain **P**ermafrost in **S**witzerland (TEMPS) funded by the Swiss National Science Foundation (project no. CRSII2 136279). The TEMPS project consisted of four interrelated subprojects, which focused specifically on the determination of the current state and the dominant processes influencing the evolution of permafrost in the Swiss Alps. Based on the analysis and integration of high mountain observations with model simulations, TEMPS aimed to create plausible evolution scenarios of mountain permafrost at specific sites and investigated the interactions between atmosphere and permafrost focusing on the evolution of ground temperature, ice content and related degradation and creep processes. The overall objective of TEMPS was to improve the understanding of the dynamics of mountain permafrost regions induced by climate change and to assess the potential impact at different field sites in the Swiss Alps. The research was based on newly acquired and existing permafrost monitoring datasets from the Swiss Alps available to the TEMPS project including data from the Swiss Permafrost Monitoring Network (PERMOS) and former research projects (such as the SPCC project (Sensitivity of mountain permafrost to climate change) funded by the German Research Foundation).

The TEMPS project was composed of four sub-projects (TEMPS A, B, C and D), each focusing on a specific approach to high mountain permafrost research (see Fig. 2).
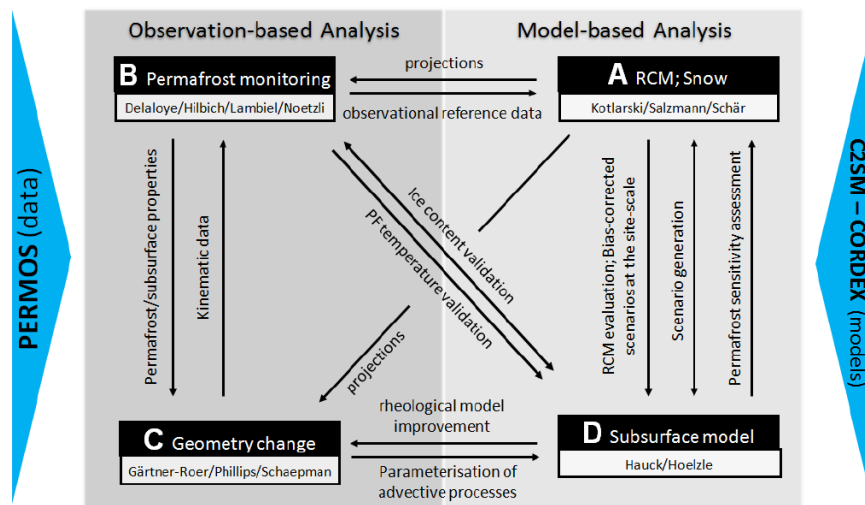

Figure 2: The organization of the TEMPS project with its subprojects and principal investigators (Source: TEMPS project proposal).

TEMPS-A focused on climatic changes and application of regional climate models in high mountain permafrost environments with special emphasis on the dominant role of the downscaling and topography effects in mountains (Rajczak et al., 2013, Rajczak et al., 2015). TEMPS-B combined meteorological data, ground temperatures and geophysical subsurface data to analyze permafrost dynamics (Staub, 2015). TEMPS-D focused on the thermal subsurface regime and its interaction with the atmosphere (Marmy, 2015).

The major objective of TEMPS-C was to improve the process understanding of permafrost creep in terms of landform dynamics. This was performed by observing and quantifying distinct geometric and kinematic changes of a landform that are related to certain atmospheric conditions, with a reaction time of weeks to months. The systematic assessment required long-term data series for the analysis of multidecennial trends, interannual variations and seasonal rhythms, as is available from PERMOS and other projects (see Table 1). Besides geometric/geomorphic changes, physical properties such as subsurface ice and sediment dynamics had to be taken into account to describe the process chain from a change in surface temperature to a rheological response (dynamics).

The subproject consisted of three work packages (WP) designed to acquire, process and analyze remote sensing data in order to quantify permafrost creep on various spatio-temporal scales (WP I); model and assess rockglacier evolution (WP II) and quantify sediment transfer rates in periglacial high mountain systems (WP III). The generated products and results of these WPs contributed significantly to this dissertation and the research questions have been strongly influenced by the goals of the project.

The results of TEMPS-C (such as kinematic data, DEMs, analysis concepts, process dynamics and quantification) were made available to the other subprojects as shown in Fig. 2.

1.4.1 Sites

As laid out above, TEMPS-C was specifically responsible for the acquisition of (intra-)annual and interannual measurements of kinematics as well as the analysis of spatio-temporal variations of rockglacier topographies in different regions of the Swiss Alps.

Figure 3 shows the core field sites of the TEMPS-C project which was mainly concerned with the rockglacier sites in the Turtmann Valley, Murtèl-Corvatsch and Muragl.
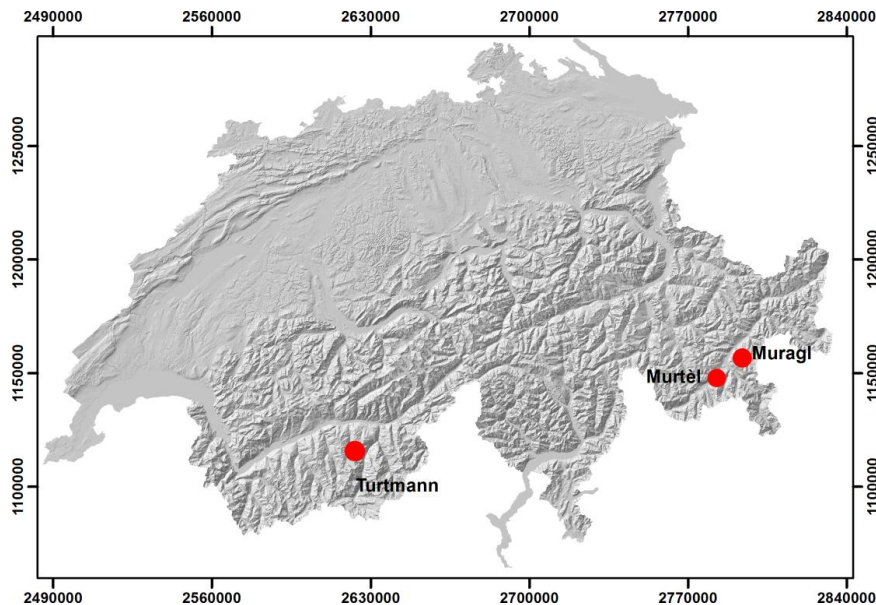
Figure 3: Overview of the study sites in Switzerland (Hillshade: SwissAlti3d).

Each subproject was concerned with some core research sites which have been equipped with specialized installations – such as kinematic monitoring networks, thermal monitoring and/or permanent geophysical monitoring systems during the TEMPS project – or have been inherited from former research projects which holds true for most of the sites. For the selection of study sites it was crucial to rely on long time series and established permafrost sites in order to get an insight on the long-term evolution of mountain permafrost. The three core sites of TEMPS-C were chosen because each of them is part of the PERMOS network, have undergone regular kinematic and thermal monitoring for many years and will continue to do so in the future; furthermore, historic remote sensing data is available. The selected sites also allow for the application of multi-sensoral analysis approaches because several in-situ, terrestrial and airborne assessments have been applied there in the past. The availability of multi-temporal and multi-sensoral data of different resolution and accuracy is especially important for the independent assessment of their accuracy, data fusion applications and process analysis on different spatial and temporal scales.

1.4.2 Remote sensing datasets

For each of the three selected sites, TEMPS-C was responsible for compiling different seasonal and annual datasets based on multiple remote sensing techniques. This was achieved by TS, TLS, airborne digital photogrammetry, ALS and UAV-based photogrammetry. Table 1 shows the previously existing and and newly collected remote sensing datasets available for each of the key field sites. In addition to newly acquired datasets, the TEMPS project attained access to historic remote sensing data made available from the German Research Foundation funded SPCC project and PERMOS.

Not all of the available datasets have yet been analyzed within the project context, e.g. the TLS and UAV data at the Muragl sites have been used for Master thesis projects at the University of Zurich. Details on data acquisition, pre and post-processing, accuracies and application of these datasets are part of the peer-reviewed publications in Part II, Sect. 1 and 2.

Table 1: Airborne and terrestrial remote sensing datasets of TEMPS-C and related projects. The bold marks show the data that was used in the publications.

Site	Data	Year / Projects												
		PERMOS						SPCC/PERMOS			TEMPS/PERMOS			
		1996	2001	2002	2005	2007	2008	2009	2010	2011	2012	2013	2014	2015
Murtel	Terrestrial Geodetic Survey							**X**	**X**	**X**	**X**	**X**	**X**	**X**
	Airborne Stereo-photogrammetry	**X**				**X**					**X**			
	Airborne laser scanning			**X**										
	Terrestrial laser scanning								**X**		**X**			
	UAV-based stereo-photogrammetry													X
Turtmann	Terrestrial Geodetic Survey							**X**	**X**	**X**	**X**	**X**	**X**	**X**
	Airborne laser scanning					**X**								
	Airborne Stereo-photogrammetry		**X**		**X**		**X**		**X**		**X**	**X**		
Muragl	Terrestrial Geodetic Survey							X	X	X	X	X	X	X
	Terrestrial laser scanning											X	X	
	UAV-based stereo-photogrammetry												X	X

2 Background

This section elaborates on the current state of mountain permafrost research focusing on distinctive landforms and their constituent processes. Further insight is given into the possibilities, challenges and current developments related to the remote assessment of mountain permafrost. Finally, the effects of climate change on high mountain permafrost dynamics and resulting landform dynamics are discussed. This dissertation's contribution to the above mentioned aspects shall be outlined throughout the following section.

2.1 Mountain Permafrost, rockglaciers and rockglacier dynamics

Permafrost is defined as lithospheric material that remains permanently at or below 0 °C for more than two consecutive years. While this presents a purely thermal definition excluding the presence of water and ice, it is due to the existence and the impact of considerable amounts of subsurface ice that permafrost derives its relevance on material properties, process rates and landscape evolution (French, 2007).

Extensive areas in mountain regions are considered to be cold climate environments that promote permafrost conditions (Owens, 2004). High mountain topography is mostly characterized by high elevation, strong terrain gradients, complex and rocky terrain and the presence of snow and ice (Barsch and Caine, 1984). This extreme variability of high mountain topography influences almost all surface and subsurface characteristics and therefore the spatial distribution and properties of permafrost and permafrost-related landforms. For an intensive review and state of the art research on mountain permafrost see Gruber and Haeberli (2009), Haeberli et al. (2010) and Etzelmüller (2013).

Mountain permafrost receives its relevance due to the fact that it is an important element in high mountain systems affecting landscape and landform evolution (French, 2007), sediment transfer systems (Barsch, 1977), and slope and rockwall stabilities (Gruber and Haeberli, 2007), therefore making it an important aspect of natural hazard assessment (Kääb et al., 2005b).

Thermal conditions and internal composition (rock and ice components) of frozen slopes in high mountain areas enable the frozen sediment to creep, so called permafrost creep, which is the progressive, slow deformation of a mass of debris supersaturated with ice (e.g. Haeberli, 1985, Barsch, 1996). Besides temperature, topographic properties (slope gradient, sediment input, etc.) and physical characteristics (particle size, ice content, unfrozen water content, etc.) determine the deformation rates of these frozen sediments which lead to the development of dynamic landforms such as rockglaciers, push moraines or creeping talus

slopes over periods of centuries and millennia (Haeberli et al. 2006). Out of these landforms, active rockglaciers are the only visible indicator that can unambiguously be related to permafrost conditions.

Already in 1959, Wahrhaftig and Cox (1959) discussed the basic genesis and evolution mechanisms of rockglaciers in the Alaska Range where they presented results of extensive field data on rockglacier topography and kinematics and formulated theories on landform evolution and dynamics. Since then, numerous publications have discussed rockglacier origin and nomenclature (e.g. Johnson, 1983, Martin and Whalley, 1987, Humlum, 1988, Barsch, 1992, Whalley and Martin, 1992, Hamilton, 1995, Barsch, 1996, Humlum, 1996, Clark et al., 1998, Haeberli et al., 2006, Berthling, 2011).

This study follows the reasoning of Barsch and Haeberli, defining rockglaciers as "*lobate or tongue-shaped bodies of perennially frozen unconsolidated material supersaturated with interstitial ice and ice lenses that move down slope or down valley by creep as a consequence of the deformation of ice contained in them and which are, thus, features of cohesive flow*" (Barsch, 1992, p. 176), although acknowledging the complex nature of the origin of rockglaciers which exists within a continuum between "*steadily creeping perennially frozen and ice-rich debris on non-glacierised mountain slopes*" experiencing permafrost conditions (termed rockglacier) and "*debris-covered glaciers in permafrost free areas*" (termed debris covered glaciers) (Haeberli et al., 2006, p. 190).

Active rockglaciers are an integral part of periglacial high mountain systems around the world experiencing permafrost conditions and representing one of the primary forms of mass wasting (Clark et al., 1998), nevertheless their long-term evolution and short-term dynamics are not yet sufficiently understood. Time series of rockglacier movement in the European Alps indicate acceleration in permafrost creep over the last decades related to an increase in ground temperatures (Delaloye et al., 2010b, PERMOS, 2013, Bodin et al., 2015). Multi-sensoral geomorphometric analyses have shown signs of destabilization such as subsidence features and structural disintegration of alpine rockglaciers which are indicative of landform degradation (Kääb et al., 2007a, Roer et al., 2008, Bodin et al., 2010, Springman et al., 2013, Micheletti et al., 2015b). Most of these studies have addressed the connection between mean annual air temperatures (MAAT) and rockglacier dynamics from a descriptive point of view (Ikeda and Matsuoka, 2002a, Roer et al., 2005, Delaloye et al., 2010, Springman et al., 2012). Wirz et al. (2015) have shown that short-term variations in creep velocities are mainly influenced by the direct impact of meteorological forcing such as warming and precipitation. Nevertheless, we argue that the long-term evolution of landform geometry and dynamics cannot solely be explained by meteorological variations but must

integrate controlling environmental factors such as sediment supply dynamics and landform characteristics (Roer et al., 2005). Already Wahrhaftig and Cox discussed in their groundbreaking paper on rockglaciers in 1959 the role of rockglaciers as part of the sediment cascade in high mountains and pointed out their role as weathering and climate indicators and sediment traps. More recent studies have used rockglaciers to quantify backweathering rates, sediment dynamics (Humlum, 2000), sediment budgets (Otto et al., 2009), and sediment transfer rates (Gärtner-Roer, 2012) over multiple time scales. Advances in remote sensing techniques allow for the assessment and quantification of sediment generation and landform connectedness and pose the opportunity to assess rockglaciers in relation to their surrounding environment.

2.1.1 Contribution

In order to understand rockglacier evolution in relation to their systemic setting, this study considers rockglaciers as constituent subsystems of the entire periglacial high mountain system that are interpreted as closed systems concerning coarse debris (Barsch and Caine, 1984) in the sense of Chorley and Kennedy (1971). Figure 4b shows such an exemplary system in the Turtmann valley in the Canton of Valais, Switzerland. In Publication II we develop a theoretical and instrumental concept of an idealized periglacial mountain slope comprised of three constituent subsystems (see Fig. 4a for the theoretical concept): The headwall and intermediate storage subsystem, the talus slope subsystem and the rockglacier subsystem. The subsystems are defined based on several characteristics: topographic features, typical landform(s) and dominating mass wasting processes. We use a multi-sensoral approach to assess backweathering rates, sediment and energy transfer rates as well as subsystem connectedness in this periglacial system. The presented findings give insight into the long-term geometric and kinematic evolution of the rockglacier in regards to material input variations in combination with temperature variations (Part II, Publication II).
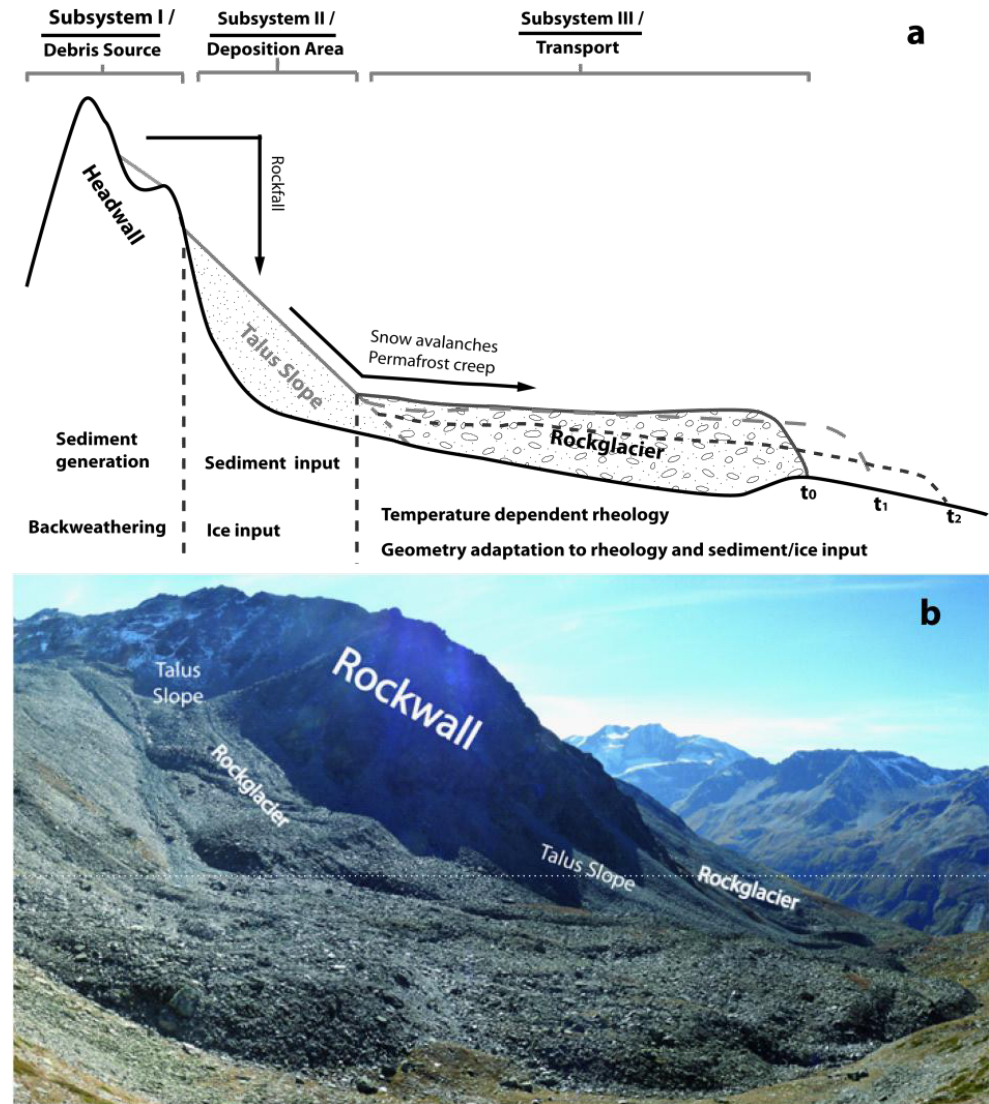
Figure 4: Theoretical concept of sediment dynamics and processes controlling rockglacier rheology and surface evolution. We assume that an increase in temperature and reduced ice input will lead to succeeding landform subsidence and acceleration (time steps t_0, t_1, t_2) (a). The geomorphological setting of a periglacial system including the subsystems Rockwall, Talus Slopes and Rockglacier in the Turtmann Valley, Valais, Switzerland (b).

2.2   Remote Sensing of high mountain permafrost systems

Due to its nature as a purely thermally defined phenomenon, permafrost is not directly observable. However, indicators, processes or boundary conditions of permafrost and permafrost-related surface dynamics can be detected remotely including for example rockglaciers, active-layer detachments, thaw slumps, vegetation types and snow cover distribution in alpine regions. A whole range of remote sensing instruments is well suited for repeated and rapid observation in remote and inaccessible areas of high mountains (Kääb, 2008). Mostly mono- and multi-temporal DEMs derived from various remote sensing systems are repeatedly used in high mountains to analyze land surface features and processes (e.g. Gruen and Murai, 2002, Kneisel and Kääb, 2007, Tarolli and Dalla Fontana, 2009, Debella-Gilo and Kääb, 2012), numerical and hydrological modeling (e.g. Storck et al., 1998, Oppikofer et al., 2011,), topographic and radiometric correction of remote sensing imagery (e.g. Goyal et al., 1998) and the assessment of multiple terrain and geophysical parameters (e.g. Li et al., 2005, Maune, 2007).

Typically, two sensor systems are used to generate high-resolution DEMs in mountain areas: stereophotogrammetrical sensors that acquire optical stereoscopic imagery (Lane, 2000) and Light Detection and Ranging (LiDAR) systems, active opto-mechanical sensing systems that generate three dimensional information based on the run time of a light signal between the sensor and the surface (Vosselman and Maas, 2010). Laser scanning and photogrammetry are traditionally mainly used on airplane-based systems but experience increased application on unmanned aerial vehicles (UAV) and terrestrial surveying approaches. TLS and terrestrial photogrammetry are established methods for assessing many kinds of natural processes in the geosciences and have been repeatedly applied in high mountain permafrost contexts (Oppikofer et al., 2008, Kenner et al., 2011, Schürch et al., 2011, James and Robson, 2012). Structure from motion (SfM) approaches and UAV-based photogrammetry have been applied to derive DEMs for geomorphological applications (Fonstad et al., 2013, Kaiser et al., 2014, Ouédraogo et al., 2014, Eltner et al., 2015, Haas et al., 2015, Micheletti et al., 2015a, Nolan et al., 2015) but rarely in a permafrost or high mountain context. Nevertheless, these approaches promise very fruitful products for high mountain permafrost applications (Cloutier et al., 2015, Gauthier et al., 2015, Lato et al., 2015).

Besides these technical and instrumental advances, stereophotogrammetric products remain the most cost-efficient method to acquire high-resolution elevation data with high accuracies over large remote areas (Bühler et al., 2012). Many multi-temporal DEM applications use several sensor systems of different age and with different technical setups (e.g. Kääb et al.,

1997, Roer and Nyenhuis, 2007), but the sensors' limited accuracy can distort the quantification of changes in process rates and mass transport. Mono- and multi-temporal application of DEMs such as the analyses of sediment transport, mass balances, morphometry and geomorphodynamics require the consideration of accuracy of remotely-sensed DEMs because their applicability and interpretability depend strongly on their accuracy (Tarolli et al., 2009, Abermann et al., 2010, Pieczonka et al., 2011). Especially in highly complex terrains such as mountainous regions, the methods of obtaining digital elevation models face several challenges and inherit numerous uncertainties leading to significant differences in the quality of the derived data (Fisher and Tate, 2006).

2.2.1 Accuracy assessment – Accuracy, Trueness and Precision

Accuracy is a term often used in remote sensing applications to describe the applicability and restrictions of data, but the fact that accuracy is a qualitative expression of performance characteristics is often neglected and a detailed assessment is often missing.

Menditto et al. (2007) stress the point that a common terminology to describe the quality of a measurement/dataset has been and still is difficult to establish due to the ambivalent use of the term accuracy in different languages, research communities and applications.

In general, the term accuracy is used to describe the qualitative performance characteristics of measurements which result from the influence of systematic and random errors. An error is defined as the "*result of a measurement minus a true value of the measurand*" (BIPM, 2008, p. 36). An error in a digital elevation dataset, for example, would describe the three-dimensional deviation of data points located in a coordinate system relative to their "true" location in said system.

Errors are traditionally viewed as having a random and systematic component. Random errors arise from unpredictable or stochastic temporal and spatial variations of influence quantities which might stem from sensor irregularities, atmospheric influences or hardware malfunctions. Systematic errors are described as the difference between the average of several measurements on the same sample and its true value (bias) (Cooper, 1998, Wise, 2000, Menditto et al., 2007). Figure 5 shows exemplarily the occurrence of systematic errors (a) and (b), spatially autocorrelated error (c) and random errors (d) by means of a digital elevation model transect and its reference.
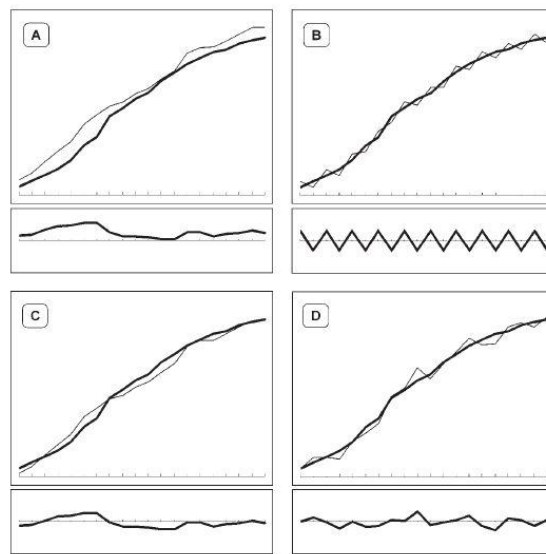
Figure 5: Comparisons of a profile through a DEM and the occurrence of error. (A) The occurrence of error with bias; (B) the occurrence of systematic error; (C) the occurrence of spatially autocorrelated error (the normal situation); (D) the occurrence of random error (no spatial autocorrelation). In each instance the upper diagram shows the ground surface as a thick line and the ground surface with the error as a thin line, and in the lower diagram the error alone. Source: Fisher and Tate, 2006, p. 470.

In order to address the implications of random and systematic errors on datasets, the International Organization for Standardization (ISO) uses the terms 'trueness' and 'precision' to describe the accuracy of a dataset (ISO 5725-1, 1998). Hereby, trueness is defined as the closeness of agreement between the arithmetic mean of a number of measurements and the reference value which quantifies the systematic error and can be addressed as a measure of such and precision refers to the closeness of agreement between test results and therefore describes the random error. Menditto et al. (2007) give the very plausible analogy that the general term fruits includes both apples and oranges just as the general term accuracy includes both trueness and precision.

When assessing accuracy it is therefore necessary to address and quantify trueness and precision. Accuracy assessment of remotely sensed digital elevation data is usually conducted by calculating the difference between the digital elevation data and some source of control data of superior accuracy (most commonly ground control points (GCP) derived by differential GPS). If the reference data is extensive enough it is possible to quantify the systematic deviation of the test data and therefore quantify the trueness and correct the data accordingly (Thapa and Bossler, 1992). Once the systematic error (trueness) is known and corrected for, the term accuracy remains to describe the precision of the DEM which is the common application of that term in the remote sensing community and used as such in this

study. Menditto et al. (2007) advocate the use of 'measurement uncertainty' as a measure for accuracy that has been corrected for bias and the statistical properties of the precision are known but the scientific literature and user community is still struggling to adapt this recommendation.

The accuracy of remote sensing data is mostly spatially heterogeneous and it is insufficient to describe a whole digital elevation dataset with only one global statistical value such as the mean error, the standard deviation of the error or the RMSE after bias correction (Fisher, 1998). This holds especially true for studies where multiple DEMs are used to quantify process rates, landform changes, system dynamics, etc. Since these measures give no information about the spatial distribution or correlations with topographic features such as slope and/or roughness of the errors (Fisher 1998, Oksanen and Sarjakoski, 2006, Wechsler, 2007), they are of limited use when they are consulted to determine the applicability of a DEM for a certain analysis (Hebeler and Purves, 2009b). Figure 5c shows a spatially autocorrelated error, which means that the spatial distribution of the error is heterogeneous but related to certain surface characteristics (slope, aspect, etc.) (Fisher and Tate, 2006).

In order to overcome the shortcomings of global accuracy measures it is possible to use modeling to assess error properties, error distributions and spatial correlation (Kyriakidis et al, 1999, Fisher, 1998, Shortridge and Goodchild, 1999, Hebeler And Purves, 2009a). Another way is to adapt the accuracy assessment to the analysis approach at hand and consult spatially extensive reference data that suffices a priori the requirements of the application (Höhle and Höhle, 2009). Especially for the assessment of environmental processes that are spatially diverse and act on longer time scales such as permafrost creep, different sensor systems are often applied and combined for long-term analysis. In these cases the different properties of the sensor systems and their products have to be considered in relation to their application. An assessment of the performance and compatibility of different modern and historical sensor systems and datasets is necessary in order to ensure that the observed processes and/or landform dynamics are in accordance with the DEMs accuracy.

2.2.2   Contribution

We present a thorough accuracy assessment of the applied remote sensing products in Part II, Publication I, in order to be able to assess the high mountain processes targeted within this thesis sufficiently. Therefore, we evaluate the vertical accuracy of DEMs derived from four different stereoscopic aerial camera systems (HRSC-A, RC30, ADS40 and ADS80) in a high alpine environment. The RC30 is an analogue stereoscopic sensor system, whereas the three other systems are stereoscopic digital pushbroom scanners of different generations

and with different instrumentation, which have been used repeatedly in high mountain areas but have not yet been checked systematically for their accuracies (Bühler et al., 2007, Kellenberger and Nagy, 2008, Bühler et al., 2012, Kenner et al., 2014). The evaluation includes the assessment of the trueness and precision of the DEMs and shows the advantages and disadvantages of different types and generations of photogrammetric sensors.

The study area is located in the Turtmann valley, Valais, Switzerland, a glacially and periglacially formed hanging valley stretching from 2400 m to 3300 m a.s.l. The photogrammetrically-derived DEMs are evaluated against geodetic field measurements and an airborne laser scan (ALS).

Several global and local accuracy measures are used to evaluate the performance of the sensor systems. The measurement uncertainty is estimated by using elevation data of superior quality acquired by an airborne laser scan and terrestrial geodetic measurements as reference. Global quality measures describe the entire area of interest using only a few parameters, but local assessment describes the quality of a DEM at a higher level of detail and is incorporated into the DEM analysis (Papasaika and Baltsavias, 2010). We show to which degree the tested DEMs can be used reliably in high mountain research and to which detail topography and process rates can be quantified.

2.3   Permafrost dynamics, permafrost degradation and climate change

In principle, climate-induced environmental changes may lead to permafrost degradation and aggradation processes. It is generally assumed that increasing air temperatures, as currently observed for Switzerland with stronger trends than for the mean Northern Hemisphere (e.g. Ceppi et al., 2012), may lead to increasing subsurface temperatures and consequently to an enhanced frequency of thaw-induced instability phenomena, affecting infrastructure and leading to rock fall and debris flow (Harris et al., 2001, Gruber and Haeberli, 2007, Harris et al., 2009, Ravanel et al., 2010). On the other hand, glacier retreat may lead to permafrost aggradation in regions where the current mean annual air temperature still favors the development of frozen ground (Hoelzle and Haeberli, 1995, Kneisel and Kääb, 2007). Projections of long-term permafrost evolution are scarce and up to now generally based on sensitivity studies with highly idealized model environments (Salzmann et al., 2007, Noetzli and Gruber, 2009, Engelhardt et al., 2010, Etzelmüller et al., 2011).

However, the latest IPCC report (2014) describes projected warming patterns and associated regional-scale features such as changes in precipitation and extreme weather events (especially an increased frequency of heat waves), which could lead to severe permafrost degradation in the Swiss Alps.

21

Statements about the state and evolution of permafrost landforms are mainly based on the analysis of subsurface temperature time series. About 75% of the permafrost boreholes for which temperature is reported in the global International Polar Year (IPY) indicate that the thermal state of permafrost is warmer than -3 °C (Delisle, 2007, Smith et al., 2010). This holds especially true for boreholes in alpine permafrost (Harris and Isaksen, 2008, Harris et al., 2009, PERMOS, 2013). At temperatures close to the freezing point, phase-change processes dominate the thermal state of permafrost. Heat flow mostly results in melting or freezing of ice and has only negligible effects on temperature. Therefore, it is insufficient to rely on temperature alone as the key variable when monitoring permafrost dynamics. Instead, the temperature measurements need to be complemented with information about surface and subsurface material characteristics, sediment and ice dynamics, water content and the energy fluxes therein in order to gain insight into the long-term evolution and short-term dynamics of permafrost systems.

A number of recent review papers have emphasized that an assessment of permafrost degradation furthermore requires strong efforts in developing direct and indirect monitoring approaches to observe changes in the composition of the surface and subsurface. Moreover, also the impacts of (changes in) sediment supply, ice, liquid water and air within debris and bedrock need to be analyzed (Haeberli et al., 2006, Kneisel et al., 2008, Riseborough et al., 2008, Harris et al., 2009).

The Swiss Permafrost Monitoring network (PERMOS, Von der Mühll et al., 2008) is designed to focus on several key parameters to monitor the state of high mountain permafrost following a landform-based approach. It collects continuous data on three key observation elements: ground temperatures, changes in ice content and permafrost creep velocities. Besides the direct measurements in boreholes, the data on rockglacier movements (kinematics) reveals information on subsurface conditions such as temperature dynamics, ice content and unfrozen water fluxes and their respective changes (PERMOS, 2013).
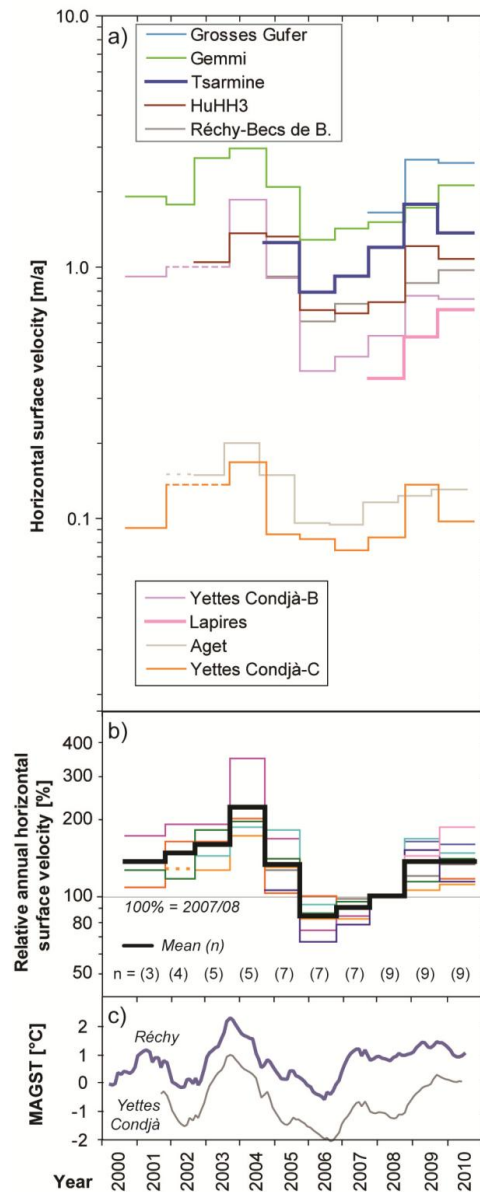
Figure 6:Annual horizontal surface velocities (reference values) of nine sites in Valais between 2000 and 2008 derived from terrestrial surveys: a) absolute horizontal velocities (m/a) and b) relative annual horizontal velocities (%) are linked to c) mean annual ground surface temperature (MAGST) (PERMOS, 2013, p. 34).

Changes in temperature and subsurface conditions are influencing the movement and geometry of permafrost landforms (see Fig. 6, Kääb et al., 2007a, Ikeda et al., 2008, Delaloye et al., 2010) and may induce geomorphological process changes, instabilities and hazards

(Kääb et al., 2005b, Roer et al., 2008). Signs of permafrost degradation such as acceleration, subsidence features and structural disintegration (forming of crevasses) have been observed at several rockglacier landforms in the Swiss Alps (Kääb et al., 2007b, Roer et al., 2008, Delaloye et al., 2011, Lambiel, 2011, PERMOS, 2013, Springman et al., 2013, Kenner et al., 2014, Bodin et al., 2015, Voelksch, 2016, Wirz et al., 2015, Wirz et al., 2016). These studies show that various factors can lead to signs of degradation and that a common thermal triggering is not sufficient to explain the magnitude of the observed rheological and geometrical changes. The rockglacier dynamics are most likely linked to the complex coupling of local topography, thermal state of permafrost (climate-induced response) and/or to variations in the sedimentation regime affecting long-term landform evolution. We expect changes related to meteorological forcing to occur on short time scales. Long-term evolution and degradation of rockglaciers, however, are most likely influenced by the supply and integration of sediment and ice in combination with climate dynamics. Frauenfelder (2004) has shown that the availability of rock debris is a very important parameter controlling the occurrence and evolution of rockglaciers during millennia and should be combined with spatio-temporally varying creep characteristics of rockglaciers.

2.3.1 Contribution

The availability of numerous remote sensing techniques to acquire data on permafrost creep (see Haeberli et al., 2006 and Kääb, 2008 for an extensive summary), high mountain geomorphometry (Bishop et al., 2003) and high mountain sediment dynamics (Gärtner-Roer, 2012, Heckmann and Schwanghart, 2013) allows for establishing a holistic assessment strategy and process coupling for rockglacier systems and their dynamics. The approach presented in Sect. 2.1.1 incorporates the quantification of sediment supply rates, ice volume estimations and rockglacier rheology in order to establish an improved understanding of rockglacier evolution (Gärtner-Roer and Nyenhuis, 2010).

Therefore, we introduce a holistic analysis concept to assess long-term rockglacier evolution and the impacts of variations in temperature, sediment supply and ice supply. We apply a modeling approach, which assesses two rockglaciers in the Swiss Alps with different topographical and rheological characteristics concerning their position in a typical coarse debris process chain in Sect. 3.3. A numerical flow model based on the conservation of mass within the debris process chain is used to calculate the evolution of rockglacier landform geometries and to generate observed rockglacier geometries and rheologies.

Variations in rockglacier geometry and velocity have been mainly attributed to changes in mean annual air temperature but are also controlled by more complex factors such as ground

temperature, slope, thickness of the deforming layer, marginal friction, density, debris/ice ratio, thermal subsurface conditions, water content, etc. (Frauenfelder et al., 2003, Roer et al., 2005). In the past, models have been applied to assess the influence of varying mean annual air temperature on rockglacier surface velocities (Kääb et al., 2007b, Springman et al, 2012). Building on that, we introduce variations in the controlling factors temperature as well as the supply of sediment and ice in order to observe kinematic and topographical adaptations of the rockglaciers.

The modeling helps to understand the driving forces of morphological changes and shows the influence of sediment supply and temperature variations on the morphological and rheological evolution of rockglaciers. We present topographic and kinematic features of the rockglaciers, which are believed to be signs of degradation and apply the model to explain the occurrence of these processes. The use of an adapted Glen-like numerical flow model for rockglaciers has been demonstrated in Olyphant (1983), Wagner (1992), Frauenfelder et al. (2008), Leysinger Vieli and Gudmundsson (2004) but such a dynamic flow model has so far not been used to assess input-dependent long-term evolution of rockglacier topography and degradation.

3 Using multi-sensoral remote sensing data to assess high mountain periglacial systems and model rockglacier evolution

In this section, the results with regard to the research objectives are presented. The presented work consists of three successive work packages. The initial step was to generate high-resolution DEMs from different airborne remote sensing systems and to check their applicability in topographically complex periglacial environments (Sect. 3.1). The findings of this study were included in the succeeding analysis. The multi-temporal DEMs were combined with datasets derived from terrestrial geodetic surveys (TS) and laser scans (TLS) and emplyed to assess the coarse sediment dynamics of high mountain periglacial systems (Sect. 3.2). This, in turn, served as basis for the geomorphometrical assessment and identification of degradation features implemented in the rockglacier evolution modeling (Sect. 3.3).

3.1 Accuracy assessment of photogrammetrically-derived airborne digital elevation models in a high mountain environment

The cornerstones of this research project's analytical part are multi-temporal DEMs derived from several remote sensing techniques. The generated DEMs are used to analyze relevant landform structures (monotemporal) and geomorphological processes (multi-temporal). High-resolution DEMs were generated by the High Resolution Stereo Camera – Airborne (HRSC-A) in 2001, the Leica Airborne Digital Sensors 40/80 (ADS40 in 2010 and ADS80 in 2012) and the analogue camera system RC30 from the year 2005. In order to apply the DEMs subsequently to assess and quantify landform structures and processes, it is necessary to know their accuracies. We conducted a thorough inaccuracy assessment in the Turtmann valley, Valais, Switzerland, a glacially and periglacially formed hanging valley stretching from 2400 m to 3300 m a.s.l., which also serves as the test in site in Publication III (see Part II). The photogrammetrically-derived DEMs were evaluated against geodetic field measurements and an airborne laser scan (ALS).

The commonly used accuracy assessment regarding height information calculates uses Δh_i between measured and reference data as accuracy measure. We used the terrestrial geodetic measurements and the ALS in two different approaches as reference data to which the photogrammetric digital elevation information is compared. Kraus et al. (2006), Mills et al. (2006) and Joerg et al. (2012) show that ALS data is of very high accuracy also in complex terrain, and can therefore be used to assess the accuracy of a photogrammetrically-derived DEM in two ways: The spatially extensive ALS dataset can be used to conduct thorough

statistical analyses of the Δh_i values and the according spatial variation of the accuracy can also be assessed.

The comparison of the photogrammetrically-derived DEMs from airborne surveys and the ALS with the geodetic reference data shows that the terrestrial geodetic measurements can not only be used to assess the accuracy of the photogrammetric data but also to check the performance of the ALS, before this data is used as a reference for further spatial and statistical analysis (Table 2).

Table 2: Accuracy assessment of the DEMs of the Turtmann valley by means of geodetic reference data (42-84 ground control points) (Absolute Mean Error (AME), Root Mean Square Error (RMSE) and Standard Deviation (SD)).

System	AME [m]	RMSE [m]	SD [m]
ALS	0.41	0.52	0.52
HRSC-A	0.87	0.96	0.97
RC30	0.61	0.72	0.71
ADS40	0.59	0.75	0.53
ADS80	0.46	0.6	0.55

The assessment is in agreement with the findings of Kraus et al. (2004) that the accuracy of ALS data is higher than the accuracy of airborne photogrammetric data. Therefore, it is reasonable to use the ALS as reference data to conduct the spatial analysis of the accuracy of the DEMs.

Using the ALS as reference data for the accuracy assessment allows not only the establishment of global quality parameters but also a locally discrete analysis. Approximately 5.1 million data points have been analyzed and show similar accuracies for the digital pushbroom scanners (HRSC-A, ADS40 and ADS80), and the lowest accuracy for the analogue RC30 System (see Table 3 and 4).

Table 3: "Traditional" accuracy measures of the ALS assessment (Absolute Mean Error (AME), Root Mean Square Error (RMSE) and Standard Deviation (SD)).

System	AME [m]	RMSE [m]	SD [m]
HRSC-A	0.72	1	1
RC30	0.85	1.30	1.28
ADS40	0.69	1.05	1.05
ADS80	0.63	1.04	0.97

Following the approach of Höhle and Höhle (2009), the error dataset is tested for normal distribution by comparing the observed and theoretical normal distribution of height differences before any other processing is applied. Höhle and Höhle (2009) introduce robust statistical methods (i.e. methods that are less influenced by outliers) to assess the accuracy of

DEMs. If the data reveal non-Gaussian distribution the authors propose the following robust measures to describe the properties of the dataset: median, normalized median absolute deviation and 68.3% and 95% quantile of the error distribution. Due to a non-Gaussian distribution of errors for all datasets, robust global accuracy measures are used to describe the vertical quality of the DEMs (see Table 4).

Table 4: Robust accuracy measures of the accuracy assessment using ALS data as reference (as proposed by Höhle and Höhle (2009)) (Median (MED), Normalized Median Absolute Deviation (NMAD) and 68.3% and 95% Quantile (Quan683) and (Quan95)).

System	MED [m]	NMAD [m]	Quan683 [m]	Quan95 [m]
HRSC-A	-0.07	0.85	0.82	1.91
RC30	0.3	0.84	0.87	1.91
ADS40	0.01	0.65	0.72	2.1
ADS80	0.01	0.62	0.66	1.92

Detailed local analysis identified slope as the main factor that determines the accuracy of the digital elevation information in all datasets. Except for the HRSC-derived DEM, all DEMs perform similarly in steep areas, and they are all able to produce accuracies better than 1 m up to a slope of 25° inclination (see Fig. 7).
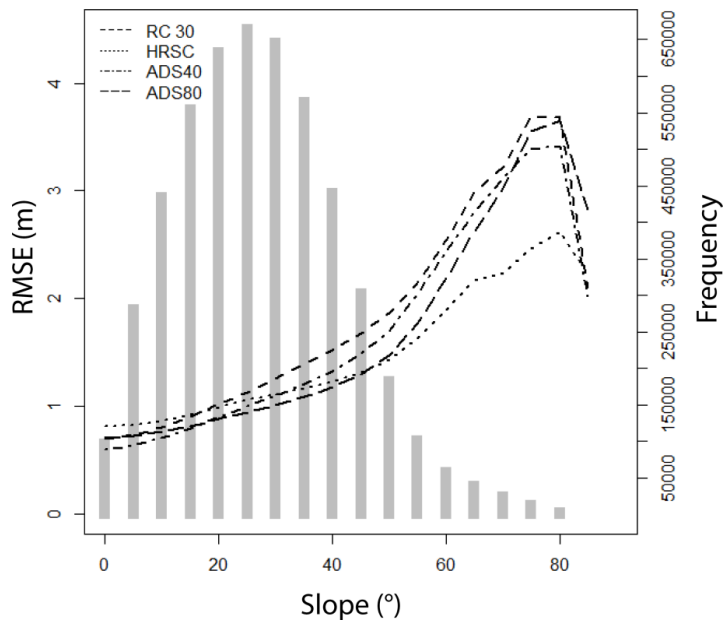

Figure 7: RMSE of the DEMs depending on slope. The grey bars show the frequency of sample points at any given slope (y-axis on the right). The values on the x-axis are in degree (°).

In general, we conclude that the modern digital pushbroom scanners can produce high-resolution DEMs in alpine environments with a very high accuracy. DEMs generated from analogue and older digital pushbroom systems have to be applied carefully, especially in steep terrain. We show that the selected sensor systems of multiple generations display only a few differences in their accuracy in complex steep terrain and can therefore be used for multi-temporal assessment.

3.2   Geomorphic work and sediment transfer in periglacial systems

This section summarizes the analysis approach and main results regarding sediment dynamics and sediment transfer in periglacial high mountain slopes.

In this contribution (see Part II, Publication II) we present a cascading, systemic model adapted from Caine (1976) (as presented in Fig. 4a) in order to describe and quantify sediment transfer rates and to derive energy fluxes in a high mountain periglacial system. Periglacial slopes are characterized by rockglaciers, ice-cored moraines and/or solifluction lobes and are often closely connected to glacial and gravitational landforms. All of these landforms are considered as significant observable indicators for changes within these systems.

Geomorphic work and sediment transfer rates are among the main components in characterizing and comparing the potential energy of geomorphological systems (Reid and Dunne, 1996, Beylich and Warburton, 2007, Micheletti et al., 2015b) and hold the opportunity to detect and quantify changes within these systems over time. The term *geomorphic work* has been introduced by Caine (1976) in order to find a universal definition for erosion and transport within geomorphological systems. In this context, the term *work* is referred to in its original physical sense as a measure of released potential energy to overcome friction and induce acceleration. Geomorphic work *GW* is defined as potential energy:

$$W = m \, g \, \Delta h \tag{1}$$

where m is the mass of the mobilized material, g the gravitational acceleration and Δh the vertical distance traveled by the material (Caine, 1976).

Based on a sediment budget approach, geomorphic work and sediment transfer rates are often assessed for entire mountain ranges (e.g. Church and Slaymaker, 1989) or single gravitational processes (e.g. Krautblatter et al., 2012). Up to now, deficits have existed in the knowledge of temporal and spatial coupling of nested geomorphological processes and complex interactions of different sediment storages (Dietrich and Dunne, 1978, Caine and

Swanson, 1989, Schrott et al., 2003).

We address these shortcomings by applying a combination of terrestrial and airborne remote sensing products derived from digital photogrammetry, TS and TLS in order to quantify sediment transfer, energy fluxes and backweathering rates in a cascading coarse debris system on a yearly scale.

The approach, using TLS and photogrammetrically-derived DEM differencing and feature tracking, allows for the quantification of vertical changes and thereof derivable quantities (such as changes in volume and energy) over time. These changes result mainly from mass movements (which holds true for the headwall) and other vertical changes due to melt of subsurface ice or from mass transport by other processes such as permafrost creep. Additional information on the kinematic behavior and/or subsurface information of the talus slope would show if alternative processes are involved but since no such information is available for this area, this study relies on the interpretation of the DEM differences and field observations.

Table 5: Detailed analysis of geomorphic work (GW) in the different subsystems and the entire catchment (total) of the two rockglacier systems Murtèl and Marmugnun. GW is given in Giga Joule [GJ].

	Rockwall		Talus Slope		Rockglacier
	GW released [GJ]	effective GW [GJ]	GW released [GJ]	effective GW [GJ]	GW released [GJ]
Murtèl	14.58	2.30	3.27	0.64	0.81
Marmugnun	86.30	27.58	13.21	3.34	0.62
Total	**100.88**	**29.88**	**16.48**	**3.99**	**1.44**

Table 5 shows the geomorphic work generated within two rockglacier systems (Murtèl and Marmugnun) in one exemplary year. The geomorphic work released (GW released) refers to the entire energy generated due to vertical mass movement over the entire feeding areas/subsystems, whereas the effective geomorphic work accounts for the energy, which is transferred to the next subsystem. The rockglacier, as the last compartment of the sediment cascade, only releases energy.

The effective volume of sediment determined by this approach in the rockwall accounts for a backweathering rate of 2 mm per year, which is consistent with values presented in Glade (2005) and Krautblatter et al. (2012). The entire system from headwall to rockglacier mobilizes 1.95×10^6 m^3 material which generate 118.8 GJ of geomorphic work.

However, only 35.3 GJ (658.9 m^3) are effectively transferred between the subsystems and the rest is retained in intermediate storages. The highest amount of energy (100.88 GJ, 29.88 GJ

effectively) is released within the headwall, whereas the rockglaciers are mobilizing the highest amount of sediment (1.93×10^6 m³) but contribute only 1.44 GJ of geomorphic work. This pattern highlights that a rockglacier can be considered a long-lasting sediment sink. It stores sediment, but it is often not connected to streams or other sediment paths downstream. Thus, rockglaciers are probably one of the best and long-lived sediment stores during interglacials.

The values presented here are significantly higher than in comparable studies (Beylich, 2000 Krautblatter et al., 2012), which is due to the spatially discrete data of the observation methods and the vertical dimension of the headwall. The spatially discrete data also allows locating active and inactive areas. The highest parts of the rockwall have been identified as most active which explains the high amounts of energy released by the headwall. Most of the material is mobilized within the rockglaciers, mainly by the Murtèl rockglacier, which by itself holds a volume of 1.4×10^6 m³. Due to their rather slow movement and low inclination the rockglaciers only contribute 1.4 GJ of geomorphic work to the entire system. Because of an existing borehole, the volume of Murtèl rockglacier is accurately known and therefore the geomorphic work precisely calculable. In the case of Marmugnun, no borehole exists, and the applied method to evaluate the thickness is not as precise. However, even if the volume of Marmugnun was underestimated by 50%, the rockglaciers would only contribute 2.06 GJ of geomorphic work to the system.

We show that a combination of observation methods is necessary to analyze each subsystem due to their specific topographies and processes. TLS is the method of choice to assess steep rockwalls and talus slopes, whereas a combination of terrestrial surveying and airborne photogrammetry has proven to show good results for rockglacier analysis (PERMOS, 2010). We quantify and locate not only the volume of material and energy mobilized within each subsystem but also the amount of material and energy which is kept and/or relocated within a subsystem. The discrepancy between mobilized and retained mass and energy lets us estimate the transfer between the subsystems but also the energy generated within the entire system. The introduced approach permits the spatial discrete analysis of mobilized and accumulated sediment volume which allows investigating the dynamics within the system, differentiating between active and inactive areas and tracking changes of process domains over time.

3.3 Rockglacier evolution

This section summarizesizes the main results of the rockglacier evolution modeling. Utilizing the results from Müller et al., 2014a (see Part, II Publication I) and Müller et al., 2014b (see Part II, Publication II) the rockglacier landforms are analyzed in a holistic setting, including their spatial and temporal long-term evolution.

Active rockglaciers are part of periglacial high mountain systems as presented in Sect. 2.1 and 2.3. The topographical evolution of the rockglacier landform is therefore relying on the production, transportation and deposition of coarse debris in the system and the generation and integration of subsurface ice. Rockglaciers are considered dynamic landforms influenced by the warming and melting of ice and changes in sediment input. A numerical flow model based on the conservation of mass within the debris process chain is used to calculate the evolution of rockglacier surfaces.

For this study the rheology of the rockglacier is reduced to a body of frozen sediment that deforms and creeps like a non-linear viscous material under the influence of gravity as proposed already in 1959 by Wahrhaftig and Cox (1959) and elaborated upon in Olyphant (1983) and Frauenfelder et al. (2008). This rheology can be described by a Glen-type flow law (Glen, 1955) as typically used for glacier ice (Cuffey and Paterson, 2010), relating the strain rate $\dot{\varepsilon}$ non-linearly to the stress τ:

$$\dot{\varepsilon} \propto A\,\tau^n \tag{2}$$

where n is a flow-law exponent that typically ranges between 2 and 3 for frozen material (Cuffey and Paterson, 2010) and A is the rate factor describing the temperature-dependent softness of the rockglacier material.

We further reduce the problem to the case of an infinite sheet of uniform thickness that creeps down an inclined plane (also known as the shallow ice approximation in glaciology, Cuffey und Paterson 2010) and thereby neglect longitudinal stress gradients. Such constitutive approximations have been applied and discussed in other studies on rockglacier creep (Whalley und Martin, 1992, Whalley und Azizi, 1994, Barsch 1996, Azizi und Whalley, 1996, Kääb et al., 2007) and their applicability further supported by results from borehole measurements and shear experiments in the laboratory on real rockglacier material (including Murtèl rockglacier; Arenson et al., 2002, Kääb and Weber, 2004, Arenson and Springman, 2005, Frehner et al., 2015).

Surface flow speeds are given by integrating rockglacier thickness h, local surface slope $\frac{\partial s}{\partial x}$, which translates into shear stress τ and strain rate ε:

$$\bar{u} = \frac{2A}{n+2} \cdot \left(\rho g \frac{\partial s}{\partial x}\right)^n h^{n+1}$$ (see Sect. 9 for a comprehensive derivation) (3)

Where ρ is the density of the rockglacier material and g the gravitational acceleration. The modeled creep rates are calibrated with the observed surface velocities and observed geometries (see Sect. 3.2).

The evolution of rockglacier thickness h and therefore the landform surface is calculated from the principle of mass conservation which takes the following form for the 1-dimensional representation along the center flowline (Oerlemans, 2001):

$$\frac{\partial h}{\partial t} = a_r - \frac{1}{w} \cdot \frac{\partial \bar{u} h w}{\partial x}$$ (4)

where t is the time, a_r is the rate of rockglacier material accumulation or removal at the surface (>0 for accumulation; in m a^{-1}), w is the rockglacier width and $\bar{u}$ is the vertically averaged horizontal flow speed.

The evolution of the rockglacier thickness and surface is calculated numerically on a regular grid of 10 m intervals along the center flowline. Using a standard implicit finite-difference scheme (Oerlemans, 2001), the surface evolution equation 4 is solved at each time step and for all grid points from the depth averaged ice flux $\bar{q} = \bar{u} \cdot h \cdot w$ and the material input a_r at the rockglacier surface.

It is assumed that the sediment and ice input from the rockwall builds up a rockglacier, which develops under a given constant climatic and geomorphic setting. Variations in temperature and sediment/ice input induce kinematic and geometric responses of the modeled rockglaciers, which can be compared to field observations of recent years.

The creep model was used to generate observed rockglacier geometries and rheologies of two selected rockglaciers (Murtèl rockglacier in the Engadine and Hungerlihorli rockglacier (Huhh1) in the Valais) with different geometric, kinematic and topographic properties (see Table 6). The modeled rockglaciers were subjected to step-change variations in driving forces such as temperature and the supply of sediment and ice.

Table 6: Comparison of observations of two rockglaciers and the model results.

		Slope [°]	Age [a]	Length [m]	Thickness [m]	Creep Vel. [ma⁻¹]	Subsidence [ma⁻¹]
Murtèl	Observations	12	6000	280	30	0.06-0.13	0.05
	Model	12	6000	300	28	0.06-0.09	0.005-0.035
Huhh1	Observations	27	600	310	12	0.75-1.55	0.16
	Model	27	600	240	16	0.63-0.79	0.02-0.13

The approach to assess rockglacier evolution in a holistic, systemic way including the dynamics and properties of relevant subsystems (headwall, deposition area and rockglacier) has proven to be well suited to reconstruct different rockglacier geometries, rheologies and their dynamics (Kääb, 2007, Frauenfelder et al, 2008). Crucial to this systemic approach are the geomorphic mapping of the different subsystems, the quantification of the sediment input rates, the ice to sediment ratio and the application of the horizontal velocities. Due to its design, the model is not capable of reproducing the exact evolution and small-scale kinematic and/or geometric properties of the two chosen real-world rock glaciers in relation to their geomorphological stetting, but is rather suitable to simulate the basic behavior of a rockglacier body evolution over time.

Despite its simplifications, the model is able to generate observed rockglacier surface, length and flow speed along the center flowline of exemplified rockglaciers on a given sediment/ice input and rockglacier rheology. It is also capable of reproducing the basic behavior of a creeping rockglacier body under environmental steady-state conditions and of simulating the impacts of step-like variations in the driving forces (see Table 6 for the model results).

Figures 8 and 9 show exemplarily the detailed results for the Murtèl and Huhh1 rockglaciers for one representative perturbation experiment. Using a reference rockglacier temperature of -1.5°C, an increase in temperature of 1 C (corresponding to an increase of rate factor *A* by factor 1.7, see Eq. 3) and a decrease of material input to 40% of the original value is applied.
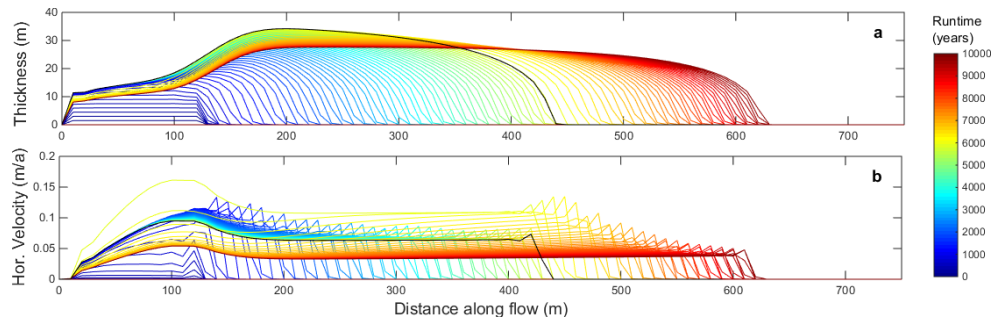

Figure 8: Modeled evolution of absolute thickness (a) and horizontal velocities (b) of the Murtèl rockglacier introducing a 1 °C temperature increase (1.7 flow-rate factor) and a reduction in material input to 40% after the rockglacier build-up (6000a, black line). The lines are plotted at 100a time steps.
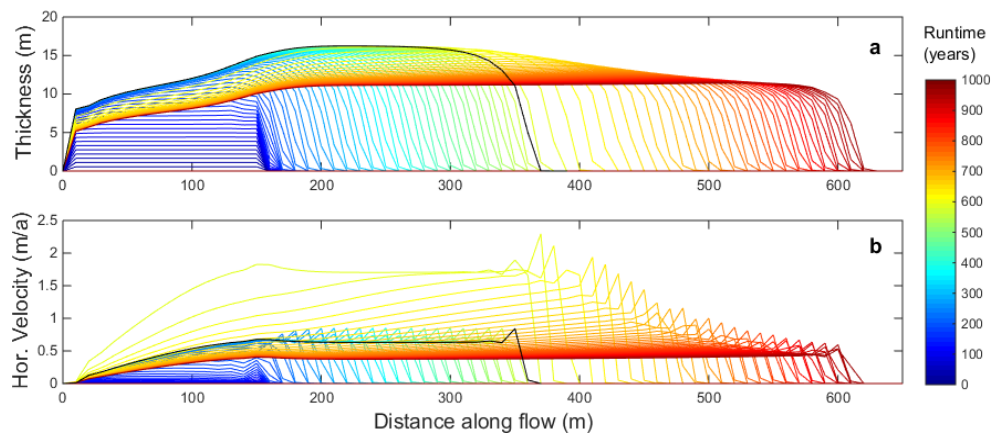

Figure 9: Modeled evolution of absolute thickness (a) and horizontal velocities (b) of the Huhh1 rockglacier introducing a 1°C temperature increase (1.7 flow-rate factor) and a reduction in material input to 40% after the rockglacier build-up (600a, black line). The lines are plotted in 10a time steps.

Figures 8 and 9 illustrate the evolution of surface geometry and horizontal velocities along the central flow line of Murtèl and Huhh1 rockglacier, respectively. This experiment shows a substantial increase in horizontal velocities (Fig. 8b and 9b) and an upstream thinning of the "initial" landform in the subsequent years (Fig. 8a and 9a) and. The maximum thinning rates occur within the first few decades of the experiment and amount to 1.6 cm a^{-1} for Murtèl and 6 cm a^{-1} for Huhh1. A new stable geometry with advancing front is successively approached,

again within roughly 1000 a and 100 a for Murtèl and Huhh1, respectively. The final thickness and velocities of the main rockglacier body remain, however, very close to the initial values.

Climatic changes, especially warming, are expected to influence rockglacier dynamics in a profound way. The dynamic rockglacier modeling approach allows not only for analyzing the impact of a direct warming by adjusting the flow rate of the rockglacier but also including the influence of changes in sediment and ice input. Variations in the driving forces temperature and supply of sediment and ice give insight into the rheological and geometrical responses of the landforms, which show that

- Short-term changes in velocities are introduced by temperature variations whereas long-term geometrical adaptations are mainly influenced by sediment/ice supply.
- Geometrical changes can be modeled, quantified and spatially addressed leading to a better understanding of the long-term evolution of rockglaciers.
- The combinations of thermal and sediment variations reproduce the variations in rockglacier velocities observed from field data.
- Rockglaciers remain active although the thermal and sediment input conditions are not favorable for their sustenance.
- Adjusted rockglacier rheologies (Arenson and Springman, 2005) close to 0 °C show much stronger reactions to thermal forcing than colder ones.

Comparing the model scenarios for localized geometrical adaptations (subsidence) with observed phenomena shows that these controlling factors are not sufficient to explain the magnitude of this process (see Table 5).

This implies that other processes than increased creep velocities and decreased sediment/ice supply are responsible for this subsidence and need further investigations. The discrepancy between the modeled and observed subsidence hints to an increased melt of subsurface ice, which can be interpreted as a sign for the degradation of the two presented rockglaciers. Degrading rockglaciers are expected to experience an increase in hazardous potential due to their instability and non-linear behavior (Arenson, 2002, Kääb et al., 2005a, Springman et al., 2013). The modeling approach presented here might serve as a tool to determine the state of alpine rockglaciers and their potential state of degradation.

4 Discussion

In the following, the scientific findings of this thesis will be discussed in the context of the formulated research questions (Sect. 1.3.2) and how the complementary papers improve the understanding of high mountain permafrost systems.

4.1 Analyzing remote high mountain systems from the air – possibilities and restrictions

Remote sensing is particularly well-suited for repeated and rapid observation in remote and inaccessible areas of high mountain environments. Mono- and multi-temporal DEMs derived from various remote sensing systems are repeatedly used to analyze land surface features and processes (e.g. Kääb et al., 1997, Gruen, 2002, Tarolli et al., 2009, Debella-Gilo and Kääb, 2012). Despite their common usage, their accuracies are only rarely considered. Lane stated already in 1998 that "*many users accept DEMs uncritically*" (Lane, 1998, p. 8) despite the fact that the applicability of digital elevation models depends on their accuracy in respect to their analytical purpose. Especially when using multi-temporal data the accuracy of the particular elevation product must be known to quantify changes within the separate time steps.

We were able to show that different methodologies have been applied to assess the accuracy of DEMs depending on their application. The comprehensive datasets enabled us to quantify and correct systematic errors addressing the trueness of the data but also to elaborate on the precision of the data. A comprehensive literature review showed that only two out of eight scientific papers were comparable to the methods and results presented in our assessment. Studies that tested the same sensor systems in less complex terrain or relied on less comprehensive reference data showed in general better results for the systems' accuracy. This shows that it is absolutely necessary to not only consider the general accuracy of photogrammetrically-derived DEMs but to also check if the accuracy measures are applicable to the research area and analysis concept in question. Interestingly, studies which were conducted by the developer/manufacturers themselves showed much higher accuracies than we were able to reproduce.

The availability of multi-sensoral reference data allowed a detailed spatial analysis of the DEM accuracy and we were able to characterize the error distributions and identify slope as the main factor that determines the accuracy of the digital elevation information in all datasets. We found that the four sensor systems produce DEMs with similar accuracy despite their different setups and generations and are therefore suitable for further application. Spatial accuracy assessments of DEMs are always limited by the quality of

reference data. An accuracy assessment which is carried out by means of reference data is regarded as defining the exterior quality (Kraus et al., 2004). Maune (2007) states that the accuracy of the reference data should be at least three times more accurate than the evaluated digital elevation data. We used two unrelated datasets as reference data (geodetic survey data and ALS data) which are of different quality. The terrestrial survey data is by far the most accurate data with accuracies of 1-2 cm. Nevertheless, the low population of the ground control points from terrestrial surveying does not allow statistically reliable conclusions about the entire dataset and their distribution is biased as they are not randomly located within the entire research area but are clustered on rockglaciers which depict certain surface characteristics. Although the ALS data has been repeatedly used for accuracy assessments (Mills et al., 2006) and is spatially extensive, it does not fulfill the requirements of Maune (2007). The quality of the ALS is also heterogeneous within the complex topography of the test site where steep slopes present the greatest difficulties. Therefore the absolute quantification of the photogrammetric data accuracy has to be interpreted with respect to the quality of the reference data.

The findings we present are especially valuable for permafrost research in high mountains because process rates that are observable by airborne remote sensing are comparably slow in permafrost environments (e.g. rockglacier creep, solifluction, thaw-induced ground subsidence, etc.), thus either high accuracies or long time spans are needed in order to quantify and assess such surface dynamics. Most statements about the state and evolution of high mountain permafrost landforms are mainly based on the analysis of time series that extend as long as methodically reasonable into the past (Kääb, 2008). Especially for remote sensing applications in these environments, it is absolutely necessary to consider the interpretative restrictions due to the accuracy of the derived products.

4.2 Quantifying sediment and energy transfer in periglacial high mountain systems

High mountain environments deserve special scientific attention, since environmental changes may occur on shorter time scales and with lasting consequences, thus reflecting the sensitivity of complex high energy environmental systems (Barsch and Caine, 1984). Especially in near-isothermal periglacial high mountain environments (such as the European Alps), it is expected that changes in the thermal regime will influence geomorphological processes such as weathering rates, mass wasting processes and landform dynamics (Diaz, 2003, Kääb, 2007b, IPCC, 2013). Periglacial landforms are considered significant indicators

for changes within the system. In order to assess the connectedness and dynamics in such a system, we developed a conceptual, cascading sediment and energy transfer model. Geomorphic work can serve as a uniform measure of system dynamics in order to quantify and characterize ongoing processes based on the energy released and stored by sediment transport in the entire mountain slope. The concept of geomorphic work is applicable in geosystems with a high level of intermediate storage and internal sediment transport (Krautblatter et al., 2012) such as periglacial mountain slopes. It can be used as a measure of geomorphic activity and compared between different systems or different time steps.

Crucial to this approach is the quantification of headwall backweathering and the according sediment generation. We identified TLS as the best suited method to derive this information but the analysis was restricted to only two years of data. This methodology allowed us to not only assess the sediment transfer from the rockwall to the talus slope but also the sediment dynamics within the rockwall. Most alpine rockwalls consist not only of 90 degree vertical cliffs but also of many steep scree slopes which serve as temporary sediment storages (Sass, 2005) and are underrepresented in our transfer model. Krautblatter et al. (2012) stated that rockfall sediment yield is dominated by high-magnitude rock avalanches (62% of total sediment input) and low magnitude rockfall (18%) whereas cliff-, boulder- and block falls account for the remaining 20% (cliff falls 10%, Boulder falls 6% and block falls 4%). Rock avalanches are high magnitude and low frequency events and very unlikely to be systematically analyzed in a single slope within two years (Clarke and Burbank, 2010). Therefore our assessment holds only true for the assumption that sediment regimes are dominated by mid- to small-scale events. Geomorphic mapping and field observations have shown that the Murtèl cirque is prone to constant rockfall activity of medium to small magnitudes (10–10^4 m^3) which could be quantified during two years of TLS.

Geomorphic work in mountain systems has been thoroughly assessed in Krautblatter et al. (2012) and the study gives also a good overview of the geomorphic work literature. The values presented in paper II are significantly higher than the results presented in preceding studies but there are only few comparable datasets available. Most of the studies concerned with geomorphic work focus on single processes such as solution (Groves and Meiman, 2005), debris flows (Lewkowicz and Hartshorn, 1998) and selected mass movements (Beylich, 2000).

In order to establish a systemic assessment of energy transfer in periglacial environments, we present a spatially differentiated analysis of the geomorphic work in a mountain slope. The available dataset covers only one year of system dynamics but prominent landforms in periglacial systems such as rockglaciers evolve over millennia. Therefore, in order to make

full use of the analysis potential of this dataset, it is necessary to conduct similar studies in other periglacial systems and/or repeatedly assess the Murtèl slope over time. We expect changes related to climatic forcing to occur on short time-scales; thus influencing the related processes. Possible implications of climate change are increased weathering rates and therefore increased sediment production (Gruber and Haeberli, 2007) which will have an impact on all succeeding process domains and the geomorphic work generated. Higher temperatures will also influence ice aggregation and segregation, ice properties and therefore permafrost creep, thus changing process rates in permafrost landforms. The findings we present serve as an energy-based approach that helps to assess the dynamic changes in such periglacial environments in the future and provides a baseline for upcoming studies. The conceptual approach of cascading process domains and resulting landforms quantifies process rates and their connectedness through the exchanged material and energy. Their changes can be analyzed by using energy fluxes and geomorphic work as indicators for their process-related evolution.

4.3   From kinematics to dynamics – Modeling rockglacier dynamics and degradation

Active rockglaciers and the corresponding cascading sediment transport systems are part of periglacial high mountain systems. The topographical evolution of the rockglacier landform is therefore relying on the production, transportation and deposition of coarse debris in the system and the generation and integration of subsurface ice. Rockglaciers are considered as dynamic landforms influenced by the existence and thermal state of ice and changes in sediment input. The variations in environmental factors translate into observable changes in geometry and kinematics which are interpreted as signs for degradation and/or destabilization of these permafrost landforms (Roer et al., 2008, Springman et al., 2013). Most rockglacier monitoring strategies focus on the *kinematics* [Greek: kínema = movement] of these landforms which are defined as the quantification of movement (velocity, acceleration) without considering the forcing factors (Roer, 2005). *Dynamics*, however, involve physical forces and their interactions as well as the resulting changes in physical systems and pose the upcoming challenges in rockglacier research.

Many studies have taken a kinematic approach to rockglacier assessment where rockglacier velocity and acceleration were measured and qualitatively compared to air or ground temperatures (Roer et al., 2005, Delaloye et al., 2010, Scapozza et al., 2014). Only few other studies have tried to establish an empirical or physical process-based concept of rockglacier

dynamics which involved shear stresses, sediment supply and/or properties of the ice/rock mélange that characterize rockglaciers in relation to variations in controlling factors such as temperature and sediment dynamics (Kääb et al., 2007b; Springman et al., 2012).

Based on the results of Publication I and Publication II, it was possible to analyze the rockglacier landforms comprehensively, including sediment dynamics, their spatial and temporal development and kinematic information in order to develop a *dynamic* model of rockglacier evolution.

Time series of rockglacier kinematics in the European Alps indicate an acceleration over the last decades related to an increase in ground temperatures (Delaloye et al., 2010, PERMOS, 2013, Bodin et al., 2015). Multi-temporal geomorphometric analyses have shown degradational processes such as subsidence features and structural disintegration of alpine rockglaciers (Kääb et al., 2007b, Roer et al., 2008, Bodin et al., 2010, Springman et al., 2013). These observations can be addressed by the model helping to understand the driving forces of these kinematic and geometric changes, showing what influence sediment supply and temperature variations have on the morphological and rheological evolution of rockglaciers. Different experiments with our model show that temperature and sediment/ice dynamics play an important role in rockglacier acceleration, whereas observed subsidence features cannot be sufficiently explained.

Besides temperature and material input, variations in rockglacier geometry and velocity are also controlled by more complex factors such as shear zone characteristics, slope and thickness of the deforming layer, marginal friction, density, debris/ice ratio, thermal subsurface conditions, water content, etc. (Frauenfelder et al., 2003, Kääb et al., 2007b, Roer et al., 2005). Due to the fact, that the role of most of these additional factors is still not clear, they can hardly be incorporated in a numerical model approach. Still further research needs to address these points in order to establish a process-based understanding of these parameters and develop a more comprehensive understanding of rockglacier dynamics.

However, the rockglacier evolution model helps to understand some of the forces that drive morphological changes of rockglaciers and shows the influence of sediment supply and temperature variations. Further, it elaborates to which degree these variations can be held responsible for signs of degradation. This may serve as a tool to determine the state of alpine rockglaciers and determine their potential state of degradation which is of great importance for a comprehensive natural hazard management.

Although simplifications such as a pure ice body, constant material input and constant thermal conditions had to be assumed for the rockglacier build-up (as already demonstrated

in Olyphant (1983), Leysinger Vieli (2004a) and Frauenfelder (2008)), the model performs well concerning the reconstruction and evolution of geometrical and kinematic properties of rockglaciers. While the model setup assumes the properties and physics of a pure ice body, the adaptations to these assumptions to represent rockglaciers have shown to be very effective in order to reconstruct and assess their evolution.

To implement climatic changes, we presented a very simplified step change approach to introduce warming to the rockglacier systems which has been suggested for sensitivity studies by Leysinger Vieli (2004a) and Wainwright (2013). It is obvisouly not feasible to assume step-like changes in temperature or sediment dynamics in natural environments but this approach delivers useful information to assess their impacts on rockglacier dynamics. In reality, permafrost temperature depends on the energy balance and heat exchange at the ground surface (Hanson and Hoelzle, 2004). Therefore, the snow cover thickness and duration and the characteristics of the surface material and matrix are important for processes that have not been included in this modeling approach. Kääb et al. (2007) and Scherler et al. (2014) have developed approaches to implement convective and advective heat transfer processes in rockglaciers material which will have to be implemented in future rockglacier studies concerned with the impacts of climate variations in rockglacier properties. Existing physically based energy balance models for debris covered glaciers address latent and sensible heat transfer as well as advective and convective heat fluxes in an unconsolidated debris cover similar to rockglacier material (Brock et al., 2010). These approaches to model energy balance, heat conduction and ice melt on glaciers with thick debris cover should theoretically be transferable to rockglaciers. In both cases the role of the debris cover/active layer poses the critical aspect of energy transfer and is crucial to the melt of subsurface ice and landform dynamics. In the case of debris covered glaciers, however, the role of precipitation is mostly reduced to its impact on heat fluxes and mostly ignored because its relevance tends to be extremely small (Reid and Brock, 2010). Precipitation however seems to play an important role in rockglacier dynamics (Wirz et al., 2015). Additionally, studies on thermal conduction and energy fluxes of debris covers on glaciers can produce reliable estimates of melt rates beneath debris layers several decimeters thick but are inappropriate for thick debris covers (Nicholson and Benn, 2006) which is the case for rockglaciers. Since rockglaciers tend to have active layers of several meters thickness, it is hence necessary to apply debris-covered glacier approaches carefully.

Nevertheless, our approach to model rockglacier movement without incorporating sophisticated heat fluxes agrees well with long-term monitoring data presented in Delaloye

et al. (2010) and PERMOS (2013) where the warm summer and exceptional snow conditions of the years 2003/2004 resulted in a speed up of various rockglacier all over the Alps of up to >300%. Most model runs in our experiment show a more moderate acceleration of about 200%, which is within the main variations of rockglacier velocities. Especially the most realistic scenarios of a -1.5 °C rockglacier and a reduction of material input agree well with the field data.

The thermally-induced acceleration of the rockglacier leads to an increase in mass transport capacity which determines the long-term horizontal velocities in combination with various mass inputs. The long-term evolution shows that a decrease in sediment/ice input results on the long term to a slower average horizontal velocity in relation to the initial temperature of the rockglacier. The spatial analysis of the model results shows an immediate and strong reaction to the perturbation at the upper parts of the rockglacier whereas the signal is weakened along the flowline. Depending on the assumed initial temperature of the rockglacier, the impacts of the perturbation are varying according to location and input scenario. The landform as a whole remains advancing at different speeds during the perturbations of the system even if the material input is completely stopped. This feature of landform thinning, especially in the upper parts of the rockglacier, has been described as a sign of degradation by Ikeda and Matsuoka (2008), Springman et al. (2013) and Roer et al. (2008) and interpreted as a destabilized rockglacier where the rockglacier landform is disconnected from its deposition area.

The sediment experiments show the establishment of a new long-term surface geometry depending on the accelerated velocity of the rockglacier and the material input conditions. Steady state conditions are not realistic but the rates of geometrical adaptation give insight into the rockglacier dynamics.

The detailed analysis of the subsidence processes can only explain subsidence rates lower than observed values. This means that the observed thinning rates in the field cannot only originate from geometrical adaptation due to thermally-induced acceleration and varying sediment dynamics but must be influenced by volume loss in the subsurface, most likely due to the disappearance of subsurface ice.

5 Conclusion and Outlook

In densely populated high mountain areas affected by the occurrence of permafrost, it is essential to obtain improved understanding of the entire „conveyor belt" system ranging from the origin of the weathered material at the rockwall to the creeping permafrost feature. Besides natural hazard management, investigations of sediment budgets and system dynamics in high mountain environments improve the understanding of geomorphological processes and recent environmental changes. Rockglaciers and frozen talus slopes are one of the main storage components of the coarse debris system within alpine environments and reflect the evolution of mountain permafrost. The combination of comprehensive airborne and terrestrial remote sensing data, novel conceptual analysis approaches and numerical rockglacier evolution modeling allowed us to contribute to the current understanding of the landform and process dynamics in high mountain systems under permafrost conditions. The presented research combines the application of contemporary remote sensing methods with existing long-term monitoring methods and data sets. The wealth of existing data available for creeping alpine permafrost features can thus be exploited to its full potential.

5.1 Main findings

Here, the major findings are condensed and organized according to the research questions formulated in Sect. 1.3. More details can be found in the full versions of the research papers in Part II.

Paper I: *How accurate are photogrammetrically-derived high-resolution airborne digital elevation models and what are the limitations in high mountain applications?*

- Modern digital photogrammetric airborne sensor systems are well suited for automatic terrain extraction in high alpine areas, including shaded and ice covered surfaces. DEMs generated from analogue and older digital pushbroom systems have to be applied carefully, especially in steep terrain.
- The accuracy assessment of the DEMs showed systematic errors as well as a non-normal distribution for all data sets. According global and local accuracy measures were found that displayed similar performances for all sensor systems (see Tables 2 & 3).
- Detailed local analysis identified slope as the main factor that determines the accuracy of the digital elevation information in all datasets. Except for the HRSC, the

DEMs perform similarly in mountainous ares. In steep areas, they are able to produce accuracies of <1 m up to a slope of 25° inclination.

- We conclude that sensor systems of different generations display only a few differences in their accuracy in complex steep terrain and can therefore be used for multi-temporal assessment.

Paper II*: What are the sediment dynamics, storages and transfer rates in a periglacial mountain slope system?*

- A novel multi-sensoral approach to assess the sediment and energy transfer of the coarse debris system within a periglacial high mountain slope was developed based on a systemic understanding of processes and landforms.

- A combination of observational methods is necessary to analyze each subsystem due to their specific topography and processes. TLS is suited best to assess steep rockwalls and talus slopes whereas a combination of terrestrial surveying and airborne photogrammetry has proven to show good results for rockglacier analysis.

- The entire assessed system consisting of headwall, talus slope and two rockglaciers mobilizes 1.95×10^6 m^3 a^{-1} of material which generates 118.8 GJ a^{-1} of geomorphic work of which only 35.3 GJ a^{-1} (658.9 m^3 a^{-1}) is effectively transferred between the subsystems and the rest is retained in intermediate storages. The highest amount of energy is released within the headwall whereas the rockglaciers are mobilizing the highest amount of sediment.

- A backweathering rate of 2 mm a^{-1} is derived from the sediment dynamics in the headwall.

Paper III: *How do rockglaciers evolve and react to changes in environmental factors?*

- A numerical creep model based on the conservation of mass within the debris process chain was developed to calculate the long-term evolution of rockglacier surfaces and velocities.

- The model is able to generate observed rockglacier surface, length and flow speed along the central flowline of two different rockglaciers on a given sediment/ice input and rockglacier rheology.

- A 1 °C temperature increase in rockglacier temperature can result in 160%-400% acceleration of rockglacier creep depending on the thermal state of the rockglacier.

- Sediment/ice input variations result in the long-term adaptation of the rockglacier geometry. An expected decrease of sediment/ice supply due to climate change is modeled to result in a spatially diverse subsidence of the landform.

- Observed subsidence features cannot be reproduced by warming and variations in sediment/ice supply which shows that these controlling factors are not sufficient to explain ongoing subsidence processes.

- Irrespective of the perturbation, the rockglaciers keep advancing and remain active although the thermal and sediment input conditions are not favorable for their sustenance.

- Rockglaciers react spatially diverse to changes in environmental factors. Changes in temperature have an immediate effect on the entire landform but the impact of material input variations are most pronounced in the sedimentation area and upper parts of the rockglacier.

- Although the absolute magnitudes in thinning and creep acceleration differ between the two rockglaciers, the changes relative to the initial thickness and creep velocity respectively are very similar thus indicating that changes scale with their geometric and dynamic characteristics.

- Based on most recent models of rockglacier rheology (Arenson and Springman, 2005) rockglaciers close to 0 °C are likely to show much stronger reactions to thermal forcing than colder ones.

- On the basis of our modeling and kinematic wave theory, we propose a typical *time scale of dynamic adjustment* to external perturbations that is given by the inverse of a few times the horizontal velocity of a rockglacier.

5.2 Conclusion

A graphical summary of the contents of this dissertation is given in Fig. 10 where the synergies and connections between the subjects of the three peer-reviewed papers are illustrated.
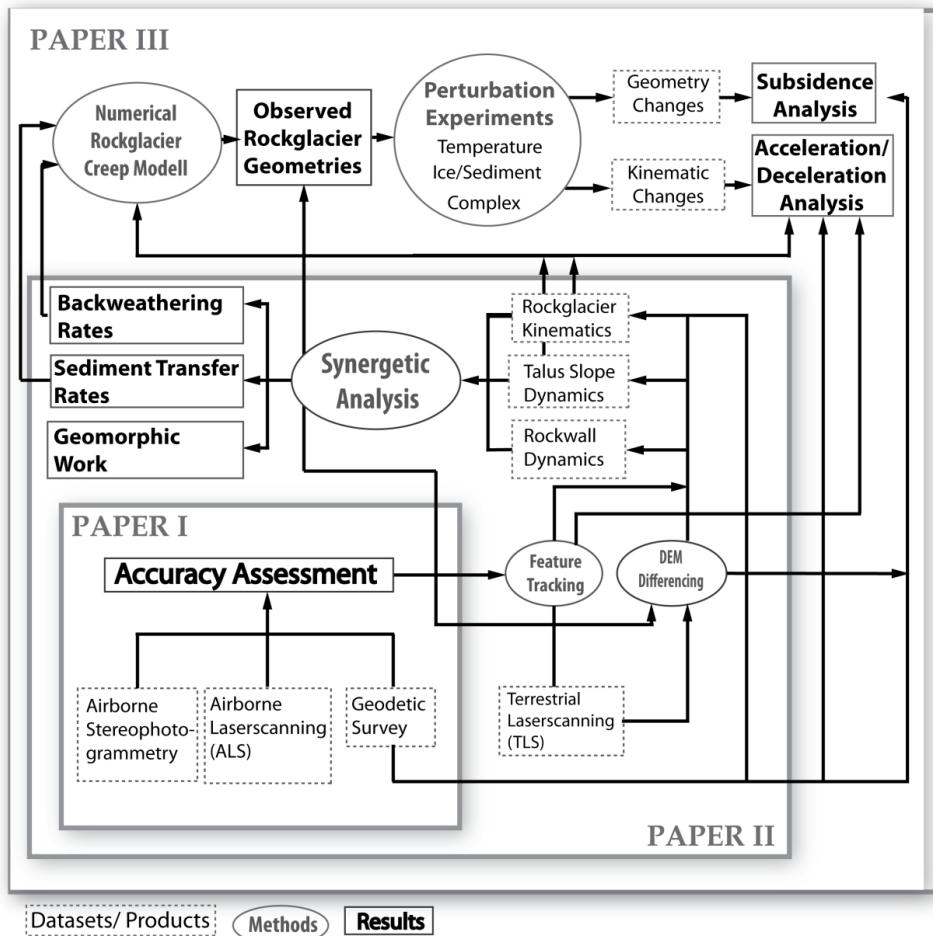

Figure 10: Schematic overview of this dissertation showing the initial datasets, processing products, methods and major results as well as the contents and relations between the three research papers.

Figure 10 shows that this research project is predicated on the processing and analysis of multi-temporal, remotely sensed digital elevation information. A variety of terrestrial and airborne remote sensing systems has been used to acquire this information, each containing different qualities and restrictions. This is why a comprehensive assessment of the

performance and compatibility of the modern sensor systems and datasets is necessary, so that these important sources of information can be safely combined and applied (see Sect. 3.1 and Publication I). As presented in the subsequent studies here, the general findings of the accuracy assessment should be considered in future studies which use multi-temporal DEMs in complex high mountain terrain to make sure the digital elevation datasets are applied according to their capabilities.

The assessment of sediment and energy transfer rates in a periglacial mountain slope (Sect. 3.2 and Publication II) exemplified the use of multi-sensoral digital elevation information with respect to the different system characteristics. We presented a novel conceptual and instrumental approach to assess an entire periglacial mountain slope holistically, coupling different process and landform domains based on quantifiable field data. Many studies have focused on large scale sediment dynamics or single landform assessment in order to assess energy and material transfer (Campbell and Church, 2003, Krautblatter et al., 2012). Here, the unique availability of a complementary instrumentation at the presented field site allowed for the quantification and coupling of coarse sediment dynamics, geomorphic work and the efficiency of landform processes in an entire mountain slope based on individual landforms and their coupling. We highlighted the important role of rockglaciers as long-time sediment traps of entire mountain slopes and their role as one of the best and long-lived sediment stores during interglacials. With the quantification of the relevant process rates such as rockfall, talus slope dynamics and permafrost creep, we present the possibility to directly compare environmental systems and geomorphological processes on different spatial and temporal scales and assess changes therein.

The findings on sediment dynamics, geomorphic work and the wealth of existing data on rockglacier kinematics were implemented in a rockglacier evolution model. This new model approach is based on the conservation of mass within a dynamic landform, and is capable of reproducing actual landform geometries and their changes, which had not been done so far. The relation between rockglacier velocity and temperature has been repeatedly addressed (Arenson and Springman, 2005, Kääb et al., 2007b) but the rockglacier evolution model introduces the role of sediment/ice production and supply in addition to the thermal controlling factors. The possibility of assessing rockglacier geometries and their dynamics in relation to changes in environmental controls offers the opportunity to address questions concerning the current state of these permafrost landforms and their potential destabilization and/or degradation.

The synergy of all aspects displayed in Fig. 10 presents a holistic and comprehensive approach to assess permafrost landform dynamics in high mountains. Beginning with data generation and evaluation, its application and quantification in the field and resulting in an approach to model process as well as landform dynamics, this dissertation presents a novel multi-sensoral approach to assess rockglacier evolution.

5.3 Outlook

Based on the results and the discussion above, it can be concluded that future progress in high mountain research concerned with periglacial systems, permafrost and rockglaciers will come from advances in the fields of observation, application, comparison and modeling. The following will give a recommendation what future research should follow up on.

5.3.1 Remote Sensing in high mountain systems

Recent advances in remote sensing technology have opened countless opportunities to apply newly developed methods and instruments in high mountain periglacial systems. These include the application of UAV-based and terrestrial digital photogrammetry, terrestrial and spaceborne radar interferometry and many more.

UAV-based photogrammetry has already been used in geomorphological contexts in some studies (Eltner et al., 2015, Ouédraogo et al., 2014, Haas et al., 2015) but, although very promising, their potential to assess periglacial high mountain systems has not been thoroughly tested (Immerzeel et al., 2014). This method of DEM generation promises very high temporal and spatial resolution, fast and cost-efficient data acquisition and will enable us to focus on selected research targets individually. As elaborated in this dissertation, a reliable application of this data will demand a thorough assessment of the applicability and accuracy, especially in complex topographies. The application of UAV technology has become effortless and versatile. Multi-temporal application of UAV-based photogrammetry will allow for (hopefully) very accurate, high-resolution (spatially in cm and temporally in h) elevation data that can be used to assess kinematics and geometric changes of permafrost and high mountain landforms.

Similar facts hold true for the application of **terrestrial photogrammetry** where the advances in **Structure from Motion** (SfM) software have become ubiquitously applicable and need to be tested for geomorphological analyses in high mountains (Westoby et al., 2012, Piermattei et al., 2015). Historic digital photogrammetry relied heavily on calibrated cameras and lenses, complex manual intervention in the scene and during pair-wise processing, often

with inferior results in uncontrolled circumstances. Recent research has shown that SfM photogrammetry can be applied in an uncomplicated manner with very promising results even in complex terrain (Micheletti et al., 2015a, Lato et al., 2014). The fact that SfM photogrammetry utilizes large number of detailed, but otherwise not specialized, digital photos to automatically generate dense three-dimensional models of remote surfaces makes it especially interesting for rapid data acquisition and offers even the possibility of crowdsourced data generation (Heipke, 2010).

A combination of the methods to derive the above mentioned DEMs with terrestrial and spaceborne radar interferometric data has already been tested to detect and quantify rockglacier kinematics and high alpine processes (Barboux et al., 2015, Strozzi et al., 2012, Caduff et al., 2014) but has never been used for assessment in a holistic manner. **Radar interferometry** is capable of detecting very small changes in topography which makes it well suited for the detection and quantification of small-scale surface subsidence and other geometrical changes. We have shown that the quantification of geometrical rockglacier destabilization is restricted by the accuracy of the observational systems but georeferenced interferometric radar data is able to detect changes in mm-resolution (Caduff et al., 2015). We expect this unprecedented level of detail to be especially beneficial for future assessments of geometrical rockglacier destabilization and seasonal landform monitoring.

The great benefits of the new technologies mentioned above can be summarized as significant improvements in the accuracy and spatial and/or temporal resolution of the data and need to be applied to improve process understanding in periglacial environments.

5.3.2 Periglacial system and rockglacier assessment

Fundamental advances in periglacial system understanding are most likely to be achieved by combining a more detailed analysis of the controlling processes in such environments with a holistic approach considering the coupling and feedback mechanism in complex environmental systems under a changing climate (Phillips, 2006).

The study of **weathering rates, rock stability and rockwall retreat** in laboratory environments and field experiments (Matsuoka and Murton, 2008, Murton et al., 2006, Weber et al., 2016), and their dependence on geological and climatic parameters on different time scales (Krautblatter et al., 2013) will be crucial to improve the understanding of the past and future evolution of high mountain permafrost systems. The study of sediment production and sediment supply will also have to address the question of the efficiency of supplying processes, namely if the most effective processes are mostly low magnitude-high frequency or rather high magnitude-low frequency events (Krautblatter et al., 2012).

Further resources should be allocated to assessing **the controlling factors of rockglacier creep**. Rockglacier creep has been intensely studied but the role of many landform properties remains unclear. The important role of different substrates and lithologies, melt water existence and infiltration, the heterogeneity of subsurface ice and its properties have been recognized in rockglacier rheology and surface dynamics but not quantified or conceptually addressed and modeled. This is of course due to the past and present difficulties of obtaining field data concerning these properties and processes. However, advances in geophysical applications, remote sensing and modeling are expected to address these issues of data acquisition (Lei and Ma, 2014, Scherler et al., 2010, Buchli et al., 2013).

Another aspect that should be addressed is the cumulative **impact of expected climate change** on periglacial systems. Warming temperatures, weather extremes and changes in precipitation are expected to influence almost all controlling factors in these environments. The short-term effects of warming are currently the topic of numerous landform and process studies but long-term evolution is very rarely investigated because uncertainties prevail in the long-term application of climate modeling and the anticipated impacts on process rates and landform responses. The terms "**degradation**" and "**destabilization**" are often used in the context of future landform evolution and process rates in periglacial/permafrost systems but a comprehensive definition is yet missing. Permafrost degradation has been in general thermally defined as the top-down or bottom-up thaw of permafrost (IPCC, 2013) but a common conceptualization of degradation is necessary to address the dynamic and topographic impacts of thawing permafrost in order to assess the state of permafrost systems and derive their further evolution.

To assess system evolution and the impacts of different climatic factors, the findings of this dissertation presented in Part II, Publication II may serve as a **baseline** example for a periglacial system experiencing warming permafrost conditions. Comparable systems can undergo a similar analysis and the comparison will show differences and similarities in energy and sediment transfer rates, which can be attributed to the climatic and/or geomorphological settings.

5.3.3 Rockglacier modeling

All models are wrong, but some are useful.

(Chatfield, 1995)

Therefore, future modeling approaches concerned with rockglacier evolution should address a number of aspects:

Firstly, despite the assumptions presented in the modeling approach of this study, in reality, rockglaciers do not consist of and behave like homogenous material but are of highly spatially and temporally heterogeneous composition. Especially when assessing the long-term evolution of rockglaciers, the **ratio between ice and sediment** is very likely to change, which impacts the rheology and therefore topography of the landforms. Therefore, the origin, aggradation and degradation of rockglacier subsurface ice should be considered in future modeling approaches and observations of how the kinematic and topographic evolution changes with varying ice content.

Secondly, the implementation of long-term evolution of sediment supply is recommended according to a **thermally controlled backweathering model**. This would introduce a dynamic, more realistic sediment input influencing rockglacier evolution.

Thirdly, as it is shown in Part II, Publication III, temperature variations play a significant role in the short- and long-term variation of rockglacier velocities. The kinematic modeling can be significantly improved if the thermal signal is implemented according to established **thermal conduction models** such as presented in Scherler et al. (2014).

Finally, the recommendations presented in the two foregoing sections should find their implications integrated in future modeling approaches. Frequent **high-resolution data on topography and kinematics** with high accuracy will provide more detailed and quantifiable information on landform evolution and possible degradation. Therefore, it is absolutely necessary to continue monitoring entire periglacial mountain slopes on different temporal and spatial scales in order to enhance the holistic understanding of high mountain rockglacier systems.

6   References

Abermann, J., Fischer, A., Lambrecht, A., and Geist, T.: On the potential of very high-resolution repeat DEMs in glacial and periglacial environments, The Cryosphere, 4, 53–65, 2010.

Arenson, L., Hoelzle, M., and Springman, S.: Borehole deformation measurements and internal structure of some rock glaciers in Switzerland, Permafrost and Periglacial Processes, 13, 117–135, 2002.

Arenson, L. U. and Springman, S. M.: Mathematical descriptions for the behaviour of ice-rich frozen soils at temperatures close to 0 °C, Canadian Geotechnical Journal, 42, 431–442, 2005.

Azizi, F. and Whalley, W.: Numerical modelling of the creep behavior of Ice-Debris Mixtures under variable thermal regimes, in: The proceedings of the Sixth (1996) International Offshore and Polar Engineering Conference, Chung, J., Braja, M., and Boesset, J. (Eds.), Los Angeles, USA, May 26-31, 1996.

Barboux, C., Strozzi, T., Delaloye, R., Wegmüller, U., and Collet, C.: Mapping slope movements in Alpine environments using TerraSAR-X interferometric methods, ISPRS Journal of Photogrammetry and Remote Sensing, 109, 178–192, 2015.

Barsch, D.: Nature and importance of mass-wasting by rock glaciers in alpine permafrost environments, Earth Surface Processes, 2, 231–245, 1977.

Barsch, D.: Permafrost creep and rockglaciers, Permafrost Periglacial Processes., 3, 175–188, 1992.

Barsch, D.: Rockglaciers: Permafrost Creep and Rockglaciers, Springer, Berlin, 331 pp., 1996.

Barsch, D. and Caine, N.: The Nature of Mountain Geomorphology, Mountain research and development, 4, 287–298, 1984.

Berthling, I.: Beyond confusion: Rock glaciers as cryo-conditioned landforms, Geomorphology, 131, 98–106, 2011.

Beylich, A.: Geomorphology, sediment budget, and relief development in Austdalur, Austfiroir, East Iceland, Arctic, Antarctic, and Alpine Research, 32, 466–477, 2000.

Beylich, A. and Warburton, J. (Eds.): Analysis of Source-to-Sink-Fluxes and Sediment Budgets in Changing High-Latitude and High-Altitude Cold Environments: SEDIFLUX Manual, One, NGU Report 2007, NGU Report 2007, 2007.

BIPM, IEC, IFCC, ILAC, ISO, IUPAC, IUPAP, OIML, 2008. Guide to the expression of uncertainty in measurement. (GUM), ISO, Geneva.

Bishop, M. P., Shroder, J. F., and Colby, J. D.: Remote sensing and geomorphometry for studying relief production in high mountains, Geomorphology, 55, 345–361, 2003.

Bodin, X., Thibert, E., Fabre, D., Ribolini, A., Schoeneich, P., Francou, B., Reynaud, L., and Fort, M.: Two decades of responses (1986 - 2006) to climate by the Laurichard rock glacier, French Alps, Permafrost and Periglacial Processes, 20, 331–344, 2009.

Bodin, X., Rojas, F., and Brenning, A.: Status and evolution of the cryosphere in the Andes of Santiago (Chile, 33.5°S.), Geomorphology, 118, 453–464, 2010.

Bodin, X., Schoeneich, P., Deline, P., Ravanel, L., Magnin, F., Krysiecki, J.-M., and Echelard, T.: Mountain permafrost and associated geomorphological processes: Recent changes in the French Alps, Journal of Alpine Research, 103-2, 2015.

Brock, B. W., Mihalcea, C., Kirkbride, M. P., Diolaiuti, G., Cutler, M. E. J., and Smiraglia, C.: Meteorology and surface energy fluxes in the 2005–2007 ablation seasons at the Miage debris-covered glacier, Mont Blanc Massif, Italian Alps, J. Geophys. Res., 115, 2010.

Buchli, T., Merz, K., Zhou, X., Kinzelbach, W., and Springman, S. M.: Characterization and Monitoring of the Furggwanghorn Rock Glacier, Turtmann Valley, Switzerland: Results from 2010 to 2012, Vadose Zone Journal, 12, 2013.

Bühler, Y., Kneubühler, M., Bovet, S., and Kellenberger, T.: Anwendung von ADS40 Daten im Agrarbereich, in: DGPF Tagungsband: Dreiländertagung SGPBF, DGPF und OVG, E Seyfert (Ed.), Deutsche Gesellschaft für Photogrammetrie, Fernerkundung und Geoinformation (DGPF), Oldenburg, 381–390, 2007.

Bühler, Y., Marty, M., and Ginzler, C.: High Resolution DEM Generation in High-Alpine Terrain Using Airborne Remote Sensing Techniques, Transactions in GIS, 16, 635–647, 2012.

Caduff, R., Kos, A., Schlunegger, F., McArdell, B. W., and Wiesmann, A.: Terrestrial Radar Interferometric Measurement of Hillslope Deformation and Atmospheric Disturbances in the Illgraben Debris-Flow Catchment, Switzerland, IEEE Geosci. Remote Sensing Lett., 11, 434–438, 2014.

Caduff, R., Schlunegger, F., Kos, A., and Wiesmann, A.: A review of terrestrial radar interferometry for measuring surface change in the geosciences, Earth Surf. Process. Landforms, 40, 208–228, 2015.

Caine, N.: A uniform measure of subaerial erosion, Geological Society of America Bulletin, 87, 137–140, 1976.

Caine, N. and Swanson, F. J.: Geomorphic coupling of hillslope and channel systems in two small mountain basins., Zeitschrift für Geomorphologie, 33, 189–203, 1989.

Campbell, D. and Church, M.: Reconnaissance sediment budgets for Lynn Valley, British Columbia: Holocene and contemporary time scales, Canadian Journal of Earth Sciences, 40, 701–713, 2003.

Clark, D. H., Steig, E. J., Potter, Jr., Noel, and Gillespie, A. R.: Genetic variability of rock glaciers, Geografiska Annaler A, 80, 175–182, 1998.Clarke, B. A. and Burbank, D. W.: Bedrock fracturing, threshold hillslopes, and limits to the magnitude of bedrock landslides: Earth and Planetary Science Letters, 297, 577–586, 2010.

Ceppi, P., Scherrer, S. C., Fischer, A. M., and Appenzeller, C.: Revisiting Swiss temperature trends 1959-2008, Int. J. Climatol., 32, 203–213, 2012.

Chatfield, C.: Model Uncertainty, Data Mining and Statistical Inference, Journal of the Royal Statistical Society. Series A (Statistics in Society), 158, 419, 1995.

Chorley, R. J. and Kennedy, B. A.: Physical geography: A systems approach, Prentice-Hall, Hemel Hempstead, 1971.

Church, M. and Slaymaker, O.: Disequilibrium of Holocene sediment yield in glaciated British Columbia, Nature, 337, 452–454, 1989.

Cloutier, C., Locat, J., Mayers, M., Noel, F., Turmel, D., Gionet, P., Jaboyedoff, M., Jacob, C., and Dorval, P. Bosse, F.: An integrated management tool for rockfall evaluation along transportation corridors: description and objectives of the parachute research project, in: 68th Canadian Geotechnical Conference GeoQuebec, Canada., Quebec, 2015.

Cooper, M. A. R.: Datums, Coordinates and Differences., in: Landform monitoring, modelling and analysis, Lane, S. N. (Ed.), British Geomorphological Research Group symposia series, Wiley, Chichester, 1998.

Debella-Gilo, M. and Kääb, A.: Measurement of Surface Displacement and Deformation of Mass Movements Using Least Squares Matching of Repeat High Resolution Satellite and Aerial Images, Remote Sensing, 4, 43–67, 2012.

Cuffey, K. M. and Paterson, W.: The physics of glaciers, 4th ed., Elsevier, Amsterdam, 693 p, 2010.

Delaloye, R., Lambiel, C., and Gärtner-Roer, I.: Overview of rock glacier kinematics research in the Swiss Alps: seasonal rhythm, interannual variations and trends over several decades, Geographica Helvetica, 65, 135–145, 2010.

Delaloye, R., Morard, S., Barboux, C., Abbet, D., Gruber, V., Riedo, K., and Gachet, S.: Rapidly moving rock glaciers in Mattertal., in: Mattertal - ein Tal in Bewegung, Graf, C. (Ed.), Jahrestagung der Schweizerischen Geomorphologischen Gesellschaft, St. Niklaus, Switzerland, 2011.

Delisle, G.: Near-surface permafrost degradation: How severe during the 21st century?, Geophys. Res. Lett., 34, 2007.

Diaz, H. F., Grosjean, M., and Graumlich, L.: Climate Variability and Change in High Elevation Regions: Past, Present and Future, Climatic change, 59, 1–4, 2003.

Dietrich, W. and Dunne, T.: Sediment budget for a small catchment in mountainous terrain., in: Field Instrumentation and Geomorphological Problems, Slaymaker, O., Rapp, A., and Dunne, T. (Eds.), Schweizerbart'sche Verlagsbuchhandlung, Stuttgart, 191–206, 1978.

Eltner, A., Baumgart, P., Maas, H.-G., and Faust, D.: Multi-temporal UAV data for automatic measurement of rill and interrill erosion on loess soil, Earth Surf. Process. Landforms, 40, 741–755, 2015.

Engelhardt, M., Hauck, C., and Salzmann, N.: Influence of atmospheric forcing parameters on modelled mountain permafrost evolution, Meteorol. Z., 19, 491–500, 2010.

Etzelmüller, B., Schuler, T. V., Isaksen, K., Christiansen, H. H., Farbrot, H., and Benestad, R.: Modeling the temperature evolution of Svalbard permafrost during the 20th and 21st century, The Cryosphere, 5, 67–79, 2011.

Etzelmüller, B: Recent Advances in Mountain Permafrost Research, Permafrost and Periglacial Processes, 24, 99–107, 2013.

Fisher, P.: Improved Modeling of Elevation Error with Geostatistics, GeoInformatica, 2, 215–233, 1998.

Fisher, P. F. and Tate, N. J.: Causes and consequences of error in digital elevation models, Progress in Physical Geography, 30, 467–489, 2006.

Fonstad, M. A., Dietrich, J. T., Courville, B. C., Jensen, J. L., and Carbonneau, P. E.: Topographic structure from motion: a new development in photogrammetric measurement, Earth Surf. Process. Landforms, 38, 421–430, 2013.

Frauenfelder, R., Haeberli, W., and Hoelzle, M.: Rockglacier occurrence and related terrain parameters in a study area of the eastern Swiss Alps., in: ICOP 2003 Permafrost: Proceedings of the Eighth International Conference on Permafrost, Haeberli, W. and Brandova, D. (Eds), Zurich, Switzerland, A.A. Balkema Publishers, Vol. 1, 253-258, 2003.

Frauenfelder, R., Schneider, B., and Kaeaeb, A.: Using dynamic modelling to simulate the distribution of rockglaciers, Geomorphology, 93, 130–143, 2008.

French, H. M.: The periglacial environment, 3rd ed., John Wiley and Sons, Chichester, England, Hoboken, NJ, 458p, 2007.

Frehner, M., Ling, Anna Hui Mee, and Gärtner-Roer, I.: Furrow-and-Ridge Morphology on Rockglaciers Explained by Gravity-Driven Buckle Folding: A Case Study From the Murtèl Rockglacier (Switzerland), Permafrost and Periglacial Processes., 26, 57–66, 2015.

Gärtner-Roer, I. and Nyenhuis, M.: Volume estimation, kinematics and sediment transfer rates of active rockglaciers in the Turtmann Valley, Switzerland, in: Landform - structure, evolution, process control: Proceedings of the International Symposium on Landform,in: Otto, J.-C., and Dikau, R. (Eds.), Lecture notes in earth sciences, 115, Springer, Berlin, 185–198, 2010.

Gärtner-Roer, I.: Sediment transfer rates of two active rockglaciers in the Swiss Alps, Geomorphology, 167–168, 45–50, 2012.

Gauthier, D., Hutchinson, J., Lato, M., Edwards, T., Bunce, C., and Wood, D.: On the precision, accuracy and utility of oblique aerial photogrammetry (OAP) for rock slope monitoring and assessment, in: 68th Canadian Geotechnical Conference GeoQuebec, Canada., Quebec, QC, 2015.

Glade, T.: Linking debris-flow hazard assessments with geomorphology, Geomorphology, 66, 189–213, 2005.

Glen, J. W.: The creep of polycristalline, Proceedingsof the Royal Society of London Series A-Mathemtical and Physical Sciences, 228, 519–538, 1955.

Goyal, S. K., Seyfried, M. S., and O'Neill, P. E.: Effect of Digital Elevation Model resolution on topographic correction of airborne SAR, International Journal of Remote Sensing, 19, 3075–3096, 1998.

Groves, C. and Meiman, J.: Weathering, geomorphic work, and karst landscape evolution in the Cave City groundwater basin, Mammoth Cave, Kentucky, Geomorphology, 67, 115–126, 2005.

Gruber, S. and Haeberli, W.: Permafrost in steep bedrock slopes and its temperature-related destabilization following climate change, Journal of geophysical research, 112, 2007.

Gruber, S. and Haeberli, W.: Mountain Permafrost, in: Permafrost soils, Varma, A. (Ed.), Springer, Berlin, 33–44, 2009.

Gruen, A. and Murai, S.: High-resolution 3D modelling and visualization of Mount Everest, ISPRS Journal of Photogrammetry and Remote Sensing, 57, 102–113, 2002.

Haas, F., Hilger, L., Neugirg, F., Umstädter, K., Breitung, C., Fischer, P., Hilger, P., Heckmann, T., Dusik, J., Kaiser, A., Schmidt, J., Della Seta, M., Rosenkranz, R., and Becht, M.: Quantification and analysis of geomorphic processes on a recultivated iron ore mine on the Italian island Elba using long-time ground-based LIDAR and photogrammetric data by an UAV, Natural Hazards and Earth System Sciences Discussions, 3, 6271–6319, 2015.

Haeberli, W.: Creep of mountain permafrost: Internal structure and flow of alpine rock glaciers, Mitteilungen der VAW/ETH Zürich, 77, 119, 1985.

Haeberli, W., Hallet, B., Arenson, L., Elconin, R., Humlun, O., Kaab, A., Kaufmann, V., Ladanyi, B., Matsuoka, N., Springman, S., and Vonder Muhll, D.: Permafrost creep and rock glacier dynamics, Permafrost and Periglacial Processes, 17, 189–214, 2006.

Haeberli, W., Noetzli, J., Arenson, L. U., Haeberli, D. R., and Roer, I.: Mountain permafrost: development and challenges of a young research field, Journal of Glaciology, 56, 1043–1058, 2010.

Hamilton, S.: Rock glacier nomenclature: A re-assessment, Geomorphology, 14, 73–80, 1995.

Hanson, S. and Hoelzle, M.: The thermal regime of the active layer at the Murtèl rock glacier based on data from 2002, Permafrost and Periglacial Processes, 15, 273–282, 2004.

Harris, C., Davies, M. C. R., and Etzelmüller, B.: The assessment of potential geotechnical hazards associated with mountain permafrost in a warming global climate, Permafrost Periglacial Processes., 12, 145–156, 2001.

Harris, C. and Isaksen, K.: Recent Warming of European Permafrost: Evidence from Borehole Monitoring, in: Proceedings of the Ninth International Conference on Permafrost, Fairbanks, Alaska, 2008.

Harris, C., Arenson, L. U., Christiansen, H. H., Etzelmüller, B., Frauenfelder, R., Gruber, S., Haeberli, W., Hauck, C., Hölzle, M., Humlum, O., Isaksen, K., Kääb, A., Kern-Lütschg, M. A., Lehning, M., Matsuoka, N., Murton, J. B., Nötzli, J., Phillips, M., Ross, N., Seppälä, M., Springman, S. M., and Vonder Mühll, D.: Permafrost and climate in Europe: Monitoring and modelling thermal, geomorphological and geotechnical responses, Earth-Science Reviews, 92, 117–171, 2009.

Hebeler, F. and Purves, R. S.: Modeling DEM Data Uncertainties for Monte Carlo Simulations of Ice Sheet Models, in: Quality aspects in spatial data mining, Stein, A. (Ed.), CRC Press, Boca Raton, Fla., 175, 2009a.

Hebeler, F. and Purves, R. S.: The influence of elevation uncertainty on derivation of topographic indices, Geomorphology, 111, 4–16, 2009b.

Heckmann, T. and Schwanghart, W.: Geomorphic coupling and sediment connectivity in an alpine catchment — Exploring sediment cascades using graph theory, Geomorphology, 182, 89–103, 2013.

Heipke, C.: Crowdsourcing geospatial data, ISPRS Journal of Photogrammetry and Remote Sensing, 65, 550–557, 2010.

Höhle, J. and Höhle, M.: Accuracy assessment of digital elevation models by means of robust statistical methods, ISPRS Journal of Photogrammetry and Remote Sensing, 64, 398–406, 2009.

Hoelzle, M. and Haeberli, W.: Simulating the effects of mean annual air temperature changes on permafrost distribution and glacier size. An example from the Upper Engadin, Swiss Alps., Annals of Glaciology, 21, 400–405, 1995.

Hoelzle, M., Mühll, D. V., and Haeberli, W.: Thirty years of permafrost research in the Corvatsch- Furtschellas area, Eastern Swiss Alps: A review, Norsk Geografisk Tidsskrift - Norwegian Journal of Geography, 56, 137–145, doi:10.1080/002919502760056468, 2002.

Huggel, C., Salzmann, N., and Allen, S.: High-Mountain Slope Failures and Recent and Future Warm Extreme Events, in: Climate Forcing of Geological Hazards, McGuire, B., and Maslin, M. (Eds.), John Wiley & Sons, Ltd, Chichester, UK, 195–222, 2013.

Humlum, O.: Rock Glacier Appearance Level and Rock Glacier Initiation Line Altitude: A Methodological Approach to the Study of Rock Glaciers, Arctic and Alpine Research, 20, 160, 1988.

Humlum, O.: Origin of rock glaciers: observations from Mellemfjord, Disko Island, central West Greenland, Permafrost and Periglacial Processes, 7, 361, 361–380, 1996.

Humlum, O.: The geomorphic significance of rock glaciers: estimates of rock glacier debris volumes and headwall recession rates in West Greenland, Geomorphology, 35, 41–67, doi:10.1016/S0169-555X(00)00022-2, 2000.

Ikeda, A. and Matsuoka, N.: Degradation of talus-derived rock glaciers in the Upper Engadin, Swiss Alps, Permafrost and Periglacial Processes, 13, 145–161, doi:10.1002/ppp.413, 2002.

Ikeda, A., Matsuoka, N., and Kääb, A.: Fast deformation of perennially frozen debris in a warm rock glacier in the Swiss Alps: An effect of liquid water, Journal of Geophysical Research F: Earth Surface, 113, 2008.

Immerzeel, P.D.A. Kraaijenbrink, J.M. Shea, A.B. Shrestha, F. Pellicciotti, M.F.P. Bierkens, and S.M. de Jong: High-resolution monitoring of Himalayan glacier dynamics using unmanned aerial vehicles, Remote Sensing of Environment, 150, 93–103, 2014.

IPCC: Climate Change 2013 - The Physical Science Basis, Cambridge University Press, Cambridge, 2014.

ISO 5725-1, 1998. Accuracy (trueness and precision) of measurement methods and results - Part 1: General principles and definitions. ISO, Geneva.

James, M. R. and Robson, S.: Straightforward reconstruction of 3D surfaces and topography with a camera: Accuracy and geoscience application, J. Geophys. Res., 117, 2012.

Joerg, P. C., Morsdorf, F., and Zemp, M.: Uncertainty assessment of multi-temporal airborne laser scanning data: A case study on an Alpine glacier, Remote Sensing of Environment, 127, 118–129, 2012.

Johnson, P. G.: Rock Glaciers. A Case for a Change in Nomenclature, Geografiska Annaler. Series A, Physical Geography, 65, 27, 1983.

Kääb, A.: Photogrammetry for early recognition of high mountain hazards: new techniques and applications, Physics and chemistry of the earth. Part A: Solid earth and geodesy, 25, 765, 2000.

Kääb, A., Haeberli, W., and Gudmundsson, G. H.: Analysing the creep of mountain permafrost using high precision aerial photogrammetry: 25 years of monitoring Gruben rock glacier, Swiss Alps, Permafrost and Periglacial Processes, 8, 409–426, 1997.

Kääb, A., Huggel C., Fischer L., Guex S., Paul, F., Roer, I., Salzmann, N., Schlaefli S., Schmutz K., Schneider D., Strozzi T., and Weidmann Y.: Remote sensing of glacier- and permafrost-related hazards in high mountains: an overview, Natural Hazards and Earth System Sciences, 5, 527–554, 2005a.

Kääb, A., Reynolds, J., and Haeberli, W.: Glacier and Permafrost Hazards in High Mountains, in: Global Change and Mountain Regions, Huber, U., Bugmann, H., and Reasoner, M. (Eds.), Advances in Global Change Research, Springer Netherlands, 225–234, 2005b.

Kääb, A., Chiarle, M., Raup, B., and Schneider, C.: Climate change impacts on mountain glaciers and permafrost, Global and Planetary Change, 56, 7, 2007a.

Kääb, A., Frauenfelder, R., and Roer, I.: On the response of rockglacier creep to surface temperature increase: Climate Change Impacts on Mountain Glaciers and Permafrost, Global Planetary Change, 56, 172–187, 2007b.

Kääb, A.: Remote sensing of permafrost-related problems and hazards, Permafrost and Periglacial Processes, 19, 107–136, 2008.

Kaiser, A., Neugirg, F., Rock, G., Müller, C., Haas, F., Ries, J., and Schmidt, J.: Small-Scale Surface Reconstruction and Volume Calculation of Soil Erosion in Complex Moroccan Gully Morphology Using Structure from Motion, Remote Sensing, 6, 7050–7080, 2014.

Kellenberger, T. and Nagy, P.: Potential of the ADS40 Aerial scanner for archaeological prospection in Rheinau Switzerland, International Archives of Photogrammetry and Remote Sensing, Vol. XXXVII, 2008.

Kenner, R., Phillips, M., Danioth, C., Denier, C., Thee, P., and Zgraggen, A.: Investigation of rock and ice loss in a recently deglaciated mountain rockwall using terrestrial laser scanning: Gemsstock, Swiss Alps, Cold Regions Science and Technology, 67, 157–164, 2011.

Kenner, R., Bühler, Y., Delaloye, R., Ginzler, C. and Phillips, M.: Monitoring of high alpine mass movements combining laser scanning with digital airborne photogrammetry, Geomorphology, 206, 492–504, 2014.

Kneisel, C. and Kääb, A.: Mountain permafrost dynamics within a recently exposed glacier forefield inferred by a combined geomorphological, geophysical and photogrammetrical approach, Earth Surface. Processes and. Landforms, 32, 1797–1810, 2007.

Kneisel, C., Hauck, C., Fortier, R., and Moorman, B.: Advances in geophysical methods for permafrost investigations, Permafrost and Periglacial Processes, 19, 157–178, 2008.

Kraus, B., Briese C., Attwenger, M., and Pfeifer, N.: Quality Measures for Digital Terrain Models, in: Proceedings and Results of XX ISPRS Congress, Commission I-VII, Altan, O. (Ed.), Geo-Imagery Bridging Continents, Istanbul, Turkey, 2004.

Kraus, K., Karel, W., Briese C., and Mandlburger, G.: Local accuracy measures for digital terrain models, The Photogrammetric Record, 342–354, 2006.

Krautblatter, M., Moser, M., Schrott, L., Wolf, J., and Morche, D.: Significance of rockfall magnitude and carbonate dissolution for rock slope erosion and geomorphic work on Alpine limestone cliffs (Reintal, German Alps), Sedimentary fluxes and budgets in natural and anthropogenically modified landscapes – Effects of climate change and land-use change on geomorphic processes, 167–168, 21–34, 2012.

Krautblatter, M., Funk, D., and Günzel, F. K.: Why permafrost rocks become unstable: a rock–ice-mechanical model in time and space, Earth Surface Processes and Landforms, 38, 876–887, 2013.

Kyriakidis, P. C., Shortridge, A. M., and Goodchild, M. F.: Geostatistics for conflation and accuracy assessment of digital elevation models, International Journal of Geographical Information Science, 13, 677–707, 1999.

Lambiel, C.: Le glacier rocheux déstabilisé de Tsaté-Moiry (VS) caractéristiques morphologiques et vitesses de déplacement., in: La géomorphologie alpine: Entre patrimoine et contrainte / actes du colloque de la Société suisse de géomorphologie, 3-5 septembre 2009, Olivone, Lambiel, C., Reynard, E., and Scappozza, C. (Eds.), Géovisions, 36, Institut de géographie de l'Univ. de Lausanne, Lausanne, 2011.

Lane, S. N. (Ed.): Landform monitoring, modelling and analysis, British Geomorphological Research Group symposia series, Wiley, Chichester, XII, 454, 1998.

Lane, S. N.: Application of digital photogrammetry to complex topography for geomorphological research, The Photogrammetric Record, 16, 793, 2000.

Lato, M., Hutchinson, J., Gauthier, D., Edwards, T., and Ondercin, M.: Comparison of ALS, TLS and terrestrial photogrammetry for mapping differential slope change in mountainous terrain., Canadian Geotechnical Journal, 52, 129–140, 2014.

Lato, M., Baumgard, A., Foster, J., kim, D., and Gauthier, D.: Hazard identification and evaluation using UAV photogrammetry, in: 68th Canadian Geotechnical Conference GeoQuebec, Canada., Quebec, 2015.

Lei, X. and Ma, S.: Laboratory acoustic emission study for earthquake generation process, Earthq Sci, 27, 627–646, 2014.

Lewkowicz, A. and Hartshorn, J.: Terrestrial record of rapid mass movements in the Sawtooth Range, Ellesmere Island, Northwest Territories, Canada, Canadian Journal of Earth Sciences, 35, 55–64, 1998.

Leysinger Vieli, G.-M.: Modeling advance and retreat of alpine and rock glaciers, Dissertation, Mitteilungen der VAW-ETH Zurich, vol. 185, Zürich, 2004.

Leysinger Vieli, G. J.-M. C. and Gudmundsson, G. H.: On estimating length fluctuations of glaciers caused by changes in climatic forcing, J. Geophys. Res., 109, 2004.

Li, Z., Zhu, Q., and Gold, C.: Digital Terrain Modeling: Principles and Methodology, CRC Press, Boca Raton, Florida, 2005.

Marmy, A.: Numerical modelling of mountain permafrost of Switzerland: sensitivity and long-term evolution, Dissertation, Geography, University of Fribourg, Fribourg, 2015.

Marmy, A., Rajczak, J., Delaloye, R., Hilbich, C., Hoelzle, M., Kotlarski, S., Lambiel, C., Noetzli, J., Phillips, M., Salzmann, N., Staub, B., and Hauck, C.: Semi-automated calibration method for modelling of mountain permafrost evolution in Switzerland, The Cryosphere Discuss., 9, 4787–4843, 2015.

Martin, H. E. and Whalley, W. B.: Rock glaciers. Part 1: rock glacier morphology, classification and distribution, Progress in Physical Geography, 11, 260–282, 1987.

Matsuoka, N. and Murton, J.: Frost weathering: recent advances and future directions, Permafrost Periglacial Processes., 19, 195–210, 2008.

Maune, D.: Digital Elevation Model Technologies and Applications: The Dem Users Manual, American Society for Photogrammetry and Remote Sensing, 2007.

Meybeck, M.: A new typology for mountains and other relief classes: An application to global continental water resources and population distribution, Mountain research and development, 21, 34–45, 2001.

Menditto, A., Patriarca, M., and Magnusson, B.: Understanding the meaning of accuracy, trueness and precision, Accred Qual Assur, 12, 45–47, doi:10.1007/s00769-006-0191-z, 2007.

Micheletti, N., Chandler, J. H., and Lane, S. N.: Investigating the geomorphological potential of freely available and accessible structure-from-motion photogrammetry using a smartphone, Earth Surface Processes and Landforms, 40, 473–486, 2015a.

Micheletti, N., Lambiel, C., and Lane, S. N.: Investigating decadal-scale geomorphic dynamics in an alpine mountain setting, J. Geophys. Res. Earth Surf., 120, 2155–2175, 2015b.

Mills, J. P., Alhamlan, A. S., Abuoliat, A. S., and Horgan, J.: Geometric Validation of Imagery and Products from a high performance airborne digital sensor, International Archives of Photogrammetry and Remote Sensing, Vol. XXXVII, 2006.

Müller, J., Gärtner-Roer, I., Thee, P., and Ginzler, C.: Accuracy assessment of airborne photogrammetrically derived high-resolution digital elevation models in a high mountain environment, ISPRS Journal of Photogrammetry and Remote Sensing, 98, 58–69, doi:10.1016/j.isprsjprs.2014.09.015, 2014a.

Müller, J., Gärtner-Roer, I., Kenner, R., Thee, P., and Morche, D.: Sediment storage and transfer on a periglacial mountain slope (Corvatsch, Switzerland), Geomorphology, 218, 35–44, 2014b.

Müller, J., Vieli, A., and Gärtner-Roer, I.: Rockglaciers on the run - Understanding rockglacier landform evolution and recent changes from numerical flow modeling, The Cryosphere Discuss., 1–40, doi:10.5194/tc-2016-35, 2016.

Murton, J. B., Peterson, R., and Ozouf, J.-C.: Bedrock fracture by ice segregation in cold regions, Science, 314, 1127–1129, 2006.

Nicholson, L. and Benn, D. I.: Calculating ice melt beneath a debris layer using meteorological data, Journal of Glaciology, 52, 463–470, 2006.

Noetzli, J. and Gruber, S.: Transient thermal effects in Alpine permafrost, The Cryosphere, 3, 85–99, 2009.

Nogués-Bravo, D., Araújo, M. B., Errea, M. P., and Martínez-Rica, J. P.: Exposure of global mountain systems to climate warming during the 21st Century, Global Environmental Change, 17, 420–428, 2007.

Nolan, M., Larsen, C., and Sturm, M.: Mapping snow depth from manned aircraft on landscape scales at centimeter resolution using structure-from-motion photogrammetry, The Cryosphere, 9, 1445–1463, 2015.

Oerlemans, J.: Glaciers and climate change, A.A. Balkema Publishers, Lisse, 148 S, 2001.

Oksanen, J. and Sarjakoski, T.: Uncovering the statistical and spatial characteristics of fine toposcale DEM error, International Journal of Geographical Information Science, 20, 345–369, 2006.

Olyphant, G.: Computer simulation of rock-glacier development under viscous and pseudoplastic flow, Geol Soc America Bull, 94, 499, 1983.

Oppikofer, T., Jaboyedoff, M., and Keusen, H.-R.: Collapse at the eastern Eiger flank in the Swiss Alps, Nature Geoscience, 1, 531–535, 2008.

Oppikofer, T., Jaboyedoff, M., Pedrazzini, A., Derron, M.-H., and Blikra, L.: Detailed DEM analysis of a rockslide scar to characterize the basal sliding surface of active rockslides, Journal of Geophysical Research F: Earth Surface, 116, 2011.

Otto, J.-C., Schrott, L., Jaboyedoff, M., and Dikau, R.: Quantifying sediment storage in a high alpine valley (Turtmanntal, Switzerland), Earth Surf. Process. Landforms, 34, 1726–1742, doi:10.1002/esp.1856, 2009.

Ouédraogo, M. M., Degré, A., Debouche, C., and Lisein, J.: The evaluation of unmanned aerial system-based photogrammetry and terrestrial laser scanning to generate DEMs of agricultural watersheds, Geomorphology, 214, 339–355, 2014.

Owens, P. N. (Ed.): Mountain geomorphology, Arnold, London, 313, 2004.

Papasaika, H. and Baltsavias, E. P.: Quality evaluation of DEMs., in: Proceedings of Accuracy 2010: 9th International symposium on spatial accuracy assessment in natural resources and envionrmental sciences, N.J.Tate and P.F. Fisher (Ed), Leicester, United Kingdom, 381-384, 2010

PERMOS: Glaciological Report Permafrost No. 10/11 of the Cryospheric Commission of the Swiss Academy of Sciences., 2013.

Phillips, J. D.: Earth surface systems: Complexity, order and scale, The natural environment, Blackwell Publishers, Malden, Massachusetts, XII, 180 S, 1999.

Phillips, J. D.: Deterministic chaos and historical geomorphology: A review and look forward, Geomorphology, 76, 109–121, 2006.

Pieczonka, T., Bolch, T., and Buchroithner, M.: Generation and evaluation of multi-temporal digital terrain models of the Mt. Everest area from different optical sensors, 5ISPRS6 Journal of Photogrammetry and Remote Sensing, 66, 927–940, 2011.

Piermattei, L., Carturan, L., Blasi, F. de, Tarolli, P., Dalla Fontana, G., Vettore, A., and Pfeifer, N.: Analysis of glacial and periglacial processes using structure from motion, Earth Surf. Dynam. Discuss., 3, 1345–1398, 2015.

Rajczak, J., Kotlarski, S., Salzmann, N., and Schär, C.: Robust climate scenarios for sites with sparse observations: a two-step bias correction approach, Int. J. Climatol., 2015.

Rajczak, J., Pall, P., and Schär, C.: Projections of extreme precipitation events in regional climate simulations for Europe and the Alpine Region, J. Geophys. Res. Atmos., 118, 3610–3626, 2013.

Ravanel, L., Allignol, F., Deline, P., Gruber, S., and Ravello, M.: Rock falls in the Mont Blanc Massif in 2007 and 2008, Landslides, 7, 493–501, 2010.

Reid, L. M. and Dunne, T.: Rapid evaluation of sediment budgets, GeoEcology, Catena, Reiskirchen, 164, 1996.

Reid, T. D. and Brock, B. W.: An energy-balance model for debris-covered glaciers including heat conduction through the debris layer, Journal of Glaciology, 56, 903–916, 2010.

Riseborough, D., Shiklomanov, N., Etzelmüller, B., Gruber, S., and Marchenko, S.: Recent advances in permafrost modelling, Permafrost Periglacial Processes., 19, 137–156, 2008.

Roer, I.: Rockglacier kinematics in a high mountain geosystem, Dissertation, Geographie, Rheinische Friedrich Wilhelms Universität, Bonn, 2005.

Roer, I., Kääb, A., and Dikau, R.: Rockglacier acceleration in the Turtmann valley (Swiss Alps): Probable controls, Norwegion Journal of Geography, 59, 157–163, 2005.

Roer, I. and Nyenhuis, M.: Rockglacier activity studies on a regional scale: comparison of geomorphological mapping and photogrammetric monitoring, Earth Surface Processes and Landforms, 32, 1747–1758, 2007.

Roer, I., Haeberli, W., Avian, M., Kaufmann, V., Delaloye, R., Lambiel, C., and Kääb, A.: Observations and considerations on destabilizing active rock glaciers in the European Alps, in: Ninth International Conference on Permafrost, 1505–1510, 2008.

Salzmann, N., Nötzli, J., Hauck, C., Gruber, S., Hoelzle, M., and Haeberli, W.: Ground surface temperature scenarios in complex high-mountain topography based on regional climate model results, J. Geophys. Res., 112, 2007.

Sass, O.: Spatial patterns of rockfall intensity in the northern Alps, Zeitschrift fur Geomorphologie, Supplementband, 138, 51–65, 2005.

Scapozza, C., Lambiel, C., Bozzini, C., Mari, S., and Conedera, M.: Assessing the rock glacier kinematics on three different timescales: a case study from the southern Swiss Alps, Earth Surf. Process. Landforms, 39, 2056–2069, 2014.

Scherler, M., Hauck, C., Hoelzle, M., Stähli, M., and Völksch, I.: Meltwater infiltration into the frozen active layer at an alpine permafrost site, Permafrost Periglacial Processes., 21, 325–334, 2010.

Scherler, M., Schneider, S., Hoelzle, M., and Hauck, C.: A two-sided approach to estimate heat transfer processes within the active layer of the Murtèl–Corvatsch rock glacier, Earth Surf. Dynam., 2, 141–154, 2014.

Schrott, L., Hufschmidt, G., Hankammer, M., Hoffmann, T., and Dikau, R.: Spatial distribution of sediment storage types and quantification of valley fill deposits in an alpine basin, Reintal, Bavarian Alps, Germany, Mountain Geomorphology - Integrating Earth Systems, Proceedings of the 32nd Annual Binghamton Geomorphology Symposium, 55, 45–63, 2003.

Schürch, P., Densmore, A. L., Rosser, N. J., Lim, M., and McArdell, B. W.: Detection of surface change in complex topography using terrestrial laser scanning: application to the Illgraben debris-flow channel, Earth Surf. Process. Landforms, 36, 1847–1859, 2011.

Settele, J.; Scholes, R.; Betts, R.A.; Bunn, S.; Leadley, P.; Nepstad, D.; Overpeck, J.T.; Taboada, M.A.; Adrian, R.; Allen, C.; Anderegg, W.; Bellard, C.; Brando, P.; Chini, L.P.; Courchamp, F.; Foden, W.; Gerten, D.; Goetz, S.; Golding, N.; Gonzalez, P.; Hawkins, E.; Hickler, T.; Hurtt, G.; Koven, C.; Lawler, J.; Lischke, H.; Mace, G.M.; McGeoch, M.; Parmesan, C.; Pearson, R.; Rodriguez-Labajos, B.; Rondinini, C.; Shaw, R.; Sitch, S.; Tockner, K.; Visconti, P.; Winter, M.,:Terrestrial and Inland Water Systems. In: Field, C.B.; Barros, V.R.; Dokken, D.J.; Mach, K.J.; Mastrandrea, M.D.; Bilir, T.E.; Chatterjee, M.; Ebi, K.L.; Estrada, Y.O.; Genova, R.C.; Girma, B.; Kissel, E.S.; Levy, A.N.; MacCracken, S.; Mastrandrea, P.R.; White, L.L. (eds) Climate Change 2014: Impacts, Adaptation, and Vulnerability. Part A: Global and Sectoral Aspects. Working Group II Contribution to the Fifth Assessment Report of the Intergovernmental Panel on Climate Change. Cambridge, New York,, Cambridge University Press. 271-359, 2014.

Shortridge, A. M. and Goodchild, M. F.: Communicating uncertainty for global data sets., in: Spatial data quality, Shi, W., Fisher, P. F., and Goodchild, M. F. (Eds.), Taylor & Francis, London, New York, 2002.

Smith, S. L., Romanovsky, V. E., Lewkowicz, A. G., Burn, C. R., Allard, M., Clow, G. D., Yoshikawa, K., and Throop, J.: Thermal state of permafrost in North America: a contribution to the international polar year, Permafrost Periglacial Processes., 21, 117–135, 2010.

Springman, S. M., Arenson, L. U., Yamamoto, Y., Mayer, H., Kos, A., Buchli, T., and Derungs, G.: Multidisciplinary investigations on three rockglaciers in the Swiss alps: Legacies and future perspectives, Geografiska Annaler: Series A, Physical Geography, 94, 215–243, 2012.

Springman, S. M., Yamamoto, Y., Buchli, T., Hertrich, M., Maurer, H., Merz, K., Gärtner-Roer, I., and Seward, L.: Rock Glacier Degradation and Instabilities in the European Alps: A Characterisation and Monitoring Experiment in the Turtmanntal, CH, in: Landslide Science and Practice, Margottini, C., Canuti, P., and Sassa, K. (Eds.), Springer Berlin Heidelberg, Berlin, Heidelberg, 5–13, 2013.

Staub, B.: The evolution of mountain permafrost in the context of climatic changes – towards a comprehensive analysis of permafrost monitoring data from the Swiss Alps, Dissertation, University of Fribourg, Fribourg, 2015.

Storck, P., Bowling, L., Wetherbee, P., and Lettenmaier, D. P.: Application of a GIS-based distributed hydrology model for prediction of forest harvest effects on peak stream flow in the Pacific Northwest, Hydrological Processes, 12, 889–904, 1998.

Strozzi, T., Werner, C., Wiesmann, A., and Wegmuller, U.: Topography Mapping With a Portable Real-Aperture Radar Interferometer, IEEE Geosci. Remote Sensing Lett., 9, 277–281, 2012.

Tarolli, P., Arrowsmith, J. R., and Vivoni, E.: Understanding Earth surface processes from remotely sensed digital terrain models, Geomorphology, 113, Editorial, 2009.

Tarolli, P. and Dalla Fontana, G.: Hillslope-to-valley transition morphology: New opportunities from high resolution DTMs: Understanding earth surface processes from remotely sensed digital terrain models, Geomorphology, 113, 47–56, 2009.

Thapa, K. and Bossler, J.: Accuracy of spatial data used in geographic information systems, Photogrammetric Engineering & Remote Sensing, 56, 835–841, 1992.

UNCED. Agenda 21. Program of action for sustainable development ; Rio Declaration on Environment and Development ; Statement of Forest Principles. The final text of agreements negotiated by governments at the United Nations Conference on Environment and Development (UNCED), Rio de Janeiro, Brazil. United Nations Dept. of Public Information, New York, NY, 1993.

Vonder Mühll, D., Noetzli, J., and Roer, I.: PERMOS – a comprehensive monitoring network of mountain permafrost in the Swiss Alps., in: Proceedings of the 9th International Conference on Permafrost, University of Alaska, Fairbanks, Alaska, June 29 - July 3, 2008, Kane, D. L., and Hinkel, K. M. (Eds.), Institute of Northern Engineering, University of Alaska, Fairbanks, Fairbanks, Alaska, 2008.

Vosselman, G. and Maas, H.-G.: Airborne and terrestrial laser scanning, Whittles Publishing, Dunbeath, 2010.

Wagner, S.: Creep of alpine permafrost, investigated on the murtel rock glacier, Permafrost Periglacial Processes., 3, 157–162, 1992.

Wahrhaftig, C. and Cox, A.: Rock Glaciers in the Alaska Range, Geological Society of America Bulletin, 70, 383, doi:10.1130/0016-7606(1959)70[383:RGITAR]2.0.CO;2, 1959.

Wainwright, J.: Environmental modelling: Finding simplicity in complexity, 2nd ed., Wiley-Blackwell, Chichester, 2013.

Weber, S., Hasler, A., Failletaz, J., Beutel, J.: Inter- and intra-annual fracture dynamics in steep fractured bedrock permafrost at Matterhorn, The Cryosphere, 2016 (in prep).

Wechsler, S. P.: Uncertainties associated with digital elevation models for hydrologic applications: A review, Hydrol. Earth Syst. Sci., 11, 1481–1500, 2007.

Westoby, M. J., Brasington, J., Glasser, N. F., Hambrey, M. J., and Reynolds, J. M.: 'Structure-from-Motion' photogrammetry: A low-cost, effective tool for geoscience applications, Geomorphology, 179, 300–314, 2012.

Whalley, W. B. and Martin, H. E.: Rock glaciers: II models and mechanisms, Progress in Physical Geography, 16, 127–186, 1992.

Whalley, W. and Azizi, F.: Rheological models of active rock glaciers -Evaluation, Critique and a possible test, Permafrost and Periglacial Processes, 5, 37–51, 1994.

Wirz, V., Geertsema, M., Gruber, S., and Purves, R.: Temporal variability of diverse mountain permafrost slope movements derived from multi-year daily GPS data, Mattertal, Switzerland, Landslides, 1–17, 2015a.

Wirz, V., Gruber, S., Purves, R. S., Beutel, J., Gärtner-Roer, I., Gubler, S., and Vieli, A.: Short-term velocity variations of three rock glaciers and their relationship with meteorological conditions, Earth Surf. Dynam., 4, 103-123, 2016.

Wise, S.: Assessing the quality for hydrological applications of digital elevation models derived from contours, Hydrological Processes, 14, 1909–1929, 2000.

PART II – Peer-reviewed publications

7   Publication I

Müller, J., Gärtner-Roer, I., Thee, P., Ginzler, C., 2014. Accuracy assessment of airborne photogrammetrically derived high-resolution digital elevation models in a high mountain environment. ISPRS Journal of Photogrammetry and Remote Sensing 98, 58–69.

The authors' contribution to the article:

J. Müller collected and processed the data, developed the methodology, designed the study, performed the analysis and wrote the manuscript. I. Gärtner-Roer designed the study and collected reference data. P. Thee processed the data. C. Ginzler designed the study and developed the methodology.

Abstract

High-resolution digital elevation models (DEMs) generated by airborne remote sensing are frequently used to analyze landform structures (monotemporal) and geomorphological processes (multi-temporal) in remote areas or areas of extreme terrain. In order to assess and quantify such structures and processes it is necessary to know the absolute accuracy of the available DEMs.   This study assesses the absolute vertical accuracy of DEMs generated by the High Resolution Stereo Camera – Airborne (HRSC-A), the Leica Airborne Digital Sensors 40/80 (ADS40 and ADS80) and the analogue camera system RC30. The study area is located in the Turtmann valley, Valais, Switzerland, a glacially and periglacially formed hanging valley stretching from 2400 m to 3300 m a.s.l. The photogrammetrically derived DEMs are evaluated against geodetic field measurements and an airborne laser scan (ALS). Traditional and robust global and local accuracy measurements are used to describe the vertical quality of the DEMs, which show a non Gaussian distribution of errors. The results show that all four sensor systems produce DEMs with similarly accuracy despite their different setups and generations. The ADS40 and ADS80 (both with a ground sampling distance of 0.50 m) generate the most accurate DEMs in complex high mountain areas with a RMSE of 0.8 m and NMAD of 0.6 m They also show the highest accuracy relating to flying height (0.14‰). The pushbroom scanning system HRSC-A produces a RMSE of 1.03 m and a NMAD of 0.83 m (0.21‰ accuracy of the flying height and 10 times the ground sampling distance). The analogue camera system RC30 produces DEMs with a vertical accuracy of 1.30 m RMSE and 0.83 m NMAD (0.17‰ accuracy of the flying height and two times the ground sampling distance). It is also shown that the performance of the DEMs strongly depends on the inclination of the terrain. The RMSE of areas up to an inclination <40° is better than 1 m. In more inclined areas the error and outlier occurrence increase for all DEMs. This study shows the level of detail to which airborne stereoscopically derived DEMs can reliably be used in high mountain environments. All four sensor systems perform similarly in flat terrain.

7.1 Introduction

High mountain environments have been identified by the Intergovernmental Panel on Climate Change (IPCC) as highly sensitive to climate change (Parry, 2007). Thus, these systems should be carefully monitored in order to observe environmental variability, quantify changes, assess natural hazards and understand mass-transport systems (Kääb, 2002). In particular, the IPCC has recognized glacial and periglacial systems as priority climate indicators and therefore, these indicators have received increasing attention from the scientific community (Houghton et al., 2001).

Remote sensing is particularly well suited for repeated and rapid observation in remote and inaccessible areas of high mountains. Mono- and multi-temporal digital elevation models derived from various remote sensing systems are repeatedly used to analyze land surface features and processes (e.g. Debella-Gilo and Kääb, 2012, Gruen, 2002, Kääb et al., 1997 and Tarolli et al., 2009), numerical and hydrological modeling (e.g. Oppikofer et al., 2011, Storck et al., 1998), topographic and radiometric correction of remote sensing imagery (e.g. Goyal et al., 1998) and the assessment of multiple terrain and geophysical parameters (e.g. Maune, 2007, Li et al., 2005).

Typically, two sensor systems are used to generate high resolution DEMs in mountain areas: stereophotogrammetrical sensors that acquire optical stereoscopic imagery (Lane, 2000) and LiDAR (Light Detection and Ranging) systems, active opto-mechanical sensing systems that generate three dimensional information based on the run time of a light signal between the sensor and the surface (Vosselman and Maas, 2010). In addition to inaccuracies resulting from system configuration and flight postprocessing, DEM acquisition in high mountain environments faces numerous challenges due to the complexity of the terrain topography, which results in illumination effects such as shading, and in areas with spectrally homogenous areas, in low texture in the imagery (Kääb, 2000). Airborne and terrestrial laserscanning has become frequently used in numerous applications in high mountain areas (e.g. Fischer et al., 2011, Abermann et al., 2010) but stereophotogrammetric products remain the most cost efficient method to acquire high resolution elevation data over large areas (Bühler et al., 2012). Nevertheless, for mono- and multi-temporal application of DEMs such as sediment transport, mass balances, morphometry and geomorphodynamics it is crucial to consider the accuracy of remotely sensed digital elevation models because their applicability and interpretability depend strongly on their accuracy (Abermann et al., 2010, Piezconka et al., 2011, Tarolli et al., 2009). Many multi-temporal DEM applications use several sensor systems of different age and with different technical setups (e.g. Kääb et al., 1997, Roer and

Nyenhuis, 2007), but the sensors' accuracy can distort the quantification of changes in process rates and mass transport. Especially for the assessment of environmental processes that are spatially diverse and act on longer timescales it is often the case that different sensor systems are applied and combined for long-term analysis. In these cases the different properties of the sensor systems and their products have to be considered. An assessment of the performance and compatibility of different modern and historical sensor systems and datasets is necessary in order to ensure that these important sources of information can be safely combined and applied.

Therefore, this study evaluates the vertical accuracy of DEMs derived from four different stereoscopic aerial camera systems (HRSC-A, RC30, ADS40 and ADS80) in a high alpine environment. The RC30 is an analogue stereoscopic sensor system, whereas the three other systems are stereoscopic digital pushbroom scanners of different generations and instrumentation. The evaluation includes the assessment of the performance of the digital elevation models and shows the advantages and disadvantages of different types and generations of photogrammetric sensors.

Several global and local accuracy measures are used to evaluate the performance of the sensor systems. The absolute accuracy is estimated by using elevation data of superior quality acquired by an airborne laser scan (ALS) and terrestrial geodetic measurements. Global quality measures describe the entire area of interest using only a few parameters, but local describe the quality of a DEM at a higher level of detail and should be incorporated into DEM application (Papasaika and Baltsavias, 2010). Both approaches, global and local, will be applied and discussed in this study.

7.2   Test Site

The accuracy assessment is conducted in a 12.2 km² area located around the *Hungerlitaelli*, a glacial and periglacially formed hanging valley of the Turtmann valley in the Canton Valais (southwestern Switzerland) (see Fig. 11). The area stretches from 2400m a.s.l. to 3278m a.s.l and is characterized by steep rockwalls, talus cones, a glacier, several moraines of different ages and multiple active and inactive rockglaciers. The geomorphic setting has been investigated previously in Nyenhuis et al. (2005), Rasemann (2003) and Roer (2005). The permafrost features are part of the PERmafrost MOnitoring Switzerland Network (PERMOS) and undergo regular kinematic and temperature monitoring (Vonder Mühll et al., 2008). The research area displays a typical high alpine environment including complex topography, sudden changes in terrain, steep slopes, rockwalls and glacial ice. Additionally, several

downhill creeping permafrost features, frozen talus cones and rockglaciers have been identified in the research area. Their dynamic behavior influences the methods of the accuracy assessment and must therefore be addressed.
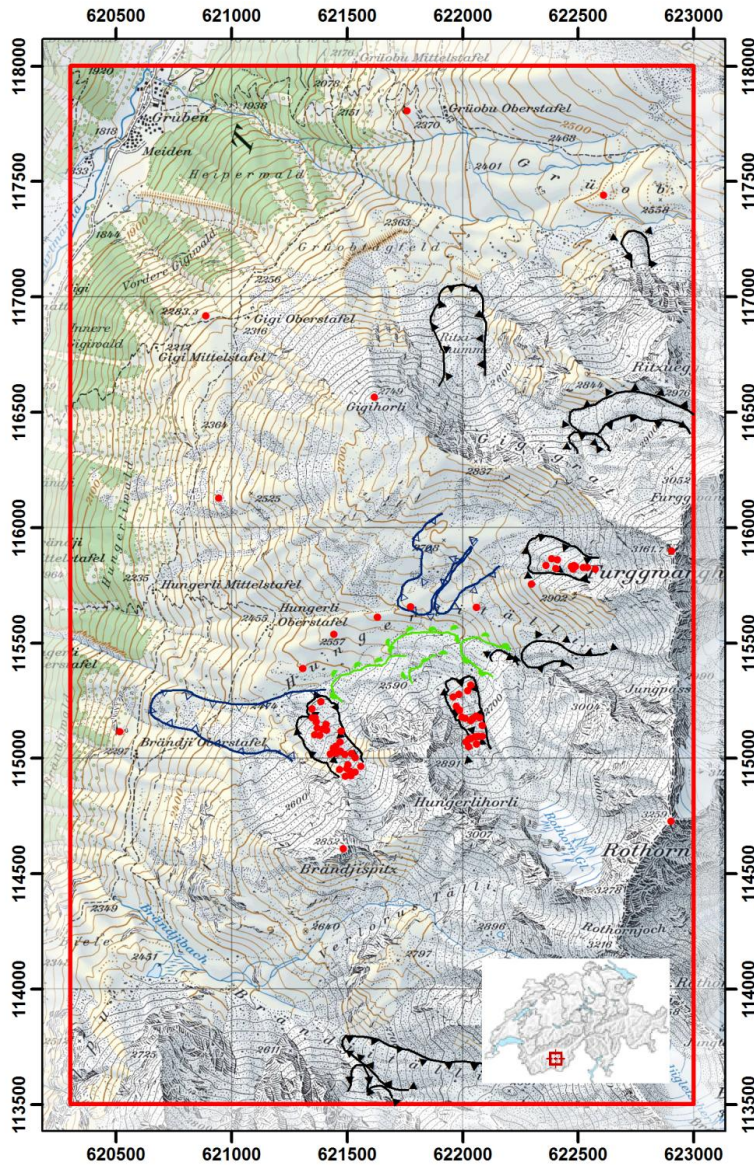

Figure 11: The research area including active (black signature), inactive (green signature) and relict (blue signature) rockglaciers. The red points mark the geodetic measurements on the rockglaciers and the SWISSTOPO control points (swisstopo - Bundesamtes für Landestopografie, 2012), both used as reference.

7.3   Datasets & Accuracy Measures

Photogrammetric sensor systems acquired imagery in 2001 (HRSC-A), 2005 (RC30), 2008 (ADS40) and 2010 (ADS80) that was used to generate digital elevation models. In addition, an airborne laserscan (ALS) was acquired in 2007 and serves as a reference dataset. The technical details of the tested sensor systems are summarized in table 1. Repeated geodetic measurements of high accuracy (1–2 cm) were provided by the DFG bundle project SPCC (Sensitivity of Mountain Permafrost to Climate Change) in order to verify the digital elevation information.

7.3.1   Test Data

High Resolution Stereo Camera - Airborne (HRSC-A)

The HRSC-A sensor is a further developed airborne version of the HRSC, which was designed by the German Aerospace Center (DLR) to explore the planet Mars within the international mars mission Mars96 (Albertz et al., 1992) and one of the first commercially available digital pushbroom scanning systems. The HRSC-A sensor is a multi-line pushbroom scanning instrument with 9 CCD line detectors mounted parallel on the focal plane of the camera. Image information is acquired by five panchromatic bands covering the spectrum from green to red under different observation angles and four color bands (blue, green, red and near infrared). In addition to its objective, to gather multispectral imagery of planetary surfaces, the HRSC-A is designed to acquire the data needed to produce digital elevation models. The sensor is able to produce imagery with a very high geometrical resolution of 10 cm as the smallest ground sampling distance (GSD) and is very well suited for the automatic generation of high resolution digital elevation models.

A flight campaign covering the entire Turtmann valley was successfully completed in September 2001 resulting in 13 overlapping stereoscopic parallel tracks, which led to a digital surface model covering the entire valley (Otto et al., 2007). The imagery was acquired with a radiometric resolution of 10 bit at a flying height of 6000 m and a ground sampling distance of 0.1 m.

RC30

The Leica RC30 is an analogue camera system that has been used from 1998 to 2005 to produce the nationwide coverage of true color orthophotos in Switzerland (Simmen and Bovet, 2007). The permafrost monitoring system Switzerland (PERMOS) acquired special RC

30 imagery in order to derive multi-temporal high resolution DEMs of several permafrost sites in the Swiss Alps (Vonder Mühll et al., 2008). The accuracy assessment of the RC 30 gives insight into the performance of analogue matrix camera systems of similar design (such as the Wild/Leica RC10 and RC20). These camera systems have also been used repeatedly to generate DEMs for research applications (Neill, 1994, Turker and Cetinkaya, 2005, Valta-Hulkkonen et al., 2004) but their accuracy has not been thoroughly tested in high mountain environments.

The sensor produces single pictures of 23 x 23 cm format that were digitized by a photogrammetric scanner with a radiometric resolution of 24 bit (8 bit per channel) and then processed in a photogrammetric workstation, where image orientation, triangulation, orthorectification and the generation of digital elevation products were completed (Kasser and Egels, 2002, Roer et al. 2005a). The 1 m DEM was generated specifically for this study. The RGB images were acquired with a 75 % overlap, so they are suitable for stereoscopic assessment and resemble a GSD of 0.4 m. The aerial photos used in this study were acquired on the 17th of August 2005 with an aperture of f/4.0 and an exposure time of 1/550.

ADS40\80

The Airborne Digital Sensor 40 (ADS40-SH2) and the ADS80 are part of the first commercially available digital large format airborne survey systems introduced in 2001 (Fricker and Rohrbach, 2005). Further improvements in the system setup and recording technology led to the third generation ADS80, which is currently used by the Swiss Federal Office of Topography swisstopo (Sandau, 2005). The ADS systems' basic design is the three-line-scanner principle, whereby linear arrays on the focal plane capture imagery looking forwards, downwards (nadir) and backwards from the aircraft (see Fig. 12). The ground surface is imaged multiple times within one flightline. The ADS sensor systems capture coregistered RGBN and panchromatic imagery (Sandau, 2005). Both sensor systems capture imagery by a total of 12 CCD lines of which four collect panchromatic information and the remaining eight red, green, and blue and near infrared data. Each line consists of 12000 CCD with a size of 6.5 µm x 6.5 µm. The multispectral imagery is stereoscopic and can be used for image matching and the extraction of 3D information. The imagery acquisition and the aerial triangulation were carried out by the Swiss Federal Office of Topography (swisstopo - Bundesamtes für Landestopografie, 2012). The data were delivered after triangulation in level1 format including orientation data and camera calibration.

The data used in this study were generated by an ADS40 of the second generation equipped

with a SH52 sensor head and the data in 2010 were acquired with the ADS80 camera system. Both flights were undertaken at a flying height of 7500 m with a GSD of 0.5 m. A radiometric resolution of 12 bit DEMs was generated in all possible channel combinations and the most accurate chosen for the accuracy assessment.
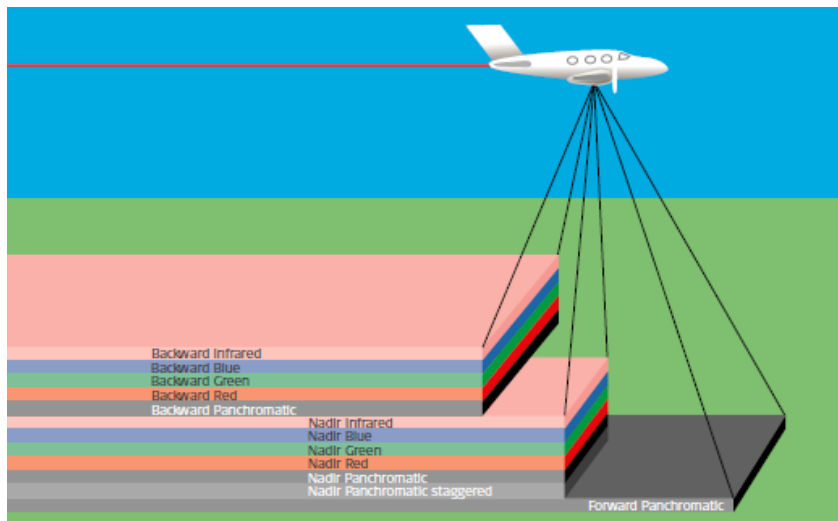

Figure 12: Three line scanner system of the ADS40 and ADS80 (Leica Geosystems AG, 2008a).

7.3.2 Reference Data

Airborne Laserscanning

Swisstopo in May 2007 acquired an Airborne LaserScan (ALS) that covered the research area, resulting in a digital surface model and a digital terrain model (swisstopo - Bundesamtes für Landestopografie, 2005 and swisstopo - Bundesamtes für Landestopografie, 2007). The ALS campaign was originally designed to generate a nationwide digital surface model (DSM) and digital terrain model (DTM) for areas in Switzerland below 2000 m a.s.l. but the entire catchment of the Turtmann valley was also covered. The flight campaigns were executed in 2007 by the TopoSys GmbH located in Biberach/Germany, which used the pulse system TopoSys Falcon II flying at 1200 m above ground to create the digital elevation data with an approximate point density of 1pt/ m^2 (Artuso et al., 2003, swisstopo - Bundesamtes für Landestopografie, 2007). For the approach presented in this study, the digital surface model as well as the digital terrain model can be used as reference data because the assessment

focuses on high mountain areas without any tall vegetation or artificial structures. The pointclouds of the DSM and DTM were used in their original, spatially heterogeneously distributed state and only corrected for outliers. No interpolation of points was conducted.

Terrestrial Geodetic Survey

Geodetic surveys with a total station (Leica TCL 1202) were undertaken each year of the aerial surveys within a six week time window in late summer and serve as reference points. The geodetic surveys with a total station allow high accuracy measurements (about 1 cm in horizontal coordinates and 2 cm in elevation), even in extreme areas such as very steep slopes and rock walls (Delaloye et al., 2010, Roer, 2003). The point measurements were originally located to monitor the kinematics of rockglaciers (see Fig. 11). Therefore, most of the points are located on the rockglacier surfaces and not equally distributed in the research area as suggested by Höhle and Höhle (2009). The number of reference points ranges from 42 to 84 due to varying field campaigns. Additional control points supplied by swisstopo were added to the reference dataset (swisstopo - Bundesamtes für Landestopografie, 2012).

Table 7: Technical details of the photogrammetric sensor systems (test data).

Sensor System		HRSC-A	RC30	ADS40-SH52	ADS80-SH82
Sensor type		CCD-line digital aerial scanner	Analogue stereo camera system	CCD-line digital aerial scanner	CCD-line digital aerial scanner
Acquisition date		28.09.2001	17.08.2005	29.08.2008	22.08.2010
Number of CCD lines		9		12	12
Numbers of sensors per line		5184		12000	12000
CCD size (µm)		7		6.5	6.5
Radiometric resolution		10 bit	24 bit (8 bit per channel)	8 bit	12 bit
Stereo viewing angle (°)	Backward	±18.9 for PAN		-16 for RGBN, -14 for PAN	-16 for RGBN, -14 for PAN
	Nadir	0 for PAN	Range from 27 to -14 at a 75% overlap of images	0 for RGBN +27 PAN	0 for RGBN +2 for PAN +27 PAN
	Forward	±12.8 for PAN			
Multispectral viewing Angle (°)		15.9 (R) 3.3(B) -3.3(G) -15.9 (NIR)		See Fig.12	
Ground sampling distance (GSD in m)		~ 0.1	~ 0.4	~ 0.5	~ 0.5
Altitude (m)		6000	6327	7500	7500
Spectral Range (nm)	Pan	585-765	RGB sensitive Film (400-670 nm)	465-680	465-676
	Red	730-770		608-662	604-664
	Green	485-575		533-587	533-587
	Blue	395-485		428-492	420-492
	Near Infrared	925-1015		833-887	833-920
Field of View (°)		±11.8	80 (angular field covered)	64	64

7.3.3   DEM Generation and Co-registration

The RC30, ADS40 and ADS80 data were processed especially for this study whereas the HRSC data were generated and processed at the DLR (German Aerospace Center). The HRSC data processing at DLR included the combined determination of position and attitude, geometric correction of the image data, image matching, digital surface model generation, orthoimage generation and mosaicing (Albertz et al., 1992, Hauber et al., 2000, Otto et al., 2007, Scholten and Wewel, 2000, Wewel et al., 1998). The end product was an orthophoto covering the whole valley and a digital surface model with a spatial resolution of one meter were delivered. The generation of the digital elevation models from the RC30 and ADS40/80 imagery was conducted using the NGATE (Next Generation Automatic Terrain Extraction) application of the commercial digital photogrammetric workstation SocetSet© 5.6 (BAE Systems). As stated in Zhang et al. (2006), the special feature of NGATE is that matching is performed for every pixel and uses area-matching and edge-matching algorithms in order to identify matching points. Additionally, NGATE is capable of multi-image matching, whereby the optimal stereo pair is selected for each area, based on the characteristics of the area's terrain and the overall geometry of the sensor positions and orientations (DeVenecia et al., 2007). Since NGATE computes an elevation for every pixel, the spacing is used to resample the internal NGATE DEM to the desired density. In addition to the vertical value, NGATE calculates the so called Figures Of Merit (FOM) for every pixel that serves as a measure of the image matching quality. Within this study, only successfully matched data points were considered and interpolated data points were neglected. NGATE offers different matching strategies optimized for certain topographies or landcover characteristics. The strategy for steep terrain and urban areas were combined by means of their figure of merit. The urban strategy was chosen because it is optimized for sudden changes and linear features in the imagery in the terrain that are common in complex high mountain topography.

Co-registration

In order to minimize the vertical error caused by a horizontal and vertical offset between the reference digital elevation model and the test dataset, the photogrammetrically derived DEMs were co-registered according to Nuth and Kääb (2011) using the ALS as the master. This method is especially designed for the co-registration of DEMs in highly dynamic areas such as glacial landscapes and has been used for similar approaches in high alpine environments (Joerg et al., 2012). It uses the unique differences in a raster cell elevation divided by the tangent of the local slope and plotted against the local aspect. This resulted in

scattered data, to which a cosine function was fitted by a least squares curve fit to derive the parameters' magnitude and direction of the horizontal shift. The method is also used to detect and correct vertical and altitude dependent bias. All four datasets show a systematic horizontal offset (see Fig. 13), which is corrected by the co-registration approach.
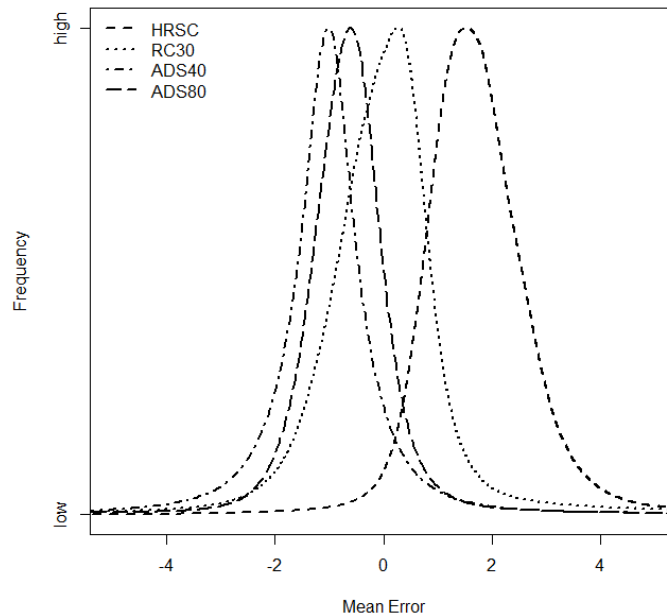

Figure 13: RMSE of the DEMs depending on slope. The grey bars show the frequency of sample points at any given slope (y-axis on the right). The values on the x-axis are in degree (°).

The co-registration assessment for the ADS40/80 and RC30 products showed a negligible offset of <0.25 m, which is less than the actual ground sampling distance of the imagery. The HRSC-A data, however, was shifted by 1.3 m in 294.4° direction. All datasets were corrected according to the co-registration results.

7.4   Accuracy Assessment

The commonly used accuracy assessment regarding height information calculates the difference in z-value Δh_i between the digital elevation data and the reference data. We used the terrestrial geodetic measurements and the ALS in two different approaches as reference data to which the photogrammetric digital elevation information is compared. Joerg et al. (2012), Kraus et al. (2006) and Mills et al. (2006) show that the ALS data is of very high accuracy, also in complex terrain and can therefore be used to assess the accuracy of a photogrammetrically derived DEM in two ways: the spatially extensive ALS dataset can be

used to conduct thorough statistical analyses of the Δh_i values and the according spatial variation of the accuracy can also be assessed.

In order to minimize the uncertainty introduced by interpolation algorithms during the generation of gridded data from the RC30, ADS40 and ADS80 data, only the raw data points of the photogrammetric processing that have been confidently matched between the image pairs (as identified by their figure of merit) are used for the accuracy assessment. A similar approach was conducted for the HRSC-A data where only those data points were considered in the accuracy assessment that were identified in all available stereopairs (Hauber et al 2000). Also, the actual ALS point cloud and not an interpolated grid is used for the further assessment. The vertical accuracy of the DEMs is determined by identifying the nearest reference data point to any given photogrammetrically derived data point in a three dimensional space (smallest XYZ distance) and then calculating the height difference. The entirety of differences can then be described statistically and the appropriate statistical measures used to describe the accuracy.

The temporal offset between the test and the reference data should be as small as possible to make sure that the area of interest is sampled under most similar circumstances. The geodetic measurements were acquired within a six week period around the flight surveys. Since the ALS was generated in 2007 and the photogrammetric products with a respective offset of several years, the dynamic surface features (glaciers, creeping permafrost) have to be excluded within the accuracy assessment. Hence, the respective areas are masked out from the digital elevation models.

It has to be considered that the analysis is performed in an area that is characterized by steep slopes and sudden changes in terrain. Therefore, short horizontal offsets can lead to great differences in elevation, which might lead to incorrect Δh_i estimates. To minimize this source of error, Kraus et al. (2006) suggest considering only reference points within a certain horizontal distance We adopted this approach, not only focusing on the horizontal distance of the reference data but selecting the three-dimensionally closest reference point to the test data points. The nearest point of the reference data was only considered when it was within a distance of 0.5 m.

If a normal distribution of the errors is assumed and there are no outliers present or have been removed, the following accuracy measures are usually used to describe the DEM globally (Höhle and Höhle, 2009):

Root Mean Square Error: $RMSE = \sqrt{(1/n \sum_{i=1}^{n} \Delta h_i^2)}$

Mean Error: $ME = 1/n \sum_{i=1}^{n} \Delta h_i$

Absolute Mean Error: $AME = 1/n \sum_{i=1}^{n} |\Delta h_i|$

Standard Deviation: $SD = \sqrt{(1/(n-1) \sum_{i=1}^{n} (\Delta h_i - ME)^2)}$

Where Δh_i is the difference between the dataset of interest and the reference data, n is the number of samples and ME the mean error.

The accuracy of a DEM is usually described by only one global accuracy parameter for the entire dataset. Kraus et al. (2006) state that using one single parameter to address an entire dataset is insufficient because errors might correlate significantly with different types of surface characteristics (e.g. flat, hilly or mountainous areas). Therefore, the authors claim that the spatial distribution of the error has to be taken into account when describing geospatial datasets (Höhle and Höhle, 2009, Karel et al., 2006, Kraus et al., 2006, Thapa and Bossler, 1992).

Höhle and Höhle (2009) claim that the previous assumption of a Gaussian distribution of Δh_i with few outliers is not valid for numerous DEM; thus, accuracy measures have to take into account that outliers may exist and that the distribution of errors might not be normal. They introduce the measure of the absolute mean error (AME) as the DEM evaluation is interested in the direction of the errors but especially in their magnitude. One approach to deal with outliers is to remove them by applying a threshold. Höhle and Potockova (2006) select a threshold for eliminating outliers of three times the RMSE. The RMSE value is calculated from an initial assessment of the Δh_i data. This approach classifies a Δh_i value as an outlier if $|\Delta h_i|$ (Maune, 2007). Despite these methods not all of the outliers can be identified and the accuracy measures might therefore be flawed. In order to minimize the influence of outliers, Höhle and Höhle (2009) introduce robust statistical methods (methods that are less influenced by outliers) to assess the accuracy of DEMs. If the data reveal non-Gaussian distribution the authors propose the following measures to describe the properties of the dataset:

Table 8: Robust accuracy measures for DEMs as proposed by Höhle and Höhle (2009).

Accuracy measure	Notional expression
Median (50% quantile)	$Q_{\Delta h}\,(0,5)= m_{\Delta h}$
Normalized median absolute deviation	$NMAD=1,4826*median_j\,(\,|\,h_i - m_{\Delta h}\,|\,)$
68.3% quantile	$Q_{|\Delta h|}\,(0,683)$
95% quantile	$Q_{|\Delta h|}\,(0,95)$

The quantiles state that a certain percentage of the absolute errors (68,3% and 95%) is found in a certain range of values. The normalized median absolute deviation (NMAD) is proportional to the median of the absolute differences between errors and median error. It generates a value similar to the standard deviation but more resilient to outliers. The measures above help to describe and compare the properties of the accuracy of DEM datasets beyond the typical measures of accuracy assessment. In order to state traditional accuracy measures the 3*RMSE is applied but for the robust measures the entire dataset including the outliers is assessed.

7.5 Results

The ADS40 and ADS80 generate forward, nadir and backward looking channel combinations that are all suited for photogrammetric application but perform differently in complex terrain. Therefore, we used all available channel combinations of the ADS40 and ADS80 imagery (see table 7) to generate digital elevation information in order to identify by a first accuracy assessment the channel combination that generates the most accurate DEM. This DEM is then subjected to the more comprehensive accuracy analysis.

Table 9 shows the results of the rough first accuracy assessment of the channel combinations for the ADS40 and ADS80 sensor systems using the ALS as reference data. For this assessment the entire Δh_i dataset was analyzed without removing outlier or any other processing. In the case of the ADS40, the combination of nadir and backward looking CIR stereopairs shows the best performance, whereas for the ADS80 the nadir and backward CIR and panchromatic channels perform equally. The ADS40's nadir panchromatic information was unfortunately not available. This results in an angle of 43° between the panchromatic image lines and worsens the performance of the image matching algorithm. Nevertheless, is it safe to assume that it would have produced similar values as the CIR stereo imagery.

Table 9: Accuracy measures of the individual channel combinations of ADS40 and ADS80. CIR = Colored near Infrared, PAN = PANchromatic, RGB= Red Green Blue, B= Backward looking channel, N= Nadir looking channel, F= Frontward looking channel. The highest accuracies are highlighted.

Sensor System	Channel	AME (m)	RMSE (m)	SD (m)
ADS40	**CIR**	**0.97**	**1.3**	**1**
	PAN BF	1.3	1.87	1.53
	RGB	1	1.31	1.02
	CIR	**1.12**	**1.59**	**1.29**
ADS80	**PAN BN**	**0.96**	**1.47**	**1.26**
	PAN BNF	1.04	2.39	2.3
	PAN FN	1.16	2.46	1.75
	RGB	1.09	2.08	1.91

This first accuracy assessment shows which channel combination of the ADS40 and ADS80 is fitted best for automatic terrain extraction within the SocetSet NGATE software.

7.6   Error Distribution

Following the approach of Höhle and Höhle (2009), the extracted data is tested for normal distribution by comparing the observed and theoretical distribution of Δh_i before any other processing is applied. This is done by visually analyzing the histogram and the quantile-quantile-plot (Q-Q plot) of the error dataset. The histogram depicts the frequency of the errors within a certain predefined interval. It gives a first impression of the normality of the data distribution. In Fig. 14 the entirety of the Δh_i errors is depicted in 100 equally spaced intervals. Superimposed on the error histograms are the expected counts from a normal distribution with mean and variance from the Δh data (red line). Fig. 14 allows a comparison between the observed distribution of Δh_i and the expected theoretical normal distribution with mean and standard deviation estimated from the observed data. The Q-Q plots show the quantiles of the distribution of the error data plotted against the theoretical quantiles of their normal distribution. In the case of a normal distribution, the Q-Q plot should yield a straight line, which is depicted as the red line in the lower row in Fig. 14.
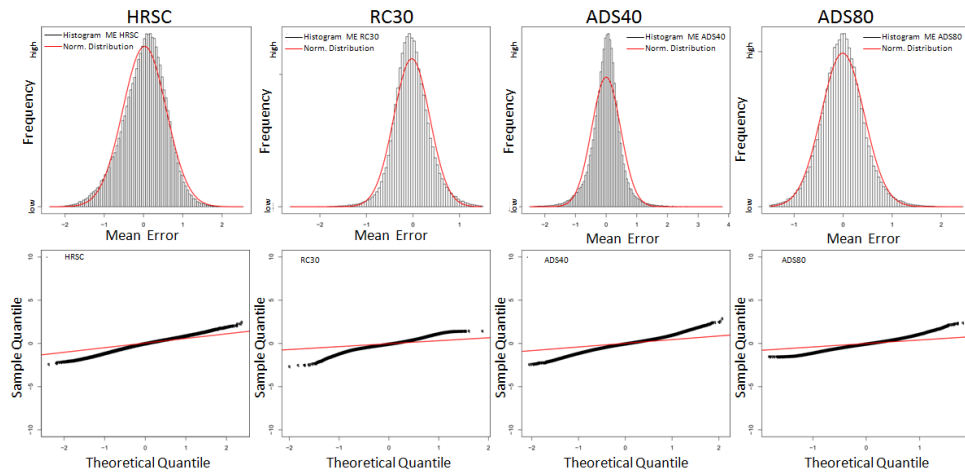
Figure 14: In the upper row the histograms show the Δhi errors in meters for the different test data sets. Superimposed on the histograms are the expected values from a normal distribution with mean and variance estimated from the actual error distribution. The histogram is truncated for better visualization. The bottom row shows the QQ plots for the distribution of Δhi. From left to right: HRSC-A, RC30, ADS40, ADS80.

Figure 14 shows that the *Δhi* distributions of all datasets are not distributed normally, which implies that additional robust measures are necessary to sufficiently describe the accuracy of the data (Höhle and Höhle 2009) and to prohibit the strong influence of outliers. Thus, the measures proposed in table 8 are applied to describe the accuracy of the DEMs and the results are shown in table 12. The Q-Q plots show that the majority of errors is normally distributed but the population depict heavy ends due to outliers.

7.6.1   Accuracy Assessment by Geodetic Measurements

The results of the comparison of the photogrammetrically derived digital elevation models and the ALS with the geodetic reference data are shown in table 5. The terrestrial geodetic measurements can not only be used to assess the accuracy of the photogrammetric data but also to check the performance of the airborne laserscan before this data is used as a reference for further spatial and statistical analysis.

The assessment is in agreement with Kraus et al. (2004) that the accuracy of the ALS is higher than the accuracy of the photogrammetric data. Therefore, it is reasonable to use the ALS as reference data to conduct the spatial analysis of the accuracy of the DEMs. Nevertheless, the low population of the GCPs does not allow statistically reliable conclusions about the entire dataset and their distribution is biased as they are not randomly located within the entire research area but are clustered on the rockglaciers (see Fig. 11). Therefore, the location of the

reference points only represents a northern exposure and does not depict the entire spectrum of possible slopes. With this approach it is not possible to check for normal or non normal distribution since the number of reference points is too small in respect to the test area.

Table 10: Accuracy assessment of the DEMs by means of geodetic reference data.

System	AME (m)	RMSE (m)	SD (m)	n	Outlier
ALS	0.51	0.62	0.59	48	2
HRSC-A	0.87	0.96	0.97	36	6
RC30	0.61	0.72	0.71	48	3
ADS40	0.59	0.75	0.53	46	4
ADS80	0.46	0.6	0.55	82	2

Table 10 shows that only a few data points have been identified as outliers and the geodetic data points are in similar numbers as in other studies that have used geodetic reference measurements (Hu et al., 2008, Hobi and Ginzler, 2012). RMSE values range from 0.6 to 0.96 m, where the newest and most technically advanced sensor system (ADS80) performs best. Even though the oldest digital camera system, the HRSC-A, acquired imagery at a 0.1 m ground sampling distance, it showed the worst performance, with a RMSE of 0.96 m and a standard deviation of 0.97 m.

7.6.2 Accuracy assessment by ALS

The accuracy assessment using the ALS as reference data allows not only the establishment of global quality parameters but also a locally discrete analysis. Approximately 5.1 million data points have been analyzed and the results of the global accuracy parameters are shown in table 11. The values show different results than the previous analysis based on the geodetic measurements. The comprehensive ALS analysis shows similar accuracies for all three sensor systems and a minimally more accurate performance of the ADS80. Also, the Q-Q plot analysis shows the most irregular distribution for the RC30 data and the highest number and values of outliers.

Table 11: "Traditional" accuracy measures of the ALS assessment.

System	AME (m)	RMSE (m)	SD (m)	n
HRSC-A	0.72	1	1	4231655
RC30	0.85	1.30	1.28	4159560
ADS40	0.69	1.05	1.05	4449695
ADS80	0.63	1.04	0.97	4359560

The robust accuracy measures reveal a similar result with similar accuracies, whereas the ADS40 and ADS80 show a slightly higher accuracy than the other systems. Especially the NMAD and the 68.3 percentile values show that the ADS40 and ADS80 generate more accurate data than the other systems. Still, the overall accuracies of the sensor systems are similar.

Table 12: Robust accuracy measures of the ALS assessment.

System	MED	NMAD	Quan683	Quan95
HRSC-A	-0.07	0.85	0.82	1.91
RC30	0.3	0.84	0.87	1.91
ADS40	0.01	0.65	0.72	2.1
ADS80	0.01	0.62	0.66	1.92

The local variance of the quality of vertical digital elevation information derived from photogrammetry can result from various sources: processing errors during flight and postprocessing, the complexity of the terrain and illumination effects (Kääb et al., 2005, Kasser and Egels, 2002). Inaccuracies arising from flight processing can unfortunately not be assessed by the data provided in this study. Extensive information about the IMU and the dGPS data during the flight surveys would be required to analyze their possible influence on the DEM. Terrain morphology (slope) has been identified as the most important influencing factor for DEM accuracy (Aguilar and Aguilar, 2007, Fisher and Tate, 2006). As stated earlier, this study's research area is characterized by highly complex terrain and therefore an evaluation of the DEMs needs to include an investigation of morphological surface characteristics. Therefore, the ALS reference data was used to calculate the slope at any given photogrammetrically derived test point in order to show the error dependency on slope.

Figure 15 shows the RMSE in dependency of slope in the research area. The underlying grey

bars present the number of data points at the particular slope and therefore the reliability of the accuracy parameter. The figure illustrates that all DEMs generate accurate data for slopes ranging from 10° to 45° inclination. In areas steeper than 45° the accuracy of the DEMs starts to decrease significantly. Especially in the very steep areas above 70° inclination the RMSE increases drastically. This is either due to the difficulties in photogrammetric image matching within steep areas or can result from the properties of the ALS reference data that also has problems gathering data from steep rock walls due to its steep viewing angle. Additionally, the low number of samples in steep areas diminishes the validity of the accuracy measures there. Figure 15 shows that the HRSC system produces more accurate data in steep terrain. The method presented here promotes the comparison of two nearest points where in steep areas even a small horizontal distance between the two points can result in very high vertical discrepancy. We tried to minimize this effect by choosing the nearest point within a 3D space instead of the only horizontally closest point. Additionally, we restrained the maximal distance to the next reference point to 0.5m.
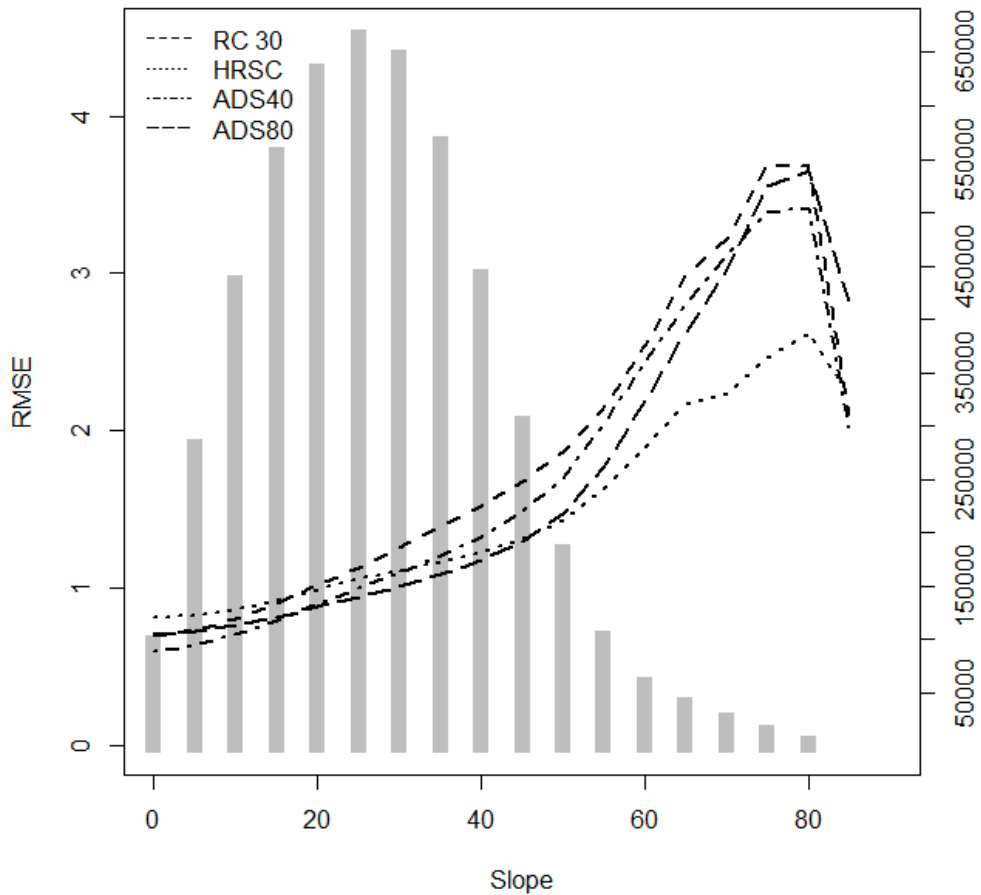
Figure 15: RMSE of the DEMs depending on slope. The grey bars show the frequency of sample points at any given slope (y-axis on the right). The values on the x-axis are in degree (°).

The stereo imagery was acquired at a very high solar zenith angle and the shaded areas coincide therefore with the steep areas assessed above. The shaded areas and areas of low texture result in the poor performance of matching algorithms of the stereo image analysis. Areas where the elevation information could not be extracted directly from the imagery and height values would have been interpolated, were not considered in the further analysis. They were removed by their figure of merit. The areas where there was no sufficient figure of merit and the reference data point was further away then 0.5m are depicted in Fig. 16. These areas are concentrated in shaded and steep areas of the study site.
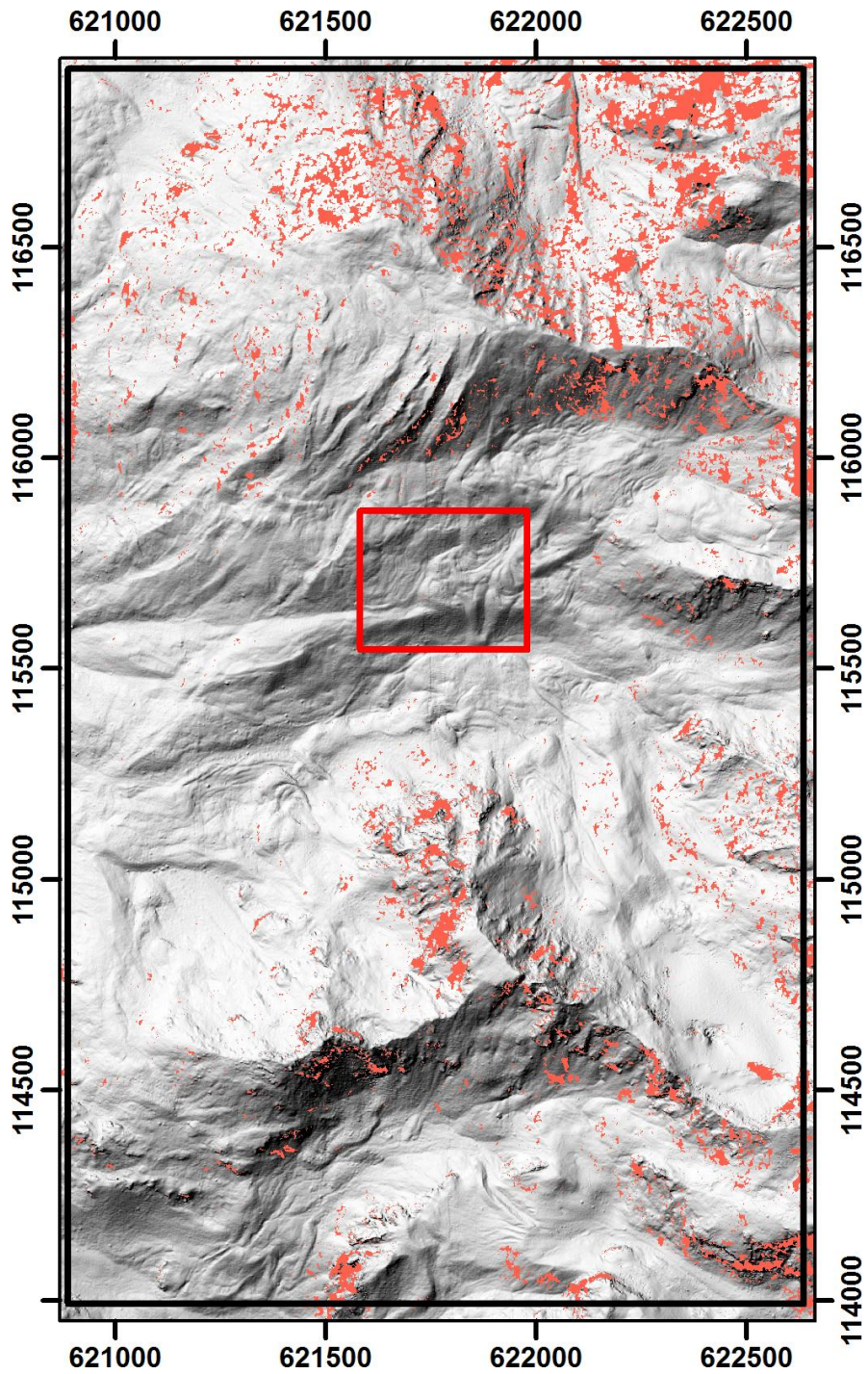
Figure 16: Shaded relief of the entire research area. The red areas mark the outliers and areas that have been excluded from the analysis due to unsuccessful image matching.
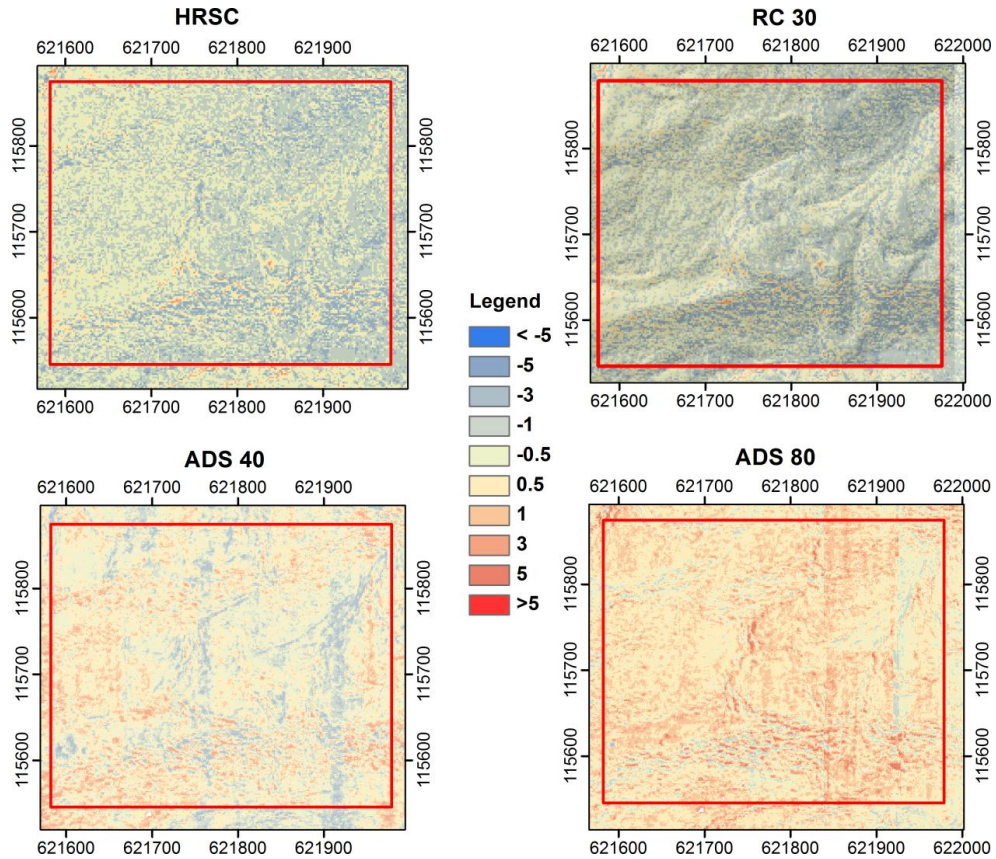
Figure 17: Local error distribution in a selected area (red square in Fig. 16). Upper left RC30, Upper Right HRSC-A, Lower Left ADS40, Lower Right ADS80.

The spatial distribution of Δh_i in a selected area is shown in Fig. 17 for each of the DEMs. The ADS40 and ADS80 show a rather heterogeneous spatial distribution of Δh_i, but, even after the co-registration, the RC30 and HRSC-A distribution exhibits a local aspect based bias that cannot be detected throughout the entire area. Since the co-registration did not correct for this, the only explanation can lie within the flight and data processing by the data provider. Linear artifacts are also visible in the ADS40 and ADS80 data that originate from the processing of the flight data and cannot be accounted for or corrected afterwards.

The global "traditional" and robust accuracy assessment of the DEMs as well as the spatial analysis show that all sensor systems perform quite similarly in complex high mountain terrain. The ADS40 and ADS80 provide better values for the traditional and robust accuracy measures but their 95 percentile is almost the same. Considering a GSD to accuracy ratio, the

RC30, ADS40 and ADS80 systems have an accuracy of approximately 2*GSD (if one considers the RMSE as the accuracy value (Casella et al. in 2008) whereas the HRSC with a GSD of 0.1m has a ratio of 10*GSD. In terms of the relationship between accuracy and flying height the HRSC and RC30 show similar results with 0.17‰ and 0.21‰, and the ADS40 and ADS80 both show an accuracy of 0.14‰ of the flying height. These results show that altogether ADS40 and ADS80 perform only slightly better than the RC30 and the HRSC, the results can be seen as generally very accurate in this kind of complex topography.

7.7 Discussion

Methodic Limitations

The terrestrial geodetic assessment within this study is only of limited validity to generate reliable information about accuracy of the DEMs in the entire research area because there is only a small population of control points and even this small number of data points is clustered in a small area. Nevertheless, the geodetic points can be used to serve as a first reference data for the assessment of the DEMs. For example the accuracy assessment by terrestrial geodetic measurements showed that the ALS has a higher accuracy than the photogrammetric products. Additionally, the geodetic assessment gives an estimate of what minimal accuracies can be expected. The comparison of the results from the geodetic (table 10) and the ALS accuracy assessment (table 11) illustrates that the approach based on the geodetic reference data produced significantly better accuracies for the tested DEMs than the assessment based on the ALS reference data. This is because the geodetic GCPs are all situated on rather flat and spectrally heterogeneous surfaces. The maximum slope value on the rock glaciers is 60°, which is still in the range where the photogrammetric products yield good accuracy measures. Nevertheless, the geodetic GCPs overestimate the global accuracy of the photogrammetric DEMs. Thus, further studies assessing the accuracy of DEMs by terrestrial point measurements have to make sure that the reference data is representatively distributed in the research area and that they are of sufficient number.

The accuracy assessment using ALS data as reference has been proven to serve as an sophisticated method to assess the performance of digital elevation models (Kraus et al., 2006). But due to the technical limitations of ALS systems, steep areas have inherent uncertainties that propagate into the accuracy assessment. Additionally, the matching algorithm of the stereophotogrammetric workstation also has difficulties performing in steep areas due to shading and imaging geometry. Therefore, the accuracy measures for steep areas are not as reliable.

Comparable studies

Three of the four sensor systems have previously been subject to accuracy assessments with different types of reference data in varying study areas. Table 13 shows a selection of studies where the vertical and horizontal accuracy of DEMs derived from the HRSC-A, ADS40 and ADS80 systems have been assessed.

Table 13: Selection and comparison of studies where the horizontal and vertical accuracy of the DEMs derived by the HRSC-A and ADS40 sensor have been assessed.

	Study	Horizontal Acc (in m)	Vertical Acc. (in m)
HRSC-A	Scholten and Wewel, 2000	0,15	0,20
	Hauber et al., 2000	0,18	0,20
	Hoffmann and Lehmann, 2001	0,15	0,20
ADS40	Casella et al., 2008	0,13 (RMSE)	0,22 (RMSE)
	Hu et al., 2008	0,80	0,90
	Mills et al., 2006	-	1,661 (RMSE)
			1,322 (St Dev)
ADS80	Bühler et al., 2012	-	0.82 (RMSE)
			2.12 (Quan95)
	Hobi and Ginzler, 2012	-	<1.2 (RMSE)

Scholten and Wewel (2000) noted a mean deviation of ± 0,15 m for planimetry and ± 0,20 m for height by using 156 dGPS checkpoints in a 1,5 x 6,0 km area near Bedburg (Germany) and the test field in Vaihingen/Enz (Germany). Both test sites are located in moderately hilly terrain but include buildings, which result in more complex surface characteristics.

Hauber et al. (2000) also tested the performance of the HRSC-A in a high mountain environment at the Sonnblick glacier in the Austrian Alps. They used the relationship between the GPS/INS measurements and the HRSC-A camera coordinate system (boresight offset) and ray intersection of identical points of adjacent image strips in order to estimate the relative and absolute accuracy of the data. They came up with a horizontal accuracy of ± 0,18 m and a vertical accuracy of ± 0,20 m. Another assessment of the HRSC-A accuracy was performed by Hoffmann and Lehmann, 2001. This study was able to define horizontal/vertical accuracy of ± 0,15 m / ± 0,20 m in the city area of Berlin (Germany).

Only Hauber et al. (2000) attempted to evaluate the performance of the HRSC-A in a high alpine environment but there, the authors used artificial reference data and no additional independent checkpoints. This study shows that the HRSC-A performs with a much lower accuracy (by a factor of 6) than previous studies have stated.

Casella et al. (2008) analyzed the ADS40 system on a test site in Pavia/Italy, using 306 dGPS GCPs to check the data. They came up with a RMSE of 0,13 m in planimetry and a RMSE of 0,22 m in height. However, they only discussed their results for an aerial survey flown at 2000m altitude in a rather flat area. The study states that the ADS40 is able to produce RMSE values of 0,65 x GSD in xy dimension and 1.1 x GSD in z dimension. If applied to this study, this would result in a horizontal RMSE of 0,32 m and 0,55 m of vertical RMSE.

Hu et al. (2008) tested the ADS40 system in China. The evaluation of the data was performed by GCPs and resulted in a RMSE of 0,80 m in xy-dimension and 0,90m in altitude for the 50 cm GSD dataset.

Mills et al. (2006) used the same method as presented here by evaluating the ADS40 data against an ALS. They came up with similar values of 1,66m RMSE and a standard deviation of 1,322 m in mountainous regions. Mills et al. (2006) also used ALS to verify the ADS40 data and came up with lower accuracies than this study for mountainous regions, even though their mountainous areas do not classify as high alpine regions. Hobi and Ginzler (2012) assessed the accuracy of the ADS80 at different landcover classes and hilly areas, resulting in an overall accuracy of 1.2 m, whereas the accuracy depended on the landcover type. Bühler et al. (2012) also compared the accuracy of ADS80 derived DEMs in a high alpine environment. Both studies used photogrammetric imagery with a GSD of 0.25 cm.

As shown above, only the studies of Bühler et al. (2012), Hobi and Ginzler (2012) and Mills et al. (2006) are comparable to the methods and results presented in this study because they used either ALS data or terrestrial checkpoints for their accuracy assessments. The results of these three studies present similar findings even though their reference data is not as extensive. Especially the findings of Bühler et al. (2012), who use a helicopter based laser scanning system which is very accurate in steep areas support the validity of the findings presented here.

Other image matching algorithms should be tested for high alpine conditions in the future. Semi global matching (Hirschmüller, 2005) is implemented in a wide range of commercial software packages and could improve the results in rough, steep terrain, although the desired high image overlap is often not given, especially from historical image campaigns.

7.8 Conclusions

Four digital elevation models derived from different high resolution airborne photogrammetric sensors systems (HRSC-A, RC30 ADS40 and ADS80) have been assessed with regard to their vertical accuracy using geodetic measurements and ALS as reference

data in a complex high mountain environment. Three of the four DEMs were specifically produced for this study using a commercial digital photogrammetric workstation (SocetSet 5.6, BAE Systems). For the multispectral pushbroom scanning systems, ADS40 and ADS80 nadir and backward looking (-16°) CIR and panchromatic imagery was identified to be suited best for automatic terrain extraction in high alpine areas, including shaded and ice covered surfaces. Furthermore, it was confirmed that sensor configurations with large discrepancies in the viewing angle between the stereo image pairs are not suited for application in complex high alpine terrain.

The accuracy assessment of the DEMs showed systematic errors as well as a non-normal distribution for all data sets. According global and local accuracy measures were found that displayed similar performances for all sensor systems. Robust statistical accuracy measures showed that the most modern sensor systems ADS40 and ADS80 deliver imagery that produces the most accurate DEMs with a RMSE of 1 m and NMAD of 0.6 m. A RMSE of 1.3 m and 0.87 m NMAD of the RC30 data displayed the worst performance with shortcomings especially in steep areas. The HRSC-A DEM is influenced by artifacts resulting from the processing of the imagery but is able to acquire an accuracy of 1 m RMSE and 0.85 m NMAD despite a GSD of 0.1 m. The small ground sampling of 0.1 m leads to high accuracies in steep areas as the high degree of detail in this high resolution depicts details of rock walls and steep slopes more reliably.

Detailed local analysis identified slope as the main factor that determines the accuracy of the digital elevation information in all datasets. Besides the HRSC, the DEMs perform similarly in steep areas as they are able to produce accuracies of <1m up to a slope of 25° inclination. In general, we conclude that the modern digital pushbroom scanners can produce high resolution digital elevation models in high mountain environments with a very high accuracy. DEM generated from analogue and older digital pushbroom systems have to be applied carefully, especially in steep terrain. We show that different sensor systems of different generations display only a few differences in their accuracy in complex steep terrain and can therefore be used for multi-temporal assessment. The limitations of their applicability have to be considered when the digital elevation products of these sensor systems are applied.

Especially within modeling and multi-temporal assessments, the individual accuracy performances of the DEMs are of importance because errors might add up and have a great impact on research results concerned with quantification of geosystem processes. Nevertheless, airborne photogrammetrical imagery remains a very useful and accurate database to obtain high resolution digital elevation models covering large areas of complex topography.

7.9 Acknowledgments

7.10 References

Abermann, J., Fischer, A., Lambrecht, A., Geist, T., 2010. On the potential of very high-resolution repeat DEMs in glacial and periglacial environments. The Cryosphere 4 (1), 53–65. doi: 10.5194/tc-4-53-2010.

Aguilar, F.J., Aguilar, M.A., 2007. Accuracy assessment of digital elevation models using a non-arametric approach. International Journal of Geographical Information Science 21 (6), 667–686. doi: 10.1080/13658810601079783.

Albertz, J., Scholten, F., Ebner, H., Heipke, C., Neukum, G., 1992. The camera experiments HRSC and WAOSS on the Mars 94 mission. International Archives of Photogrammetry and Remote Sensing, Part B1. Amsterdam (29(B1)), 130–137.

Artuso, R., Bovet, S., Streilein, A., 2003. Practical Methods for the Verification of a countrywide terrain and surface models, in: Maas, H., Vosselman, G., Streilein, A. (Eds.), Proceedings of the ISPRS working group III/3 workshop `3-D reconstruction from airborne laserscanner and InSAR data'.

Bühler, Y., Marty, M., Ginzler, C., 2012. High Resolution DEM Generation in High-Alpine Terrain Using Airborne Remote Sensing Techniques. Transactions in GIS 16 (5), 635–647. doi: 10.1111/j.1467-9671.2012.01331.x.

Casella, V., Franzini, G., Banchini, G., Gentili, G., 2008. Initial Evaluation of the second Generation Leica ADS40 Camera, in: Proceedings and Results Vol. XXXVII. Silk Road from Information from Imagery, Beijing, China. 3-11 Jul.

Debella-Gilo, M., Kääb, A., 2012. Measurement of Surface Displacement and Deformation of Mass Movements Using Least Squares Matching of Repeat High Resolution Satellite and Aerial Images. Remote Sensing 4 (1), 43–67. doi: 10.3390/rs4010043.

Delaloye, R., Lambiel, C., Gärtner-Roer, I., 2010. Overview of rock glacier kinematics research in the Swiss Alps: seasonal rhythm, interannual variations and trends over several decades. Geographica Helvetica 65 (2), 135–145.

DeVenecia, L., Walker, S., Zhang, B., 2007. New Approaches to Generating and Processing High Resolution Elevation Data with Imagery. Photogrammetric Week 17 (5), 1442–1448.

Fischer, L., Eisenbeiss, H., Kääb, A., Huggel, C., Haeberli, W., 2011. Monitoring topographic changes in a periglacial high-mountain face using high-resolution DTMs, Monte Rosa East Face, Italian Alps. Permafrost and Periglacial Processes. 22 (2), 140–152. doi: 10.1002/ppp.717.

Fisher, P.F., Tate, N.J., 2006. Causes and consequences of error in digital elevation models. Progress in Physical Geography 30 (4), 467–489. doi: 10.1191/0309133306pp492ra.

Fricker, P., Rohrbach, A., 2005. Pushbroom Scanners Provide Highest Resolution Earth Imaging Information in Multispectral Bands, in: Proceedings ISPRS Workshop High Resolution Earth Imaging for Geospatial Information. High Resolution Earth Imaging for Geospatial Information, Stuttgart, Germany. 17 - 20 May.

Gruen, A., Murai, S., 2002. High-resolution 3D modelling and visualization of Mount Everest. ISPRS Journal of Photogrammetry and Remote Sensing 57 (1–2), 102–113.

Goyal, S.K., Seyfried, M.S., O'Neill, P.E., 1998. Effect of Digital Elevation Model resolution on topographic correction of airborne SAR. International Journal of Remote Sensing 19 (16), 3075–3096. doi: 10.1080/014311698214190.

Hauber, E., Slupetzky, H., Wewel, F., Gwinner, K., Neukum, G., 2000. A Digital and automated high resolution stereo mapping of the Sonnlbick glacier (Austria) with HRSC, in: Proceedings of EARSeL-SIG-Workshop Land Ice and Snow. EARSeL-SIG-Workshop Land Ice and Snow, Dresden. June 16-17, pp. 246–254.

Hirschmüller, H., 2005. Accurate and Efficient Stereo Processing by Semi-Global Matching and Mutual Information, in Proceedings of the IEEE Conference on Computer Vision and Pattern Recognition, 20-26 June 2005, San Diego, CA, USA, Volume 2, pp. 807-814.

Hobi, M.L., Ginzler, C., 2012. Accuracy Assessment of Digital Surface Models Based on WorldView-2 and ADS80 Stereo Remote Sensing Data. Sensors 12 (5), 6347- 6368. doi: 10.3390/s120506347.

Hoffmann, A., Lehmann, F., 2001. Vom Mars zur Erde: Die erste digitale Orthobildkarte Berlin mit den Daten der Kamera HRSC–A. Kartographische Nachrichten (50), 61–71.

Höhle, J., Höhle, M., 2009. Accuracy assessment of digital elevation models by means of robust statistical methods. ISPRS Journal of Photogrammetry and Remote Sensing 64 (4), 398- 406. doi: 10.1016/j.isprsjprs.2009.02.003.

Höhle, J., Potockova, M., 2006. The EuroSDR Test "Checking and Improving of Digital Terrain Models", Utrecht, The Netherlands.

Houghton, J.T., MacCarthy, J.J., Metz, B., 2001. Climate change 2001: Contribution of Working Group II to the third assessment report of the Intergovernmental Panel on Climate Change, 1st ed. Cambridge Univ. Press, Cambridge [u.a.], X, 1032 S.

Hu, W., Yang, G., Yuan, H., 2008. Application and accuracy evaluation of Leica ADS40 for large scale mapping, in: Proceedings and Results Vol. XXXVII. Silk Road from Information from Imagery, Beijing, China. 3-11 Jul.

ISO 5725-1, 1998. Accuracy (trueness and precision) of measurement methods and results - Part 1: General principles and definitions. ISO, Geneva.

Joerg, P.C., Morsdorf, F., Zemp, M., 2012. Uncertainty assessment of multi-temporal airborne laser scanning data: A case study on an Alpine glacier. Remote Sensing of Environment 127 (0), 118–129.

Kääb, A., 2000. Photogrammetry for early recognition of high mountain hazards: new techniques and applications. Physics and chemistry of the earth. Part A: Solid earth and geodesy 25 (9), 765 -770, doi:10.1016/S1464-1909(00)00099-X.

Kääb, A., 2002. Monitoring high-mountain terrain deformation from repeated air- and spaceborne optical data: examples using digital aerial imagery and ASTER data. ISPRS Journal of Photogrammetry and Remote Sensing 57 (1-2), 39–52. doi: 10.1016/S0924-2716(02)00114-4.

Kääb, A., Haeberli, W., Gudmundsson, G.H., 1997. Analysing the creep of mountain permafrost using high precision aerial photogrammetry: 25 years of monitoring Gruben rock glacier, Swiss Alps. Permafrost and Periglacial Processes 8 (4), 409–426. doi: 10.1002/(SICI)1099-1530(199710/12)8:4<409:AID-PPP267>3.0.CO;2-C.

Kääb, A., Huggel C., Fischer L., Guex S., Paul, F., Roer, I., Salzmann, N., Schlaefli S., Schmutz K., Schneider D., Strozzi T., Weidmann Y., 2005. Remote sensing of glacier- and permafrost-related hazards in high mountains: an overview. Natural Hazards and Earth System Sciences 5 (4), 527–554.

Karel, W., Pfeifer, N., Briese C., 2006. DTM Quality Assessment. International Archives of Photogrammetry, Remote Sensing and Spatial Information Sciences 36 (2), 7-12.

Kasser, M., Egels, Y., 2002. Digital photogrammetry. Taylor & Francis, London, 351 pp.

Kraus, K., Briese C., Attwenger, M., Pfeifer, N., 2004. Quality Measures for Digital Terrain Models, in: Proceedings and Results of XX ISPRS Congress, Commission I-VII. Geo-Imagery Bridging Continents, Istanbul, Turkey. 12 - 23 July.

Kraus, K., 2004. Photogrammetrie: Geometrische Informationen aus Photographien und Laserscanneraufnahmen, 7th ed. de Gruyter, Berlin, 516 pp.

Kraus, K., Karel, W., Briese C., Mandlburger, G., 2006. Local accuracy measures for digital terrain models. The Photogrammetric Record 21 (116), 342- 354.

Lane, S.N., 2000. Application of digital photogrammetry to complex topography for geomorphological research. The Photogrammetric Record 16 (95), 793-821.

Li, Z., Zhu, Q., Gold, C., 2005. Digital Terrain Modeling: Principles and Methodology. CRC Press: Boca Raton, FL, 323 pp.

Maune, D.F., 2007. Digital elevation model technologies and applications: The DEM user manual, 2nd. edition, 2nd ed. ASPRS, Bethesda, 655. S.

Menditto, A., Patriarca, M., and Magnusson, B.: Understanding the meaning of accuracy, trueness and precision, Accreation and Quality Assurance, 12, 45–47, doi:10.1007/s00769-006-0191-z, 2007.

Mills, J.P., Alhamlan, A.S., Abuoliat, A.S., Horgan, J., 2006. Geometric Validation of Imagery and Products from a high performance airborne digital sensor. International Archives of Photogrammetry and Remote Sensing, Vol. XXXVII.

Neill, L.E., 1994. Photogrammetric Heighting Accuracy. The Photogrammetric Record 14 (84), 917- 922. doi: 10.1111/j.1477-9730.1994.tb00292.x.

Nuth, C., Kääb, A., 2011. Co-registration and bias corrections of satellite elevation data sets for quantifying glacier thickness change. The Cryosphere 5 (1), 271–290. doi: 10.5194/tc-5-271-2011.

Nyenhuis, M., Hoelzle, M., Dikau, R., 2005. Rock glacier mapping and permafrost distribution modelling in the Turtmanntal, Valais, Switzerland. Zeitschrift für Geomorphologie 49 (3), 275–292.

Oppikofer, T., Jaboyedoff, M., Pedrazzini, A., Derron, M.-H., Blikra, L., 2011. Detailed DEM analysis of a rockslide scar to characterize the basal sliding surface of active rockslides. Journal of Geophysical Research F: Earth Surface 116 (2) doi:10.1029/2010JF001807.

Otto, J.-C., Kleinod, K., Konig, O., Krautblatter, M., Nyenhuis, M., Roer, I., Schneider, M., Schreiner, B., Dikau, R., 2007. HRSC-A data: a new high-resolution data set with multipurpose applications in physical geography. Progress in Physical Geography 31 (2), 179–197. doi: 10.1177/0309133307076479.

Papasaika, H., Baltsavias, E.P., 2010. Quality evaluation of DEMs., in: P. Tate, N.; Fisher(Eds.), Accuracy 2010 - Proceedings of the Ninth International Symposium on Spatial Accuracy Assessment in Natural Resources and Environmental Sciences.

Parry, M.L., 2007. Climate change 2007: Impacts, adaptation and vulnerability : contribution of Working Group II to the fourth assessment report of the Intergovernmental Panel on Climate Change. Cambridge University Press, Cambridge, U.K. ;, New York, ix, 976.

Pieczonka, T., Bolch, T., Buchroithner, M., 2011. Generation and evaluation of multi-temporal digital terrain models of the Mt. Everest area from different optical sensors. ISPRS Journal of Photogrammetry and Remote Sensing 66 (6), 927–940.

Rasemann, S., 2003: Geomorphometrische Struktur eines mesoskaligen alpinen Geosystems. Bonner Geographische Abhandlungen 111. 2004. Sankt Augustin.

Roer, I. Rock glacier kinematics in the Turtmanntal, Valais, Switzerland – observational concept, first results and research perspectives, in: Phillips, M., Springman, S., Arenson, L.U. (Eds.), Permafrost. Proceedings of the Eighth International Conference on Permafrost, 21-25 July 2003, Zurich, Switzerland, Lisse ; Abingdon.

Roer, I. (2005): Rockglacier kinematics in a high mountain geosystem. Bonner Geographische Abhandlungen 117, 2007. Sankt Augustin.

Roer, I., Kääb, A., Dikau, R., 2005. Rockglacier kinematics derived from small-scale aerial photography and digital airborne pushbroom imagery. Zeitschrift für Geomorphologie 49 (1), 73–87.

Roer, I., Nyenhuis, M., 2007. Rockglacier activity studies on a regional scale: comparison of geomorphological mapping and photogrammetric monitoring. Earth Surface Processes and Landforms 32 (12), 1747–1758. doi: 10.1002/esp.1496.

Sandau, R., 2005. Digitale Luftbildkamera: Einführung und Grundlagen. Wichmann, Heidelberg, IX, 342 S.

Scholten, F., Wewel, F., 2000. Digital 3D Acquisition with the High Resolution Stereo Camera-Airborne (HRSC-A). International Archives of Photogrammetry and Remote Sensing, Part B4. Amsterdam, 901–908.

Simmen, J.-L., Bovet, S., 2007. Landesweite Orthophoto dank der Digitalkamera ADS40. Geomatik Schweiz - Geoinformation und Landmanagement 105 (6), 293–296.

Storck, P., Bowling, L., Wetherbee, P., Lettenmaier, D.P., 1998. Application of a GIS-based distributed hydrology model for prediction of forest harvest effects on peak stream flow in the Pacific Northwest. HYDROLOGICAL PROCESSES 12 (6), 889–904.

swisstopo - Bundesamtes für Landestopografie, 2005. DOM: Die Geodaten der Schweiz des Bundesamtes für Landestopografie für den professionellen Einsatz. http://www.swisstopo.admin.ch/internet/swisstopo/de/home/products/height/dom_dtm-av.parsysrelated1.75334.downloadList.60037.DownloadFile.tmp/domflyerdefr.pdf. (accessed 31 July 2013)

swisstopo - Bundesamtes für Landestopografie, 2007. geodata-news: Die Laser Höhenmodelle DTM-AV und DOM. Nr. 14. http://www.swisstopo.admin.ch/internet/swisstopo/de/home/docu/pub/topography/geodatanews.parsys.1829.downloadList.48896.DownloadFile.tmp/gn142007defr.pdf. (accessed 31 July 2013)

swisstopo - Bundesamtes für Landestopografie, 2012. Rasterpixel maps 1:25000 swisstopo (5704 000 000) RC30, ADS40, ADS 80. License swisstopo (5704 000 000).

Tarolli, P., Arrowsmith, J.R., Vivoni, E., 2009. Understanding Earth surface processes from remotely sensed digital terrain models. Geomorphology 113 (1-2), Editorial.

Thapa, K., Bossler, J., 1992. Accuracy of spatial data used in geographic information systems. Photogrammetric Engineering & Remote Sensing 56 (6), 835–841.

Turker, M., Cetinkaya, B., 2005. Automatic detection of earthquake-damaged buildings using DEMs created from pre- and post-earthquake stereo aerial photographs. International journal of remote sensing 26 (4), 823–832.

Valta-Hulkkonen, K., Kanninen, A., Pellikka, P., 2004. Remote sensing and GIS for detecting changes in the aquatic vegetation of a rehabilitated lake. International journal of remote sensing 25 (24), 5745–5758. doi: 10.1080/01431160412331291170.

Vonder Mühll, D., Noetzli, J., Roer, I., 2008. PERMOS – a comprehensive monitoring network of mountain permafrost in the Swiss Alps., in: Kane, D.L., Hinkel, K.M. (Eds.), Proceedings of the 9th International Conference on Permafrost, University of Alaska, Fairbanks, Alaska, June 29 - July 3, 2008. Institute of Northern Engineering, University of Alaska, Fairbanks, Fairbanks, Alaska.

Vosselman, G., Maas, H.-G., 2010. Airborne and terrestrial laser scanning. Whittles Publishing, Dunbeath.

Wewel, F., Scholten, F., Neukum, G., Albertz, J., 1998. Digitale Luftbildaufnahme mit der HRSC - Ein Schritt in die Zukunft der Photogrammetrie. Photogrammetrie - Fernerkundung - Geoinformation (6), 337–348.

Zhang, B., Miller, S., DeVenecia, L., Walker, S., 2006. Automatic terrain extraction using multiple image pair and back matching, in: Proceedings of ASPRS 2006 Annual Conference, Reno, Nevada.

8 Publication II

Müller, J., Gärtner-Roer, I., Kenner R., Thee, P., Morche, D., 2014. Sediment storage and transfer on a periglacial mountain slope (Corvatsch, Switzerland). Geomorphology 218, 35–44.

The author's contribution to the article:

J. Müller collected and processed the data, developed the methodology, designed the study, performed the analysis and wrote the manuscript. I. Gärtner-Roer designed the study, developed the methodology, collected data and wrote the manuscript. R. Kenner, P.Thee and D. Morche collected the data.

Abstract

High mountain geomorphology is mostly characterized by high elevation, steep gradients, rocky terrain, the presence of snow and ice and the related processes occurring in a high energy environment. Large sources of sediment and sediment storages often exist within high mountain systems and are controlled by the processes occurring within this setting. The purpose of this study is to describe sediment paths on a periglacial mountain slope and quantify geomorphic work within one example year in order to analyze and compare sediment budgets in high mountain geosystems. This energy related approach helps to characterize a periglacial slope on account of the effectiveness of its geomorphological processes and might help to understand the complex dynamic behavior of its constituent sub systems.

A periglacial mountain slope is investigated in Eastern Switzerland (Corvatsch). The environment is characterized by a typical coarse debris cascade: rock wall → rock fall → talus slope → permafrost creep → rockglacier. Rockglaciers are considered to be sediment traps of the coarse debris system, reflecting the erosion history of the corresponding catchment. Headwall recession and creep processes of the talus slopes and rockglaciers are quantified by a multi-method-approach combining remote sensing and terrestrial methods. Multi-temporal DEMs of the last two decades enabled the quantification of sediment transfer of the slow moving landforms (frozen talus slopes and rockglaciers). Sediment input from the rock wall is quantified by repeated laser scanning over the last 4 years. With the introduced cascading approach it is possible to assess dynamics within the coarse debris system. The mountain slope is divided into three subsystems (headwall, talus cone and rockglacier) and their dynamics are analyzed individually but also in relation to the entire mountain slope on a yearly base. A backweathering rate of 2 mm can be derived for the headwall and an energy transfer of 29.8 GJ from the headwall to the slope, 4 GJ from the talus slope to rockglacier where 1.44 GJ of geomorphic work are released by the downwards creep of the landform. This study is the first to include an analysis of the geomorphic work generated on the basis of vertically differentiated sediment production and transport processes.

Keywords: High mountain, Periglacial, Geomorphic Work, Rockglacier, Sediment transfer, Terrestrial laser scanning

8.1 Introduction

High mountain geomorphology is characterized by high elevation, steep gradients, rocky terrain, the presence of snow and ice and the resulting processes, forming a high energy environment (Barsch and Caine, 1984). Therefore, mountains deserve special attention within geomorphology, since environmental changes may occur on shorter time-scales and with lasting consequences and thus reflect the sensitivity of complex environmental systems. In a periglacial high mountain environment, it is assumed that changes in the temperature regime lead to respective changes in geomorphological processes such as weathering rates and transport rates. The outstanding landforms in such systems evolve over millennia and are related to constant temperature regimes during these periods, but we expect certain changes related to climate change to occur on shorter time scales; thus influencing the related processes. In most mountain ranges the topography is dominated by major erosional landforms (e.g., cirques) reflecting former dynamics, superimposed by more contemporary meso-relief-forms (e.g. moraines, talus cones), reflecting diverse process domains (Roer, 2007). Periglacial slopes are characterized by rockglaciers, ice-cored moraines or solifluction lobes and are often in close connection to glacial and gravitational landforms. All of these landforms are considered as significant indicators for changes within the system. The dynamic behavior of rockglaciers especially has been assessed in relation to regional climatic influences (Delaloye et al., 2010) but some rockglaciers still show erratic rheologies which cannot be accounted for by climatic drivers (Roer et al., 2008, Springmann et al., 2013,). An energy-based approach might help to understand the behavior of the rockglacier as a result of the state of the entire slope system. In order to describe sediment transfer in high mountain environments in a systematic context, Caine (1974) developed a conceptual model of alpine sediment cascades. This model describes the logical, cascade-like sequence of processes, based on an idealized slope profile. This approach has been adapted and applied within this study in order to assess an entire periglacial mountain slope

Geomorphic work, energy fluxes and sediment transfer rates are among the main components in characterizing and comparing the potential energy of geomorphological systems (e.g., Reid and Dunne, 1996, Beylich and Warburton, 2007). The energy-based approach establishing geomorphic work as a measure for erosion intensity (Caine, 1976) allows the direct comparison of environmental systems and geomorphic processes on different spatial and temporal scales. Process rates and their changes can be analyzed by using energy fluxes and geomorphic work as indicators for their effectiveness. Based on the

sediment budget approach, geomorphic work, energy fluxes and sediment transfer rates are often assessed for entire mountain ranges (e.g., Church and Slaymaker, 1989) or single gravitational processes (e.g. Krautblatter et al., 2012) but have rarely been used on a scale in between. Barsch and Caine (1984) pointed out that the sedimentary features such as talus cones and rockglaciers receive a lot of scientific attention whereas information on the source area, the rockwall and its connection to the cascading sediment system is lacking. Up to now, deficits exist in the knowledge of temporal and spatial coupling of nested geomorphological processes and complex interactions of different sediment storages (Dietrich and Dunne, 1978, Caine and Swanson, 1989, Schrott et al., 2003). Connectivity studies such as Fryir, 2007 and Heckmann and Schwanghart, 2013 have assessed the linkage of landforms and coupling between systemic entities. These connectivity approaches allow accounting for the discrepancy between erosion / mobilization of material and the sediment yield at the outlet of the system compartment which has been challenging to sediment budget studies (Caine and Swanson, 1989, Hooke 2003, Fryir et al., 2007).

In order to describe and quantify sediment transfer rates and to derive energy fluxes, information on geometrical changes within the system is required. Remote sensing data and geodetic measurements are frequently used to assess geometrical changes in periglacial high mountain areas (e.g. Campbell and Church, 2003, Roer et al., 2005, Avian et al., 2009, Bodin et al., 2009). These observations deliver information on ongoing processes and process changes and have so far not been applied for the investigation on energy fluxes on an entire slope. The study presented here combines three different methods to derive landform parameters for the analysis of sediment transfer rates and the calculation of geomorphic work. The study focuses on the sediment and energy transfer within one example year where the multi-temporal data have been averaged. The process rates of old landforms (rockglaciers) are also quantified to fit a one year period. Beside DEM analyses derived from digital photogrammetry and geodetic field survey, terrestrial laser scanning (TLS) is applied in order to achieve a better understanding of geometry changes in the steep parts of the slope (upper talus slope and headwall). Sediment transfer paths of the rockglaciers have already been described by combining movement rates and sediment volumes (Gärtner-Roer and Nyenhuis, 2010; Gärtner-Roer, 2012).

The purpose of this study is to assess and quantify sediment transfer sediment paths on a periglacial and mountain slope and quantify geomorphic work in order to analyze and compare sediment budgets in high mountain geosystems.

8.2 Murtèl / Corvatsch Cirque

The field site is the well-studied Murtèl cirque situated below the northern face of Piz Corvatsch (3300 m a.s.l.) in Grison, which lies in the south-eastern part of Switzerland (at about 46 26'N / 9 49'E) and expands over an area of 0.48 km². The lithology mainly consists of granite, granodiorite and greenschist. The density of the in-situ rock types are assumed to correspond with the values given in the literature with a density of 2.65-2.8 g/cm³ (Tarbuck et al., 2011). The climate is characterized by air masses from the south-west. The annual precipitation averages 800 mm in the valley and 1000-2000 mm in higher altitudes. Gubler et al. (2011) show the distribution of ground surface temperatures within the entire Corvatsch area by using an extensive network of randomly distributed temperature loggers. Their temperature data show that the entire slope is situated within the permafrost belt as the existing rockglaciers (Murtèl and Marmugnun) already suggest. Due to the fact of easy accessibility the Murtèl site is one of the best investigated permafrost sites and numerous datasets (such as borehole, ground surface temperatures and kinematics) are available, especially from the rockglacier sites (Hoelzle et al., 2002, Schneider et al., 2012). Based on several studies it is known that the entire slope, down to an altitude of 2620 m a.s.l. (rockglacier front) is situated in discontinuous permafrost.

The north slope of Piz Corvatsch gives a typical periglacial mountain slope with a sequence of characteristic landforms: headwall, talus slopes or cones and rockglaciers. The Murtèl rockwall, the northern face of Piz Corvatsch, comprises the headwall of an ice-free cirque in which the Murtèl rockglacier has formed. The headwall consists of heavily shattered crystalline rocks and has been part of a more detailed analysis on frost weathering and rockwall erosion by Matsuoka (2008) which identified heavy shattering of the headwall with a mean crack width of 2 mm. The headwall supplies coarse bouldery debris to the entire cirque which has developed into the talus cone and two rockglaciers during the Holocene (Barsch, 1996, Haeberli, 1998 and Matsuoka, 2008). The rockwall can be divided into two source areas supplying the rockglaciers with sediment. The entire headwall has a mean slope of 45° but most bedrock outcrops are 80°-90°. Small ledges within the headwall are covered with debris which developed into small debris cones. These cones lessen the overall steepness of the headwall. The talus cone is characterized by linear transport processes originating in the headwall. It serves as the subsequent sedimentary body to the headwall and consists of heterogeneous loose material. A sudden change in slope and the absence of bedrock identify the talus cone in the geomorphological setting. Permafrost creep and snow avalanches are considered to be processes responsible for sediment transport within the talus

cone and on-/into the rockglacier. The Murtèl rockglacier has been identified as a talus derived rockglacier (Haeberli et al., 2006) where the buildup of subsurface ice (segregation ice and the incorporation of perennial snow banks and avalanche snow (Isaksen et al., 2000, Humlum et al., 2007)) within talus slope has led the material to behave fluidly and creep downwards. Therefore the talus slopes supply sediment by permafrost creep and secondary transport by avalanches and debris flows to the rockglacier. The Murtèl rockglacier can be identified by its well developed furrow and ridge topography and the outstanding rheological features. Despite the topographical differences between the landforms, their boundaries are often not detectable as clear lines but can be depicted as transition zones (see Fig. 18 and 19).

8.3   Concept, Methods & Data

8.3.1   Cascading Concept

The periglacial high mountain system at hand can be interpreted as a closed system concerning coarse debris (Barsch and Caine, 1984) in the sense of Chorley and Kennedy (1971). The boundaries of the coarse debris system are clearly defined by the ridge of the headwall and the bottom of the rockglacier. There is no possible input of clastic material from outside the system and within this approach it can be assumed that there is no loss of sediment since only the coarse debris system is assessed. Suspended material and material in solution within the drainage water are of course existent but will not be assessed (Barsch and Caine, 1984, Jordan and Slaymaker, 1991). Sediment transfer rates and geomorphic work have repeatedly been used to describe and compare such geomorphological systems (Barsch and Jakob, 1998, Humlum, 2000: see Krautblatter et al., 2012 for a thorough compilation of geomorphic work literature).
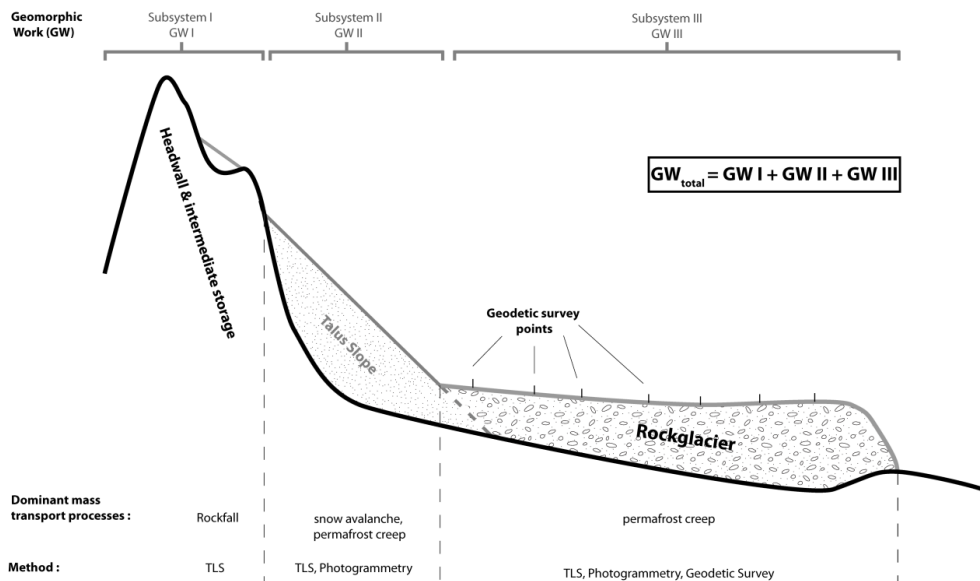
Figure 18: Idealized concept of a typical periglacial mountain slope: subsystems and the associated potential energy.

Figure 18 shows the theoretical concept of an idealized periglacial mountain slope which builds the basis of this study. Three main subsystems make up the entire mountain slope: The headwall and intermediate storage subsystem, the talus slope subsystem and the rockglacier subsystem. Each subsystem can be described by characteristic parameters (e.g., change in slope, change in grain size distribution) and has a typical setting in the landscape. The subsystems are defined based on several characteristics: topographic features, typical landform(s) and dominating mass wasting processes. Subsystem I (Headwall and Intermediate Storage) is dominated by steep rockwalls (within this study > 45 degree) consisting of consolidated rock, small debris storages where eroded material is stored for short periods of time and remobilized by avalanches or heavy precipitation (Sass, 2005). The dominant process of mass transport is rockfall and snow avalanches. Backweathering of the exposed rockwall and resulting rockfall of all magnitudes are the most effective mass wasting processes (Krautblatter et al., 2012) and supply the entire system with sediment. Subsystem II (talus slope) results from the active sedimentation of the mobilized material in subsystem I. The dominant mass wasting processes are rockfall and secondary transport by snow avalanches and probably permafrost creep. The talus slope consists of unconsolidated material of different seizes and shows a rather homogeneous sedimentation regime.

Subsystem III (rockglacier) develops from the talus slope located in permafrost conditions which begins to creep and forms the characteristic appearance of these landforms over millennial timescales (Barsch, 1996).

In order to assess the entire system, the characteristics, processes and connections of the constituent subsystems have to be identified, individually analyzed and then holistically interpreted. This multitude of parameters calls for an approach using a combination of several methods such as geomorphological mapping, photogrammetry, terrestrial laserscanning and surveying to assess and quantify the contributing processes. A holistic conceptual approach based on sediment and/or energy transfer considers the entire cascade of subsystems if a whole mountain slope is to be assessed.

8.3.2 Geomorphological mapping

The site has been analyzed by geomorphological mapping in the field as well as by interpretation of digital elevations models (DEM) and orthophotos derived from digital photogrammetry. Especially the DEMs served as basis for geomorphometric analyses to determine spatial dimensions, slope, aspect and curvature of the system. The DEMs derived from digital photogrammetry perform best in flat and moderately inclined slopes whereas terrestrial laser scanning (TLS) produces high quality digital elevation information in steep areas (see Fig. 18). Thus the DEMs derived from TLS are used for the analysis of the headwall and the talus slopes whereas the photogrammetrically derived DEMs covering the talus slopes and rockglaciers are utilized to interpret these areas. The datasets covering the overlapping area allow for an assessment of the different techniques.

The three subsystems are defined by typical landforms and corresponding processes. Crucial is the delineation of the source area (headwall and intermediate storage), of the talus slope and of the rockglaciers, which was performed by including the surface features (e.g. changes in slope, grain size distribution,) as well as the velocity information, that indicate the transition zone of the different subsystems. Unfortunately there is no subsurface information available to delineate more accurately the three sub systems.
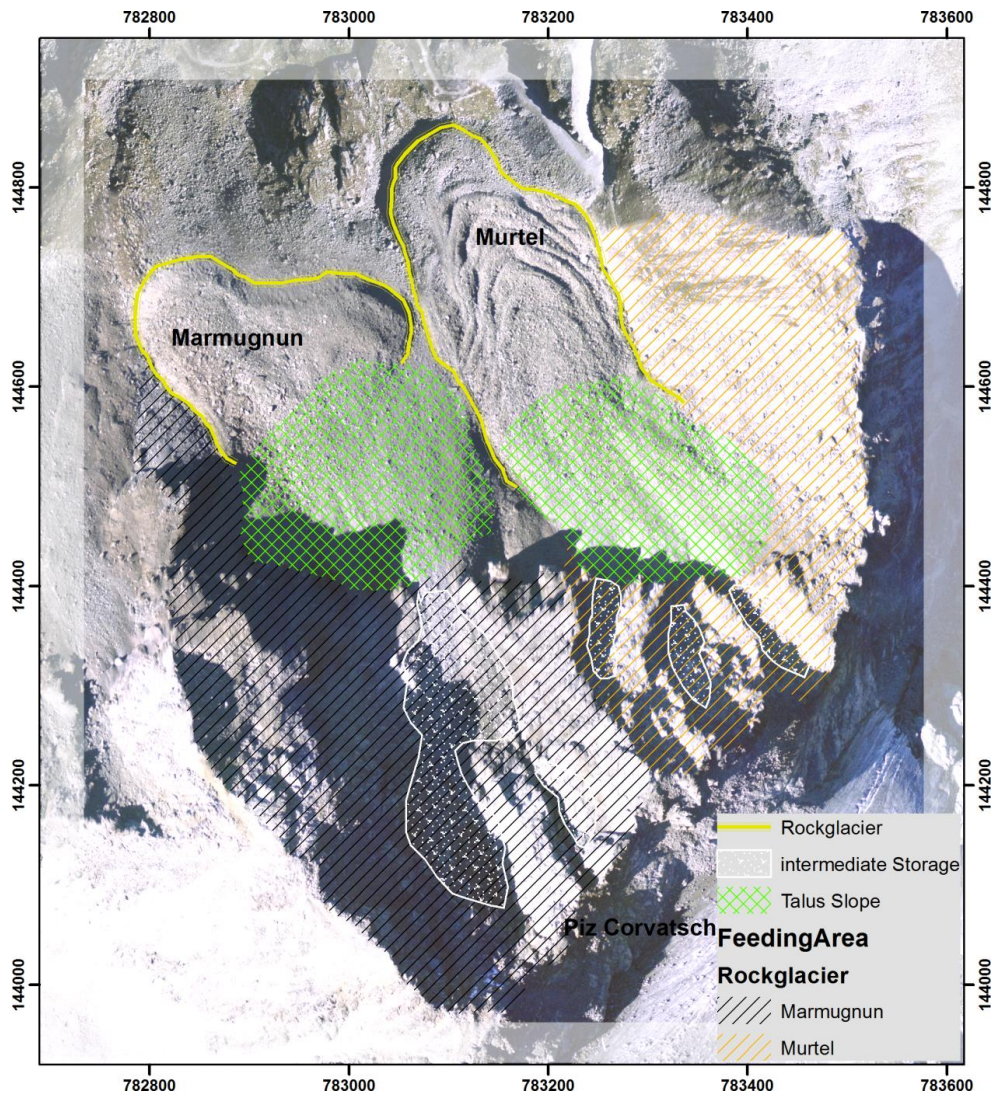
Figure 19: Geomorphological map of the Murtèl slope. The delineation of the subsystems are not as distinct as depicted but rather transition zones between the subsystems.

8.3.3 Geometry changes

Within this study a multi-sensoral approach uses TLS data, photogrammetric imagery and terrestrial geodetic measurements to derive vertical and horizontal changes within the system. Feature tracking and DEM differencing methods enable the quantification of spatially discrete changes. For the assessment of rockglacier activity, permafrost creep needs

to be quantified with a high accuracy. This is best performed by the combination of remote sensing and terrestrial methods, allowing the analysis of permafrost creep on various spatial and temporal scales (PERMOS, 2010).

Within PERMOS (Swiss Permafrost Monitoring Network), aerial photographs from low altitudes (scale 1:6000) are taken by Swisstopo for selected sites such as Murtèl with a temporal resolution from 5-7 years (1996, 2002 and 2007). Based on these data, geometry changes of entire landforms are quantified on a multiannual basis. The products of the airborne survey are digital elevation models and orthophotos with a resolution of 0.3-1m. Geometry changes are described by vertical changes derived from repeated DEM differencing (pixel based), as well as by horizontal changes derived from matching of multi-temporal orthophotos (vectors). Details on raw data, processing and accuracies are given by Kääb and Vollmer (2000), Roer et al. (2005) and Roer (2007). In addition to remote sensing, terrestrial survey using a total station (Leica TLS 1200) has been conducted since 2009 with a high temporal resolution (seasonal and annual) for a number of selected blocks on each rockglacier. Terrestrial survey points (TSPs) are measured twice a year and based on their three dimensional coordinates (x,y,z) horizontal (Δxy) and vertical (Δz, ratio of slope) changes are quantified with a resolution of 1-2 cm. Terrestrial surveying of selected blocks within the rockglacier matrix has proven as a reliable method to derive horizontal velocities and vertical displacement (Roer et al., 2008, Bodin et al., 2009, Delaloye et al., 2010,).

In order to assess the steep areas of the mountain slope, terrestrial laser scanning (TLS) has been performed annually since 2009 and produced digital elevation models with a resolution 0.5 m. Repeated surveys allow for the quantification of geometry changes in the wall as well as on the talus slope. Limitations are given in shaded areas, such as the furrow-and-ridge topography on the rockglacier surface or the complex topography of the headwall. TLS has been repeatedly used to assess geometrical and volumetric changes in vertical rockwalls (Oppikofer et al., 2008, 2011, Kenner et al., 2011, Heckmann et al., 2012) and the movement of rockglaciers (Avian et al., 2009). Several accuracy assessments of TLS surveys have shown that an accuracy of 5-7 cm is achievable depending on sampling distance (Rabatel et al., 2008, Oppikofer et al., 2009, Lim et al., 2010). TLS surveys were conducted yearly from 2009 to 2012 to assess the rockglacier movement but only the datasets of 2011 and 2012 were fit to derive sufficient information about the entire headwall to quantify changes. For the TLS surveys in 2011 and 2012 the Riegl LPM-321 instrument was used.

The multi-temporal high resolution TLS allows distinguishing and quantifying several processes within the different subsystems. The areas and volume of erosion and mobilization

of material can be located and quantified (mobil. Vol. in Table 1). Besides that, location and volume of accumulated material can also be spatially assessed and quantified (acc. Vol. in table 1). The discrepancy between the mobilized volume and the accumulated volume is referred to as the effective volume which, if positive shows the amount of material transferred to the next subsystem, or if negative, the dynamic within the intermediate storages.

8.3.4 Geomorphic Work

Geomorphic work has been introduced by Caine (1976) in order to find a universal definition for erosion and transport within geomorphological systems. The term "work" is referred to in its original physical sense: as a measure of released potential energy to overcome friction and induce acceleration. Geomorphic work is defined as potential energy

$$w = m\,g\,\Delta h$$

Where m is the mass of the mobilized material, g the gravitational acceleration and Δh the vertical distance travelled by m (Caine, 1976). The energy released can be measured in Joule or Watts (Kg m^2 s^{-3}) if the time span of the released energy is known. Other definitions have been introduced (Wolman and Gerson, 1978, Costa and O'Connor, 1995) but will not be accounted within this study. The quantification of geomorphic work (GW) within the multi-sensoral approach presented here enables the assessment of the energy regime within one entire mountain slope and the effectiveness of numerous coupled processes involved in releasing this energy. The total geomorphic work generated in the study area is the sum of the energy released in the several subsystems (see Fig. 18):

$$GW_{total} = GW\,I + GW\,II + GW\,III$$

Where GW I is the geomorphic work of the headwall and intermediate storage subsystem, GW II the geomorphic work generated in the talus slope and GW III the energy released in the rockglacier subsystem.

The multi-sensoral approach presented allows for the quantification of the energy released in the headwall by using multi-temporal TLS data to quantify the mobilized and intermediately stored sediment. The high resolution of the TLS data allows for the spatially discrete and therefore precise calculation of GW. Previously, GW has been mainly calculated by quantifying the mobilized material at the bottom of the slope by rock collectors and applying an average travelling distance for the entire sediment (e.g., Krautblatter et al., 2012). This

approach can only produce spatially restricted information about the sedimentation process and relies highly on the interpolation over the entire rockwall or catchment.

The GW within this context is calculated by quantifying the volume loss and volume gain derived from DEM differencing for the subsystems headwall / intermediate storage and talus slope. The available TLS-derived DEMs are unfortunately not adequate for an assessment of the entire rockglacier area. The mass loss of the headwall subsystem is considered as mobilized material and entirely interpreted as released energy since it is the first step of the energy / sediment cascade whereas the talus slope can be attributed with an energy in- and output (gain and release). Following the equation to calculate GW, h is considered the vertical distance of every pixel to the highest point of the subsequent system which in case of the headwall is the top of the talus slope located at 2700 m a.s.l. The peak of the rockwall, Piz Corvatsch is situated at 3185 m which leaves a maximal vertical distance of 485 m. The mass of the mobilized material is derived from the DEM differencing information and thus the geomorphic work on a pixel basis can be calculated. The DEM differencing does not only show the released material and therefore released energy but also the accumulation of that material within the subsystem. The accumulated volume is considered as intermediate storage (accumulated volume) in the headwall and talus slope.

Due to its steep slope, the GW of the talus slope subsystem is also best assessed by the TLS. For the talus slope subsystem it is possible to derive an energy input and an energy output since the headwall supplies quantifiable sediment and therefore energy to the talus slope. Energy release / output is obtained by identifying the mass loss in the talus slope and inferring the GW from that. The height (h) is here considered the vertical difference of each pixel to the highest point of the rockglacier area (2650m a.s.l.) This approach ensures the comparability to geomorphic work data from studies which used stone collectors at the foot of the rockwall (e.g. Krautblatter et al., 2012). In order to quantify the entire GW released in either one of the subsystem, GW is calculated for each pixel and the positive values are summed up to describe the entire work released. If the sum of the negative values of GW (GW$_{stored}$, resulting from mass gain within the DEM differencing) is subtracted from the released GW, it is possible to quantify the energy transfer between the subsystems. Therefore, similar to the geometry changes, it is possible to differentiate between the entire geomorphic work released in the subsystem and the energy kept by intermediate storages.

$$GW_{efficient} = GW_{released} - GW_{stored}$$

The discrepancy between the two can be referred to as effective energy (GW$_{efficient}$) because it is the energy that is transferred to the next subsystem.

The sediment transfer / geomorphic work assessment of the rockglacier is based on work in Gärtner-Roer (2012) where the sediment volumes and transport rates have already been addressed for the Murtèl rockglacier. Direct information on rockglacier thickness is only available at the Murtèl site (e.g., Haeberli et al., 1998), this data were assessed by a semi-quantitative approach for the adjacent landform Marmugnun. The thickness for Marmugnun has been determined in different parts of the front and at the lateral margins and an average value has been calculated for each rockglacier (Gärtner-Roer, 2012). The calculation of sediment volumes is based on a simplified three-layer-model of the internal structure of rockglaciers (Haeberli, 1985, Barsch, 1996, Humlum, 2000): the uppermost layer is up to three meters thick and consists of very coarse blocks. The second layer represents the ice-rich, deforming permafrost core which is moving down slope and therefore covers the third layer, which results from blocks that toppled from the front and are overridden by the rockglacier. The amount of sediment stored within rockglaciers is estimated to vary between 30 and 50% (Barsch, 1996, Humlum, 2000). The rockglacier thicknesses according to the method described before were used to calculate different sediment volumes. An ice volume of 40% was assumed for the Marmugnun rockglacier and a density of the sediment of 2.8 g cm^{-3} was applied (Gärtner-Roer and Nyenhuis, 2010).

For simplification, it is assumed that the entire rockglacier creeps and the vertical distance is based on the average slope and the horizontal distance travelled. The vertical distance travelled per year can be deducted from the horizontal velocity per year (v) derived from geodetic survey and the average slope:

$$\Delta h_{rockglacier} = v * \sin (slope)$$

The average slope for Murtèl is 12 degree and for Marmugnun 18 degree which results in 0.02 cm/a (Murtèl) and 0.05 cm/a of height covered.

8.4 Results

The results of the geomorphic mapping based on interpretation of various types of remote sensing data and field observations are depicted in Fig. 19. The spatial categorization following the concept presented in Fig. 18 cannot be seen as a spatially discrete delineation but rather as transition zones between several process domains. Both rockglaciers, Murtèl and Marmugnun, serve as sediment traps for the coarse debris system of the entire slope.
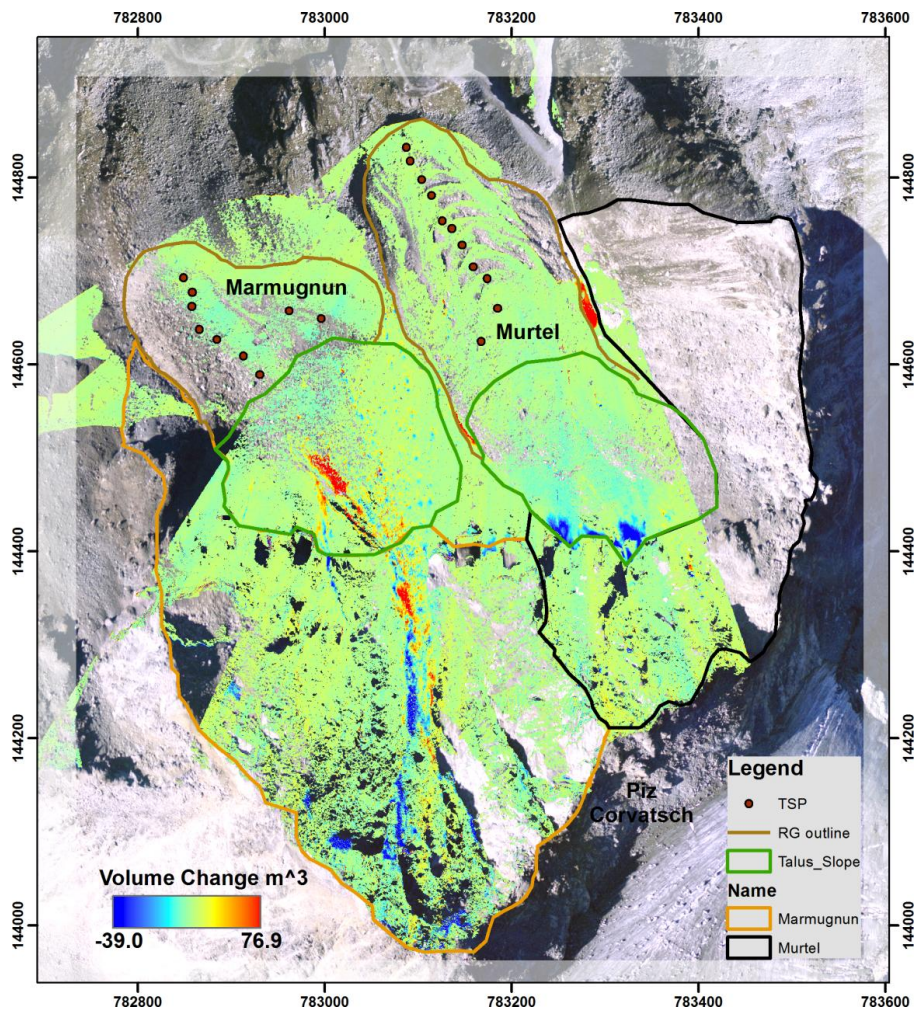

Figure 20: The TLS derived volume changes within the mapped subsystems between the year 2011 and 2012. Areas without volume change information are either due to gaps in the TLS dataset or areas where no change happens. High isolated patches of volume change are due to the melt of avalanche and have not been incorporated in the volume assessment.

Figure 20 depicts the mobilized volume (in m^3) of sediment in the mountain slope which is detected by the TLS. In total, a volume 1.95x10^6 m^3, the equivalent of 5.4 Mt of material was mobilized. The entire system released 120.31 GJ a^{-1} of geomorphic work which corresponds to 7.9 kW km^{-2}. The detailed analysis of the different subsystems is shown in table 14 and table 15.

Table 14: The detailed analysis of the sediment dynamics in the different subsystems. The mobilized volume (mobil. Vol.) is the sum of activated mass all whereas the intermediate storage is quantified as accumulated volume (acc Vol.). The rockglaciers show no direct input from the upper subsystems. Therefore sediment is only mobilized by permafrost creep.

	Rockwall / Intermediate Storage (Slope>45°)				Talus Slope (Slope 15°-45°)				Rockglacier (Slope 12° & 18°)		
	Area m²	mobil. Vol (m³)	acc. Vol (m³)	effective. vol (m³)	Area m²	Mobil. Vol (m³)	acc. Vol (m³)	effective Vol. (m³)	Area m²	Mobil. Vol (m³)	creep veolocity m/a
Murtèl	125675.35	1986.16	3022.17	-1036.01	40735.82	2110.49	970.03	1140.46	45885.74	1480000.00	0.09
Marmugnun	188317.24	10465.70	8770.79	1694.91	44931.19	4561.36	3585.19	976.17	33522.26	454787.95	0.15
Total	313992.59	12451.86	11792.96	658.90	85667.01	6671.85	4555.22	2116.63	79408.00	1934787.95	-

Table 15: The detailed analysis of geomorphic work (GW) in the different subsystems. Geomorphic work released (GW released) refers to the entire energy generated due to vertical mass movement over the entire feeding areas / subsystems whereas the effective geomorphic work accounts for the energy which is transferred to the next subsystem. The rock glacier, as the last compartment of the sediment cascade gerenates only released energy.

	Rockwall		Talus Slope		Rockglacier
	GW released (GJ)	effective GW (GJ)	GW released (GJ)	effective GW (GJ)	GW released (GJ)
Murtèl	14.58	2.30	3.27	0.64	0.81
Marmugnun	86.30	27.58	13.21	3.34	0.62
Total	100.88	29.88	16.48	3.99	1.44

8.4.1 Headwall

The headwall of the entire system mobilizes 12'451 m^3 of material of which 11'792 m^3 are held by intermediate storages within the headwall itself. Small storage areas like cavities, minor depressions and debris slopes gather material which is most likely transported onwards by snow avalanches. This shows that only a small part of the mobilized material is fed directly into the next section of the sediment cascade. Altogether, the headwall releases geomorphic work of 100.88 GJ within the years 2011 and 2012. Most of the released energy is buffered in intermediate storages und only 29.9 GJ of energy are directly transferred into the next subsystem. Figure 20 depicts the spatial distribution of the mobilized material within the headwall. It is apparent that the highest parts of the headwall are most active and deliver material into a channel where the sediment either passes to the talus cone or is stored in the lower parts of the channel. The feeding area of the Marmugnun rockglacier is largely covered by the TLS dataset, whereas the eastern slope of Murtèl was not observed by the instrument. Observations in the field have shown that this slope is not very active and contributes only small amounts of sediment into the system. The lack of a distinct talus slope supports this assumption. The effective volume of sediment generated by this approach would account for a backweathering rate of 2 mm per year.

The negative effective volume of sediment for the entire Murtèl feeding area shows, that more material is accumulated or relocated than added by rockwall erosion or transferred to the next system. This shows that the storage capacity for sediment and energy of the subsystem are not yet filled. Besides the transported volume of sediment, Fig. 20 also depicts the gaps within the TLS dataset which mostly originate from shading effects of the area.

8.4.2 Talus slope

The talus slopes are supplied with material by several distinctive channels in the headwall. The Marmugnun talus slope is mainly fed by one major channel depositing material linearly on the slope whereas there are two smaller linear areas contributing diffusely to the Murtèl talus slope. The TLS data for both talus slopes shows a mobilized volume of 6671m^3 and an accumulated volume of 4555.22m^3. Thus, the effective volume transferred through the subsystem is 2116.3 m^3. The released energy of both talus slopes sums up to 16.48 GJ in the area and the effective geomorphic work which is channeled through the system adds up to 3.99 GJ. Unfortunately there is no kinematic monitoring installed on the talus slopes thus the movement can only be derived by the interpretation of the DEMs. Singular features such as

huge boulders can be identified wandering downwards within the multi-temporal DEM analysis but the underlying transport process, permafrost related or gravitational mass wasting cannot be recognized. Distinct periglacial creeping features such as compression lobes, extension features or bound and unbound solifluction lobes are absent. Nevertheless, temperature data based on Gubler et al. (2011) suggest that the talus slope is situated in permafrost conditions thus the material is probably transported by permafrost creep before it is incorporated into the rockglacier.

8.4.3 Rockglaciers

Following the systemic concept introduced in Sect. 8.3.1 the rockglaciers develop out of frozen talus slope material and show no direct input from the headwall. The horizontal velocities of the rockglaciers are in average 0.09 m/a for Murtèl rockglacier and 0.15 m/a for Marmugnun rockglacier (see Table 15). The distribution of the rockglacier velocities over a three year period are depicted in a transect from the front to the rooting zone in Fig. 21 and show the highest velocities at the rockglacier front. Due to their high storage capacity, the rockglaciers transport the highest volume of sediment during a year within the system although the dominant process of permafrost creep shows only slow horizontal velocities (see Table 14). The GW is calculated for both rockglaciers separately using different vertical distances traveled (app. 0.02 m/a for Murtèl and 0.05 m/a for Marmugnun).Murtèl rockglacier generates only 0.81 GJ of GW although the landform mobilizes $1.49*10^6$ m^3 of sediment per year. Marmugnun rockglacier which mobilizes $0.45*10^6$ m^3 of sediment generates 0.62 GJ of GW. Marmugnun rockglacier shows higher vertical velocities per year than Murtèl which account for the similar GW generated. The combined GW of 1.44 GJ released by the rockglaciers accounts for only 1.2% of the GW released in the entire mountain slope although the rockglacier mobilize 99% of the coarse debris system.
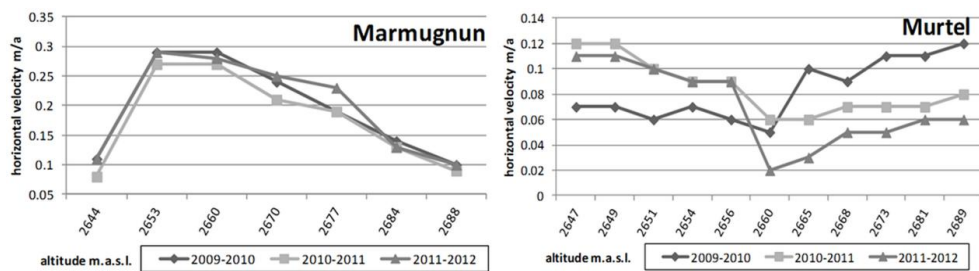

Figure 21: Annual horizontal velocities of selected blocks (in a transect from the front to the rooting zone) at the rockglaciers Marmugnun and Murtèl . The measurements were taken by terrestrial geodetic survey (TSPs).

8.5   Discussion

This study investigates the mass and energy transfers of an entire periglacial mountain slope. The method of quantifying volume mobilization and accumulation in steep areas is multi-temporal terrestrial laser scanning which allows for the discrete localization of mobilized and accumulated material. Unfortunately, the characteristic of the site in combination with the TLS does not enable distinction to be made between material which is freshly produced by backweathering of bedrock and the relocation of temporarily accumulated debris within the headwall. In the case of a vertical rockwall, all of the supplied material at the talus slope would be freshly eroded material because almost no intermediate storages exist in vertical rockwalls. Therefore, the quantification of dynamic material in the headwall using TLS data includes the freshly eroded material supplied by the bedrock as well as the remobilized material from intermediate storages. The complexity of the headwall topography prohibits the mapping of all intermediate storages. Nevertheless, the approach introduced permits the spatial discrete analysis of mobilized and accumulated volume. This allows investigating the dynamics within the system, differentiating active from inactive areas and tracking changes of process domains over time. In case of the headwall, the discrepancy between the mobilized and accumulated volume (effective volume in Table 14) represents the volume of material transferred to the talus slope. Traditionally, mobilized rockwall material is quantified using rockfall collectors at the foot of the rockwall which gather the transported material (Krautblatter et al., 2012, Rapp, 1960). The volume derived from this approach yields 658.9 m^3 of material into the next subsystem which translates into a backweathering rate of the headwall of 2 mm/a. This backweathering rate is consistent with values presented in Glade (2005) and Krautblatter et al. (2012) but the TLS analysis shows that the actual mobilized material in the headwall is much higher than the input in the next subsystem would suggest. This is also in accordance with Krautblatter and Dikau (2007) and Matsuoka (2008) who emphasize the importance of intermediate storage of loose material in step rockfalls. Therefore it is questionable how well rock collector experiments really quantify the material produced by the rockwall or if they underestimate the volumes stored in intermediate storages.

The geomorphic work derived from mobilized sediment volumes is presented in two measures: released geomorphic work and effective geomorphic work. In order to calculate the geomorphic work it is assumed that the entire mobilized material generates energy by covering the vertical distance to the next subsystem. This overestimates the amount of energy released because the majority of the mobilized material in the headwall is just

relocated and not transferred the entire vertical distance to the talus slope. The discrepancy between the total GW released in the headwall and the GW stored in intermediate storages (`negative` geomorphic work in the headwall) is transferred to the next compartment in the energy cascade. This effective GW is comparable to values presented in other studies. Geomorphic work in mountain systems has been thoroughly assessed in Krautblatter et al. (2012) and the study gives also a good overview over geomorphic work literature. The values presented by other studies are significantly lower than the results presented here but there are only a few comparable datasets available. Most of the geomorphic work studies focus on single processes such as solution (Groves and Meiman, 2005), debris flows (Lewkowicz and Hartshorn, 1998) and selected mass movements (Beylich, 2000). This study is the first to include a spatially differentiated analysis of the geomorphic work generated. Therefore it is possible to describe the released geomorphic work depending on the actual vertical distance travelled. Although the exact vertical distance per pixel cannot be derived, the released energy can serve as a value of potential energy stored in the entire headwall system.

The effective energy of 29.8 GJ/a in the headwall for mass movement of the entire coarse debris system also agrees with values presented in Krautblatter et al. (2012) who calculate 67.1 (±25.7) GJ/a for a rockwall of 4.1 km² vertical extension. In order to define a uniform measure and allow for comparison, the geomorphic work generated is referenced over the entire rockwall. The power released in the entire rockwall covers a vertical extension of 0.3 km². This translates into 99.6 GJ/km² which is five times as high as the geomorphic work presented in Krautblatter et al., 2012 but probably due to the greater vertical distances covered and faster process rates in high mountain environments.

With the introduced cascading approach it is possible to assess each of the subsystems individually but also in relation to the other. Thus a backweathering rate of 2 mm can be derived for the headwall and an energy transfer of 29.9 GJ from the headwall to the slope, 4 GJ from the talus slope to rockglacier where 1.44 GJ of geomorphic work are released by the downwards creep of the landform. In the entire system geomorphic work of 35.3 GJ was effectively released which shows that most of the geomorphic work stays within the subsystems and is not transferred from one subsystem to another. Therefore massive storages of mass and energy persist in the subsystems which are available for mobilization. The approach using TLS and photogrammetrically derived DEM differencing allows for the quantification of vertical changes and their derivable measures (volume, energy, etc). These changes can result mainly from mass movement (which holds true for the headwall) but other vertical changes due to melt out of subsurface ice or mass transport by other processes

such as permafrost creep cannot be addressed. Since there is no spatial subsidence detected on the talus slope which would correspond with the melt out of subsurface ice and field observations have shown that there are no creeping structures visible, it is feasible to assume that the elevation changes are solely caused by deposited material.

The majority of material is mobilized within the rockglaciers, mainly by the Murtèl rockglacier which by itself holds a volume of 1.4 x 10^6 m^3. Due to their rather slow movement and low inclination the rockglaciers only contribute 1.4 GJ of geomorphic work to the entire system. Because of borehole information, the volume of Murtèl rockglacier is accurately determinable and therefore the geomorphic work precisely calculable. In the case of Marmugnun, where there is no borehole existing, the method to evaluate the thickness is not as precise. But even if the volume of Marmugnun was underestimated by 50% the rockglaciers would only contribute 2.06 GJ of geomorphic work to the system.

8.6 Conclusion

This study introduces a multi-sensoral approach to assess the sediment and energy transfer of the coarse debris system within a periglacial high mountain slope. The sediment cascade is divided in three subsystems based on dominant processes and topographical features. We show that a combination of observational methods is necessary to analyze each subsystem due to their specific topography and processes. TLS is the method of choice to assess steep rockwalls and talus slopes whereas a combination of terrestrial surveying and airborne photogrammetry has proven to show good results for rockglacier analysis (PERMOS, 2010). We quantify and locate the volume of material and energy mobilized within each subsystem but also the amount of material and energy which is kept and/or relocated within a subsystem. The discrepancy between mobilized and retained mass and energy lets us estimate the transfer between the subsystems but also the energy generated within the entire system. The entire system from headwall to rockglacier mobilizes 1.95 x 10^6 m^3 material which generate 118.8 GJ of geomorphic work of which only 35.3 GJ (658.9 m^3) are effectively transferred between the subsystems and the rest is retained in intermediate storages. The highest amount of energy (100.9 GJ, 29.9 GJ effectively) is released within the headwall whereas the rockglaciers are mobilizing the highest amount of sediment (1.93 mill. m3) but contribute only 1.44 GJ of geomorphic work. This pattern highlights that a rockglacier can be considered a long lasting sediment sink: it stores sediment, but it is often not connected to streams or other sediment paths downstream. Thus rockglaciers are probably one of the best and long-lived sediment stores during interglacials. The values presented here are significantly higher than in comparable studies which is due to the spatially discrete data of

119

the observation methods and the vertical dimension of the headwall. The spatially discrete data also allows locating active and inactive areas. The highest parts of the rockwall have been identified as most active which explains the high amounts of energy released by the headwall.

The methodical approach introduced has previously not been applied to quantify sediment transfer and geomorphic work in an entire periglacial high mountain slopes and we showed that the results for the subsystems are mostly higher than the results generated by traditional methods. Additional studies in similar environments will show how the results presented here can be conclusively interpreted.

8.7 Acknowledgements

8.8   References

Avian, M., Kellerer-Pirklbauer, A., Bauer, A., 2009. LiDAR for monitoring mass movements in permafrost environments at the cirque Hinteres Langtal, Austria, between 2000 and 2008. Nat. Hazards Earth Syst. Sci. 9, 1087–1094. doi: 10.5194/nhess-9-1087-2009.

Barsch, D., 1996. Rockglaciers: Permafrost Creep and Rockglaciers. Springer, Berlin, 331 pp.

Barsch, D., Caine, N., 1984. The Nature of Mountain Geomorphology. Mountain research and development 4, 287–298.

Barsch, D., Jakob, M., 1998. Mass transport by active rockglaciers in the Khumbu Himalaya. Geomorphology 26, 215–222. doi: 10.1016/S0169-555X(98)00060-9.

Beylich, A., 2000. Geomorphology, sediment budget, and relief development in Austdalur, Austfiroir, East Iceland. Arctic, Antarctic, and Alpine Research 32, 466–477.

Beylich, A., Warburton, J. (Eds.), 2007. Analysis of Source-to-Sink-Fluxes and Sediment Budgets in Changing High-Latitude and High-Altitude Cold Environments: SEDIFLUX Manual. First Edition. NGU Report 2007.053. 158pp.

Bodin, X., Thibert, E., Fabre, D., Ribolini, A., Schoeneich, P., Francou, B., Reynaud, L., Fort, M., 2009. Two decades of responses (1986 - 2006) to climate by the Laurichard rock glacier, French Alps. Permafrost Periglacial Processes. 20, 331–344. doi: 10.1002/ppp.665.

Caine, N., 1974. The geomorphic processes of the Alpine environment., In: Ives, J.D., Barry, R. (Eds.), Arctic and Alpine Environments. Methuen, London, pp. 721–748.

Caine, N., 1976. A uniform measure of subaerial erosion. Geological Society of America Bulletin 87 137-140.

Caine, N., Swanson, F.J., 1989. Geomorphic coupling of hillslope and channel systems in two small mountain basins. Zeitschrift für Geomorphologie 33, 189–203.

Campbell, D., Church, M., 2003. Reconnaissance sediment budgets for Lynn Valley, British Columbia: Holocene and contemporary time scales. Canadian Journal of Earth Sciences 40, 701–713.

Chorley, R.J., Kennedy, B.A., 1971. Physical geography: A systems approach. Prentice-Hall, Hemel Hempstead, pp 370. doi: 10.1002/qj.49709841818

Church, M., Slaymaker, O., 1989. Disequilibrium of Holocene sediment yield in glaciated British Columbia. Nature 337 , 452–454. doi: 10.1038/337452a0.

Costa, J.E., O'Connor, J.E., 1995. Geomorphically effective floods, In: Costa, J.E. (Ed.), Natural and Anthropogenic Influences in Fluvial Geomorphology, Geophys. Monogr. Ser., vol. 89. AGU, Washington, DC, pp. 45–56.

Delaloye, R., Lambiel, C., Gärtner-Roer, I., 2010. Overview of rock glacier kinematics research in the Swiss Alps: seasonal rhythm, interannual variations and trends over several decades. Geographica Helvetica 65, 135–145.

Dietrich, W., Dunne, T., 1978. Sediment budget for a small catchment in mountainous terrain., In: Slaymaker, O., Rapp, A., Dunne, T. (Eds.), Field Instrumentation and Geomorphological Problems. Schweizerbart'sche Verlagsbuchhandlung, Stuttgart, pp. 191–206.

Fryirs, K.A., Brierley, G.J., Preston, N.J., Kasai, M., 2007. Buffers, barriers and blankets: The (dis)connectivity of catchment-scale sediment cascades. Catena70, 49–67.

Gärtner-Roer, I., 2012. Sediment transfer rates of two active rockglaciers in the Swiss Alps. Geomorphology 167–168, 45–50. doi: 10.1016/j.geomorph.2012.04.013.

Gärtner-Roer, I., Nyenhuis, M., 2010. Volume estimation, kinematics and sediment transfer rates of active rockglaciers in the Turtmann Valley, Switzerland, In: Otto, J.-C., Dikau, R. (Eds.), Landform - structure, evolution, process control. Proceedings of the International Symposium on Landform organised by the Research Training Group 437. Springer, Berlin, pp. 185–198.

Glade, T., 2005. Linking debris-flow hazard assessments with geomorphology. Geomorphology 66, 189–213.Groves, C., Meiman, J., 2005. Weathering, geomorphic work, and karst landscape evolution in the Cave City groundwater basin, Mammoth Cave, Kentucky. Geomorphology 67, 115–126. doi: 10.1016/j.geomorph.2004.07.008.

Gubler, S., Fiddes, J., Keller, M., Gruber, S., 2011. Scale-dependent measurement and analysis of ground surface temperature variability in alpine terrain. The Cryosphere 5, 431–443. doi: 10.5194/tc-5-431-2011.

Haeberli, W., 1985. Creep of mountain permafrost: Internal structure and flow of alpine rock glaciers. Mitteilungen der VAW/ETH Zürich 77. 142 pp

Haeberli, W., Hoelzle, M., Kääb, A., Keller, F., Vonder Mühll, D., Wagner, S. 1998. Ten years after drilling through the permafrost of the active rock glacier Murtèl, Eastern Swiss Alps: answered questions and new perspectives. In: Lewkowicz, A. G. and Allard, M. (Editor), 7th International Conference on Permafrost. Proceedings. Collection Nordicana. Yellowknife, Canada, pp. 403-410.

Haeberli, W., Beniston, M., 1998. Climate Change and Its Impacts on Glaciers and Permafrost in the Alps. Ambio 27, 258–265.Haeberli, W., Hallet, B., Arenson, L., Elconin, R., Humlun, O., Kaab, A., Kaufmann, V., Ladanyi, B., Matsuoka, N., Springman, S., Vonder Muhll, D., 2006. Permafrost creep and rock glacier dynamics. Permafrost and Periglacial Processes 17, 189-214

Heckmann, T., Bimböse, M., Krautblatter, M., Haas, F., Becht, M., Morche, D., 2012. From geotechnical analysis to quantification and modelling using LiDAR data: a study on rockfall in the Reintal catchment, Bavarian Alps, Germany. Earth Surf. Process. Landforms 37, 119–133. doi: 10.1002/esp.2250.

Hooke, J., 2003. Coarse sediment connectivity in river channel systems: A conceptual framework and methodology. Geomorphology 56, 79–94.

Hoelzle, M., Mühll, D.V., Haeberli, W., 2002. Thirty years of permafrost research in the Corvatsch- Furtschellas area, Eastern Swiss Alps: A review. Norsk Geografisk Tidsskrift - Norwegian Journal of Geography 56, 137–145. doi: 10.1080/002919502760056468.

Humlum, O., 2000. The geomorphic significance of rock glaciers: estimates of rock glacier debris volumes and headwall recession rates in West Greenland. Geomorphology 35, 41–67. doi: 10.1016/S0169-555X(00)00022-2.

Humlum, O., Christiansen, H.H., Juliussen, H., 2007. Avalanche-derived rock glaciers in Svalbard. Permafrost and Periglacial Processes 18, 75- 88.

Isaksen, K., Ødegård, R.S., Eiken, T., Sollid, J.L., 2000. Composition, flow and development of two tongue-shaped rock glaciers in the permafrost of Svalbard. Permafrost and Periglacial Processes 11, 241- 257.

Jordan, P. and Slaymaker, O., 1991. Holocene sediment production in Lillooet River basin: a sediment budget approach. Geographie physique et Quaternaire 45, 45-57.

Kääb, A., Vollmer, M., 2000. Surface Geometry, Thickness Changes and Flow Fields on Creeping Mountain Permafrost: Automatic Extraction by Digital Image Analysis. Permafrost Periglacial Process 11, 315–326. doi: 10.1002/1099-1530(200012)11:4<315:AID-PPP365>3.0.CO;2-J.

Kenner, R., Phillips, M., Danioth, C., Denier, C., Thee, P., Zgraggen, A., 2011. Investigation of rock and ice loss in a recently deglaciated mountain rock wall using terrestrial laser scanning: Gemsstock, Swiss Alps. Cold Regions Science and Technology 67, 157–164. doi: 10.1016/j.coldregions.2011.04.006.

Krautblatter, M., Dikau, R., 2007. Towards a uniform concept for the comparison and extrapolation of rockwall retreat and rockfall supply. Geografiska Annaler A 89, 21–40.

Krautblatter, M., Moser, M.,. Schrott, L., Wolf, L., Morche, D., 2012. Significance of rockfall magnitude and carbonate dissolution for rock slope erosion and geomorphic work on Alpine limestone cliffs (Reintal, German Alps). Geomorphology 167–168, 21–34.

Lewkowicz, A., Hartshorn, J., 1998. Terrestrial record of rapid mass movements in the Sawtooth Range, Ellesmere Island, Northwest Territories, Canada. Canadian Journal of Earth Sciences 35, 55–64.

Lim, M., Rosser, N., Allison, R., Petley, D., 2010. Erosional processes in the hard rock coastal cliffs at Staithes, North Yorkshire. Geomorphology 114, 12–21.

Matsuoka, N., 2008. Frost weathering and rockwall erosion in the southeastern Swiss Alps: Long-term (1994-2006) observations. Geomorphology 99, 353-368.

Oppikofer, T., Jaboyedoff, M., Keusen, H.-R., 2008. Collapse at the eastern Eiger flank in the Swiss Alps. Nature Geoscience 1, 531–535.

Oppikofer, T., Jaboyedoff, M., Blikra, L., Derron, M.-H., Metzger, R., 2009. Characterization and monitoring of the Åknes rockslide using terrestrial laser scanning. Natural Hazards and Earth System Science 9, 1003–1019.

Oppikofer, T., Jaboyedoff, M., Pedrazzini, A., Derron, M.-H., Blikra, L.H., 2011. Detailed DEM analysis of a rockslide scar to characterize the basal sliding surface of active rockslides. Journal of Geophysical Research: Earth Surface 116, doi: 10.1029/2010JF001807.

PERMOS, 2010. Permafrost in Switzerland 2006/2007 and 2007/2008, In: Noetzli, J., Vonder Mühll, D. (Eds.), Glaciological Report Permafrost No. 8/9 of the Cryospheric Commission of the Swiss Academy of Science., 68 pp.

Rabatel, A., Deline, P., Jaillet, S., Ravanel, L., 2008. Rock falls in high-alpine rock walls quantified by terrestrial lidar measurements: A case study in the Mont Blanc area. Geophysical research letters 35 L10502, doi:10.1029/2008GL03342410.1029/2008GL033424.

Rapp, A. Recent Development of Mountain Slopes in Kärkevagge and Surroundings, Northern Scandinavia. In: Geografiska Annaler 17, pp. 71–200.

Dubois, J.-M.M. (2000), Rapid evaluation of sediment budgets by Leslie M. Reid and Thomas Dunne, Catena Verlag, Reiskirchen, 164 pp.Roer, I., 2007. Rockglacier kinematics in a high mountain geosystem. Bonner Geograpische Abhandlungen 117,pp 217.

Roer, I., Kääb, A., Dikau, R., 2005. Rockglacier kinematics derived from small-scale aerial photography and digital airborne pushbroom imagery. Zeitschrift für Geomorphologie 49, 73–87.

Roer, I., Avian, W., Kaufmann, V., Delaloye, R., Lambiel, C., Kääb, A., 2008. Observations and considerations on destabilizing active rock glaciers in the European Alps., In: Kane, D.L., Hinkel, K.M. (eds.) Proceedings of the 9th International Conference on Permafrost,

University of Alaska, Fairbanks, Alaska, June 29 - July 3, 2008. Institute of Northern Engineering, University of Alaska, Fairbanks, Fairbanks, Alaska, pp. 1505–1510.

Sass, O., 2005. Spatial patterns of rockfall intensity in the northern Alps. Zeitschrift für Geomorphologie Suppl. Vol. 138, 51-65. Schneider, S., Hoelzle, M., Hauck, C., 2012. Influence of surface and subsurface heterogeneity on observed borehole temperatures at a mountain permafrost site in the Upper Engadine, Swiss Alps. The Cryosphere 6, 517–531. doi: 10.5194/tc-6-517-2012.

Schrott, L., Hufschmidt, G., Hankammer, M., Hoffmann, T., Dikau, R., 2003. Spatial distribution of sediment storage types and quantification of valley fill deposits in an alpine basin, Reintal, Bavarian Alps, Germany. Geomorphology 55, 45-63.

Springman, S.M., Yamamoto, Y., Buchli, T., Hertrich, M., Maurer, H., Merz, K., Gärtner-Roer, I., Seward, L., 2013. Rock Glacier Degradation and Instabilities in the European Alps: A Characterisation and Monitoring Experiment in the Turtmanntal, CH. In: Margottini, C., Canuti, P., Sassa, K. (Eds.), Landslide Science and Practice. Springer Berlin Heidelberg, Berlin, Heidelberg, pp. 5–13.

Tarbuck, E., Lutgens, F., 2011. Earth: an introduction to physical geology. 10th ed. Prentice hall. 724 pp.

Wolman, M.G., Gerson, R., 1978. Relative scales of time and effectiveness of climate in watershed geomorphology. Earth Surface Processes 3, 189-208. doi: 10.1002/esp.3290030207.

9   Publication III

Müller, J., Vieli, A., Gärtner-Roer, I., 2016. Rockglaciers on the run - Understanding rockglacier landform evolution and recent changes from numerical flow modeling. The Cryosphere Discussions, (in review).

The author's contribution to the article:

J. Müller collected and processed the data, developed the methodology, designed the study, performed the analysis and wrote the manuscript. I. Gärtner-Roer designed the study, developed the methodology and collected data. A. Vieli developed the methodology, designed the study and wrote the manuscript.

Abstract

Rockglaciers are landforms indicative of permafrost creep and received considerable attention concerning their dynamical and thermal changes. Observed changes in rockglacier motion on seasonal to decadal timescales and have been related to ground temperature variations and related changes in landform geometries interpreted as signs of degradation due to climate warming. Despite the extensive kinematic and thermal monitoring of these creeping permafrost landforms, our understanding of the controlling factors remains limited and lacks robust quantitative models for rockglacier evolution in relation to their environmental setting.

Here, we use a holistic approach to analyze the current and long-term dynamical development of two rock glaciers in the Swiss Alps. A numerical flow model, that couples the process chain from material deposition to rockglacier flow, is presented and is able to reproduce observed rockglacier geometries and their general dynamics. Modelling experiments exploring the impact of variations in rockglacier temperature and sediment/ice supply show that these forcing processes are not sufficient for explaining the currently observed short-term geometrical changes derived from multi-temporal digital terrain models at the two different rockglacier. The modelling also shows that rockglacier thickness is dominantly controlled by slope and rheology while the advance rates are mostly constraint by rates of sediment/ice supply. Further, timescales of dynamical adjustment are found to be strongly linked to creep velocity. Overall, we provide a useful modelling framework for a better understanding of the dynamical response and morphological changes of rockglaciers to changes in external forcing..

9.1   Introduction

Rockglaciers and their dynamics have received much attention in permafrost research and beyond, most prominently by the International Panel on Climate Change (IPCC) in context of impacts of a warming climate on high mountain permafrost (IPCC, 2014). Time series of rockglacier movement in the European Alps indicate acceleration in permafrost creep over the last decades related to an increase in ground temperatures (Delaloye et al., 2010b, PERMOS, 2013, Bodin et al., 2015). Further, multi-temporal geomorphometric analysis have shown subsidence features and structural disintegration of alpine rockglaciers which are indicative of landform degradation and destabilization (Kääb et al., 2007, Roer et al., 2008b, Bodin et al., 2010, Springman et al., 2013, Micheletti et al., 2015). Many studies have addressed the connection between mean annual air temperatures (MAAT) and rockglacier dynamics from a descriptive point of view (Ikeda and Matsuoka, 2002a, Roer et al., 2005a, Delaloye et al., 2010b, Springman et al., 2012) or have used modeling approaches to assess rockglacier dynamics (Jansen and Hergarten, 2006, Kääb et al., 2007, Springman et al., 2012). Most of these studies focus on the process of permafrost creep in relation to air or ground temperature in order to assess rockglacier creep. Other authors stressed that rockglacier dynamics cannot solely be explained by temperature variations and should integrate flow and controlling environmental factors such as sediment supply dynamics and landform characteristics (Roer et al., 2005a, French, 2007, Frauenfelder et al., 2008). Rockglaciers have been defined as 'lobate or tongue-shaped bodies of perennially frozen unconsolidated material supersaturated with interstitial ice and ice lenses that move down slope or down valley by creep as a consequence of the deformation of ice contained in them and which are, thus, features of cohesive flow' (Barsch, 1992, p. 176). Such a definition includes information on form, material and process and therefore, the observable rockglacier characteristics are influenced by sediment and ice input, permafrost conditions and the geomorphological setting which in turn control rheology and landform geometry (Barsch, 1996). Very few studies have addressed rockglacier dynamics in such a holistic approach including backweathering rates, sediment and ice dynamics, and climate variations to gain insight into the long-term evolution of rockglaciers (Olyphant, 1983, Frauenfelder et al., 2008) and were limited regarding validation by observational data.

Recent observations show signs of rockglacier destabilization such as acceleration, subsidence features and structural disintegration (forming of crevasses) at several rockglacier landforms in the Swiss Alps (Kääb et al., 2007, Roer et al., 2008b, Delaloye et al., 2011, Lambiel, 2011, Springman et al., 2013, PERMOS, 2013, Kenner et al., 2014, Bodin et al.,

2015). These studies indicate that various factors can lead to such degradation but a common triggering for all the cases has not been identified. These potential factors are most likely connected to the complex combination of the local topography, the thermal state of the permafrost (climate-induced response) and/or to variations in the sedimentation regime affecting the sediment load during long-term landform evolution.

Numerous remote sensing techniques are available for acquiring data on permafrost creep (see Haeberli et al., 2006 and Kääb, 2008 for an extensive summary), high mountain geomorphometry (Bishop et al., 2003) and high mountain sediment dynamics (Gärtner-Roer, 2012, Heckmann and Schwanghart, 2013, Müller et al., 2014a). This provides the necessary constraints for a holistic assessment strategy that includes the coupling of relevant landforms and processes and in which sediment supply rates can be quantified, ice volumes estimated and rockglacier rheologies derived (Frauenfelder et al., 2008, Gärtner-Roer and Nyenhuis, 2010).

Here we present such a holistic analysis approach to assess long-term rockglacier evolution and the impacts of variations in temperature, sediment and ice supply on rockglacier geometry and movement. We apply a numerical flow model to two rockglaciers in the Swiss Alps with different topographical, morphometrical and rheological characteristics. The modeling is motivated by observations of topographic and kinematic changes for the two rockglaciers revealing signs of degradation as presented in this study. The aim of the modeling approach is to relate these changes to long-term evolution and short-term adaptation of rockglacier systems to changing environmental factors and ultimately to a better understanding of the currently observed dominant controls of kinematic and morphological changes. We thereby consider rockglaciers as an integral part of a coarse-debris cascading system in periglacial environments.

9.2   Conceptional approach to high mountain periglacial systems

The topographical evolution of the rockglacier landform relies on the production, transportation and deposition of coarse debris in the periglacial system and the generation and integration of subsurface ice (Wahrhaftig & Cox 1959, Barsch, 1996). The development of rockglaciers is therefore dependent upon the supply of debris from the source headwall(s) and the long-term preservation of an ice matrix or ice core inducing creep (Morris, 1981). Rockglaciers are also dynamic landforms that are influenced by the warming and melting of

ice and changes in sediment input. The variations in environmental factors translate into observable changes in geometry and kinematics which can be interpreted as a sign for degradation and/or destabilisation of these permafrost landforms (Roer et al., 2008b, Springman et al., 2013).

Figure 22 shows the theoretical concept of an idealized periglacial mountain slope with a corresponding rockglacier system and builds the conceptual basis for this study. Two main subsystems contribute to the temporal and topographical development of the rockglacier landforms: The upper headwall and talus slope system generate the sediments which are transported into the lower rockglacier system. The rockglacier system is besides the sediment input also controlled by the existence, generation and state of subsurface ice and permafrost creep (see Fig. 22). The two subsystems differ on the basis of several characteristics: topographic features, typical landform(s) and the dominating mass transporting processes. Backweathering of the exposed rockwall and resulting rockfall are the most effective mass wasting processes (e.g. Krautblatter et al., 2012, Müller et al., 2014a) and supply the entire system with sediment. Backweathering rates and rockwall dynamics are strongly influenced by the geological structures, lithological conditions as well as characteristics and dynamics of cleft ice which are in turn thermally controlled (Hasler et al., 2012). The progressive accumulation of sediment and ice on an inclined surface at the foot of the rockwall under permafrost conditions, leads to permafrost creep and develops into a rockglacier (Barsch, 1992, Haeberli et al., 2006). The existence of ice and its properties within the sediment obviously plays an important role as process agent in these systems and environmental changes influence erosion and transport processes and result therefore in topographical and kinematic changes. (White, 1973, Arenson et al., 2004, Haeberli et al., 2006).
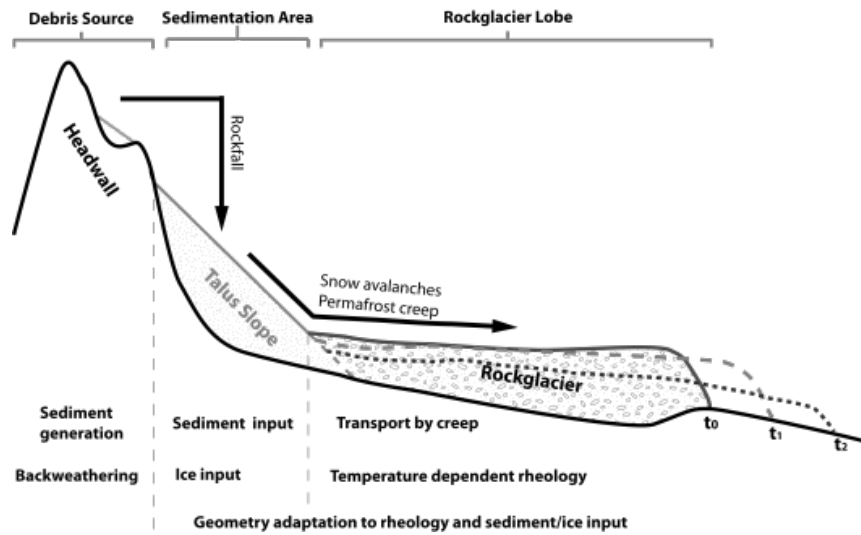
Figure 22: Conceptual model of the dynamic evolution of a rockglacier system. Black arrows show the sediment transport. t0, t1 and t2 show the rockglacier surface geometries at different time-steps resulting from variations in environmental factors such as warming and a decrease of sediment/ice input.

We transfer this conceptual approach into a numerical flow model that integrates the whole debris process chain and couples the different subsystems and related mass fluxes. It assumes a uniform sediment and ice input from the rockwall to an inclined surface, builds up a talus slope that is supersaturated with ice and then starts to creep as a viscous non-linear media similar to ice. This rheological assumption has repeatedly been used to assess rockglacier kinematics (Wahrhaftig and Cox, 1959, Olyphant, 1983, Whalley and Martin, 1992, Barsch, 1996, Kääb et al., 2007, Frauenfelder et al., 2008). A few studies e.g. Olyphant (1983), Wagner (1992), Leysinger-Vieli and Gudmundsson (2003) and Frehner et al. (2015) have demonstrated that such a rheology can in principal be used in a numerical flow model for rockglaciers.

9.3 Recent observations of rockglacier change

The modeling work in this study is motivated by detailed observations of geometric changes of two rockglacier systems both in Switzerland. We present in this section comprehensive new datasets of the two landforms, rockglacier Huhh1 in the Turtmann valley and the well studied Murtèl rockglacier in the Engadine. Both show changes in surface geometry and kinematic behaviour but have distinctly different landform characteristics (see Tab. 16 for an overview). In order to assess the controlling mechanisms of rockglacier evolution and potential degradation, we use a "backward" approach: We quantify and discuss distinct observed changes in surface geometry and kinematics of the two rockglaciers, propose potential controlling forcing factors (sediment and ice input as well as ground temperature) and then assess these observations and related forcings with a numerical creep model.

Table 16: Characteristics of the two selected rockglaciers (excluding their talus slopes).

	Murtèl rockglacier	Huhh1 rockglacier
Average thickness	30 m	12 m
Length	280 m	310 m
Slope	12°	27°
Age	~ 5000- 6000 a	~600 a
Hor. Velocity	0.06 -0.13ma^{-1}	0.75 - 1.55 m a^{-1}
Headwall area	74687.1 m^2	82781.6 m^2
Depositing area	45930.8 m^2	32355.5 m^2

9.3.1 Murtèl rockglacier, upper Engadine

The first rockglacier site is the well-studied Murtèl (UTM 563'112, 5'142'072 (zone 32T))(Hoelzle et al. 2002, Haeberli et al. 2006, Springman et al. 2012,) situated below the northern face of Piz Corvatsch (3300 m a.s.l.) in the upper Engadine, in the south-eastern part of Switzerland. The lithology mainly consists of granite and granodiorite. The density of the in-situ rock types are based on values given in the literature with a density of 2.65-2.75 kg cm^{-3} for granite and 2.7-2.8 kg m^{-3} for granodiorite (Tarbuck et al. 2011). Studies on backweathering at this site have shown backweathering rates of 2mm a^{-1} (Müller et al., 2014a). Murtèl is one of the best investigated rockglaciers and observations from this permafrost site have been discussed in great detail (see summary in Haeberli et al., 1998). As part of the PERMOS network (Permafrost Monitoring Switzerland), parameters such as borehole temperatures, ground surface temperatures and horizontal velocity are monitored since 1987 (Vonder Mühll et al., 2008). Borehole data also revealed a layered internal

structure with a shear horizon in 32 m depth where almost all of the deformation takes place (Haeberli et al., 1998). Attempts to determine the age of this rockglacier (Haeberli et al. 1999, Laustela et al. 2003) obtained an age of 5000 to 6000 years as a minimum value (Haeberli et al., 2003). These values were calculated from present day surface velocity fields assuming constant environmental conditions over the rockglacier development (Kääb und Vollmer 2000, Frauenfelder and Kääb, 2000, Haeberli et al 2003). The rockglacier is characterized by rather slow creep velocity (0.06-0.13 m a^{-1}) and is considered a thick and ice rich landform with volumetric ice contents of 60% (Haeberli et al., 1998, Arenson et al., 2002).

9.3.2 Huhh1 rockglacier, Turtmann Valley, Valais

The second rockglacier is located in one of the hanging valleys of the Turtmann Valley, a tributary of the Rhone valley in southern Switzerland (UTM 401'580, 5'116'471 (zone 32T)). The valley's lithology mainly consists of Palaeozoic gneisses and schists and based on this lithology rather constant backweathering rates of $2mma^{-1}$ are expected (Glade, 2005, Krautblatter et al., 2012, Müller et al., 2014a). The valley stretches from 2400 m a.s.l. to 3278 m a.s.l and is characterized by steep rockwalls, talus cones, a glacier, several moraines of different ages and multiple active and inactive rockglaciers (Roer and Nyenhuis, 2007). The focus within this study lies on the rockglacier Huhh1 which can be considered a thin, moderately fast moving rockglacier (see Tab. 16). This site is also part of the PERMOS network and has undergone several scientific assessments (Rasemann 2003, Roer, 2005, Nyenhuis et al. 2005). There is no direct subsurface information available but Gärtner-Roer (2012) used a semi-quantitative approach to derive the rockglacier thickness and sediment storage assuming an ice volume of 50%-70%. The age of the landform is estimated at 500-600 years using the same approach as Haeberli et al. (2003) and Kääb und Vollmer (2000), where the current velocity fields are assumed to be constant over the rockglacier evolution time span. Therefore the age estimates can be seen as minimum ages.

9.3.3 Observations of rockglacier dynamics

Complementary to the PERMOS related kinematic monitoring, we used a combination of remote sensing and terrestrial surveying methods for deriving multi-temporal elevation and displacement data in order to assess changes in geometry and creep.

Multi-temporal stereophotogrammetrically DEMs are available for the analysis between the years 1996 and 2007 for the Murtèl rockglacier. Five high resolutions DEMs have been generated in this study for the Turtmann valley between the years 2001 and 2010. For the

technical details on these DEMs an overview is given in Tab. 17. New elevation change maps are derived from differencing of the DEMs over the periods 1996 and 2007 for Murtèl and 2001 and 2012 for Huhh1. The limitations concerning processing, uncertainties and application are presented in Kääb and Vollmer (2000), Roer et al. (2005c), Roer and Nyenhuis (2007) and Müller et al. (2014b).and applied in this assessment.

Additionally, kinematic data is available for both rockglaciers from yearly terrestrial geodetic surveys of approximately 20 points as described in PERMOS (2013) and Roer (2005). Horizontal and vertical changes are quantified annually with an accuracy of 1–2 cm. The extracted vertical elevation change from these 3-dimensional displacement vectors is obtained from subtracting the surface-parallel component of the vertical displacement component.

Table 17: Airborne and terrestrial remote sensing data available at the rockglacier sites.

Data type	Murtèl	Huhh1
Airborne remote sensing (Photogrammetry and Airborne Laserscanning (ALS))	RC30 in 1996 (PERMOS) RC30 in 2002 (PERMOS) ALS in 2003 RC30 in 2007 (PERMOS)	HRSC-A in 2001 (Otto et al. 2007) RC 30 in 2005 (Roer 2005) ALS in 2007 (Müller et al. 2014a) ADS 40 in 2010 (Müller et al. 2014a) ADS 80 in 2012 (Müller et al. 2014a)
Geodetic Point Surveys	2009-2015 (annually)	2001-2015 (annually)

Based on the above DEMs, new elevation change maps have been derived for both rockglaciers and the subsystem units of the main rockglacier body and contributing talus slope have been identified (Fig. 23). This analysis (over decadal time periods) showed distinct subsidence features in the deposition area (outline with green in Fig. 23) of the rockglacier systems of different magnitudes. A more detailed assessment of the subsidence is shown in Fig. 24 where the histograms of the yearly subsidence in the deposition area (talus slope/sedimentation area) shows an overall negative average of annual subsidence of -0.04ma^{-1} for the Murtèl rockglacier and -0.16ma^{-1} for the Huhh1 rockglacier. Such subsidence features have been described as signs of permafrost degradation (Roer et al., 2008a, Springman et al., 2013, Bodin et al., 2015) and are assessed by the rockglacier evolution model in Sect. 9.6.2.4. These observed subsidence rates are calculated considering the uncertainties resulting from the DEM differencing (see Müller et al., 2014b). Additional vertical displacement data from terrestrial surveys conducted from 2001/2009 – 2015 corrected for slope parallel movement agree with the results from the DEM-differencing.

The main lobes of the rockglacier landforms (outlined red in Fig. 23) have also been analysed for subsidence, but the typical 'furrow and ridge structure' of the rockglacier and the topographical dynamics introduced by the creep process complicate the subsidence quantification. Depending on the methodology, annual average surface elevation change in the terminus area of the rockglaciers range from -0.03m a^{-1} (derived from terrestrial point surveys corrected for slope-parallel movement) to +0.01 m a^{-1} (digital photogrammetry) at Murtèl and -0.2 m a^{-1} (terrestrial point surveys corrected for slope) to +0.06 m a^{-1} (digital photogrammetry) at Huhh1. At the front of both rockglaciers, the elevation change signal is less clear and close to the measurement uncertainty and thus, no clear subsidence seems apparent.

Theoretically, subsidence features can result from surface lowering by ice melt (Phillips et al., 2009), reduced ice and sediment input, acceleration of the entire landform, potentially thermally-induced, leading to a 'creeping away' and thinning of the rockglacier from its feeding area or, and most likely, a combination of the above (Roer et al., 2005a).

Our elevation change data also shows the continuing advance of the rockglacier front and the "furrow and ridge" structure. This shows that the rockglacier continues to be active although it is probably no longer fully connected to its sediment source and therefore not in an equilibrium state with the current sedimentation and/or thermal state of the system.
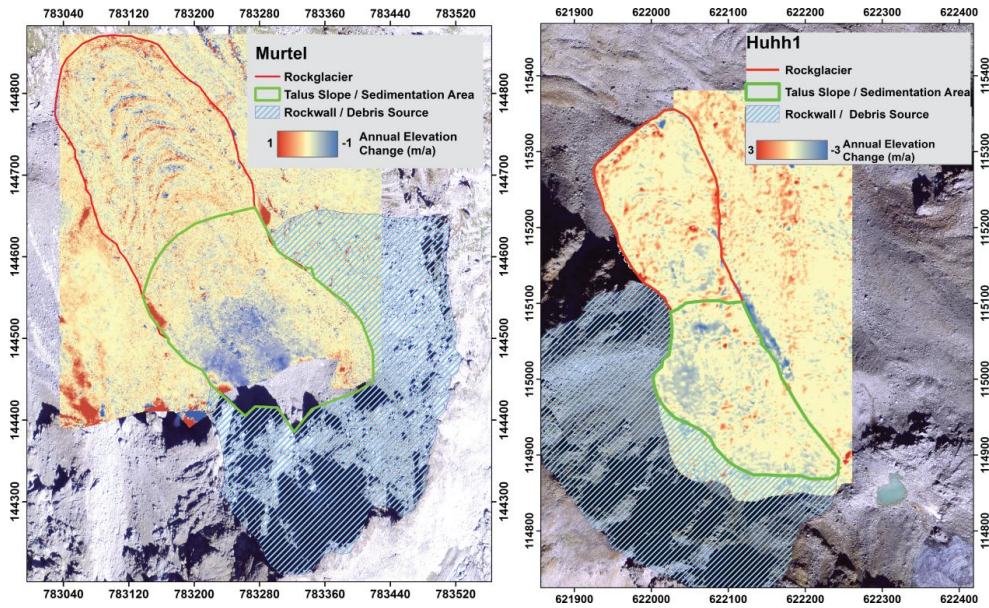
Figure 23: The Murtèl (left) and Huhh1 annual elevation change of the two rockglacier systems (right) including the geomorphic mapping of the subsystem units of the rockglacier lobe, the deposition area debris source area as outlined in Fig. 22 for Murtèl (period 1996-2007) and Huhh1 (period 2001-2012). The annual rates are derived from multi-sensoral and multi-temporal remote sensing products (Tab. 17) (Underlying the Swisstopo Swissimage.
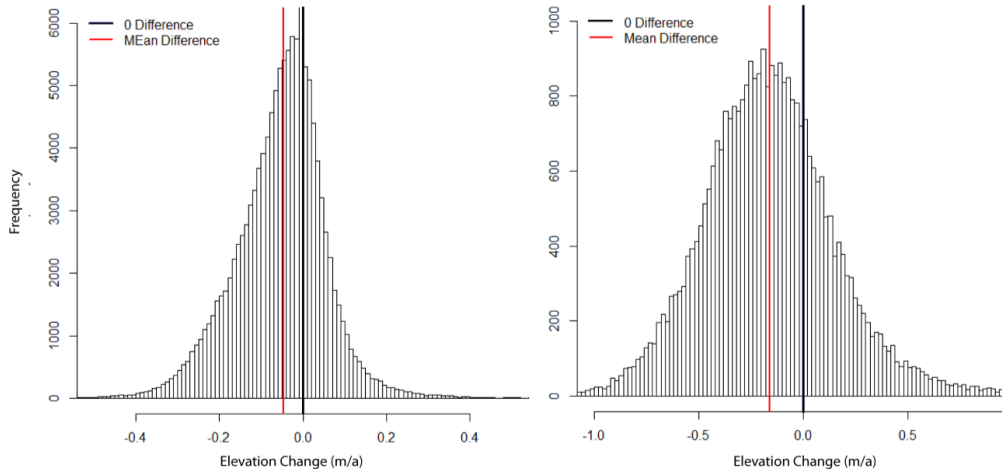

Figure 24: The frequency distribution of annual vertical surface change (m a^{-1}) from DEM-differencing in the talus slope/ sedimentation area of the two rockglacier systems. Both systems show negative mean values (red lines). The black lines refer to 0 m a^{-1} difference.

9.4   Rockglacier evolution- modeling approach

We present here a quantitative rockglacier evolution modeling approach that is based on the conservation of mass and includes the entire debris process chain in high mountain environments (see Fig. 22).

9.4.1   Geomorphological Setting

In order to initialize and evaluate the numerical model, it is necessary to derive geometrical information on the headwall, talus slope and rockglacier. Therefore, the two rockglacier sites have been analyzed according to the concept introduced in Sect. 9.2 for their along flow geometry and the quantification of sediment input and sediment deposition. Geomorphological mapping in the field as well as by interpretation of DEMs and orthophotos are used to identify the contributing headwall areas, deposition areas and rockglacier landforms (see Fig. 23). Surface features (e.g. slope, substrate) as well as velocity fields are further used to delimit the different subsystems.

The DEMs served as basis for geomorphometric analyses to determine spatial dimensions, slope, and surface geometry of the periglacial high mountain systems.

.

9.4.2   Rockglacier creep modeling approach

A 1-dimensional time-dependent numerical flow model is used to simulate the evolution of the rockglacier surface, length and creep velocity along the central flowline based on a given sediment/ice input and rockglacier rheology. In this study we are not aiming to reproduce the exact evolution or small scale geometric features of the two chosen real-world rockglaciers, but rather use the model to simulate the basic behaviour of a rockglacier body creeping down a slope and investigate the first order dynamic response of the geometry on changing external factors such as temperature and sediment supply. Specifically, we will investigate potential causes for the observed surface geometry changes (subsidence, front advance and velocity variations) as set out above (Sect. 9.3.3)

Rockglacier creep

For our study we therefore reduce the rheology of the rockglacier to a body of frozen together sediment that deforms and creeps like a non-linear viscous material under the influence of gravity as proposed already in 1959 by Wahrhaftig and Cox (1959) and applied similarly by Olyphant (1983) and Frauenfelder et al. (2008). This rheology can be described

by a Glen-type flow law (Glen, 1955) as typically used for glacier ice (Cuffey and Paterson, 2010) which relates the strain rate $\dot{\varepsilon}$ non-linearly to the stress τ

$$\dot{\varepsilon} \propto A\tau^n \tag{1}$$

where n is a flow law exponent that is typically between 2 and 3 for frozen material (Paterson, 2010) and A the rate factor describing the softness of the rockglacier material. Such a constitutive relationship has been applied and discussed in other studies on rockglacier creep (Olyphant, 1983, Whalley und Martin, 1992, Whalley und Azizi, 1994, Barsch 1996, Azizi und Whalley, 1996, Kääb et al., 2007, Frauenfelder et al., 2008) and further supported by results from borehole measurements and shear experiments in the laboratory on real world rockglaciers (including Murtèl rockglacier; Arenson et al., 2002, Kääb and Weber, 2004, Arenson and Springman, 2005, Frehner et al., 2015).

For simplification we assume the rockglacier material to be a homogenous mixture of ice and sediment, meaning the rheological parameters such as the rate factor A and flow exponent n do not change within the rockglacier body. However, from boreholes we know that the rheology within rockglaciers is variable (Haeberli et al., 1998) and typically enhanced deformation in ice rich shearing zones are observed, as for example for the case of the Murtèl rockglacier. Such shearing zones are typically near the bottom of the moving body of the rockglacier, where shear stresses are highest, and thus they dominate creep process. Consequently, potential variations in rheology in the material above are not substantially changing the non-linear viscous creep behaviour. The modeled flow is calibrated with observed surface velocities (see Sect. 9.4.3) and is dominated by the rheology of the material near the base and thus our modeling implicitly includes the shear zone in its vertically averaged rheology.

Therefore and because the rheology within rockglaciers in general is poorly known for the purpose of our study of first order controls on relatively short-term geometric changes, the assumption of a uniform rheology is justified.

We simplify the problem to the case of an infinite sheet of uniform thickness that creeps down an inclined plane (Cuffey und Paterson 2010, also known as the shallow ice approximation in glaciology (SIA)) and thereby neglect longitudinal stress gradients. As our focus is the evolution of the surface and not the detailed stress field within the landform, according to Leysinger Vieli and Gudmundsson (2004) this approximation is justified even for relatively high length to thickness ratios such as occurring for rockglaciers. For this 2-

dimensional case along a central flowline the vertical strain rate $\dot{\varepsilon}_{xz}$ is directly related to the shear stress τ_{xz} through

$$\dot{\varepsilon}_{xz} = A \cdot \tau_{xz}{}^n \tag{2}$$

where x is the horizontal coordinate along the central flowline and z the vertical coordinate. The shear stress τ_{xz} at the base is given by the local surface slope $\frac{\partial s}{\partial x}$ and material thickness h

$$\tau_d = \rho_r g \frac{\partial s}{\partial x} h \tag{3}$$

where ρ_r is the density of the rockglacier material and $\frac{\partial s}{\partial x}$ the surface slope.

Integration of Eq. (2) over the rockglacier thickness results in a surface flow speed u_s from deformation of the rockglacier material of

$$u_s = \frac{2A}{n+1} \left(\rho_r g \frac{\partial s}{\partial x} \right)^n h^{n+1} \tag{4}$$

and accordingly a vertically averaged horizontal flow speed $\bar{u}$ of

$$\bar{u} = \frac{2A}{n+2} \cdot \left(\rho g \frac{\partial s}{\partial x} \right)^n h^{n+1} \tag{5}.$$

Although this equation is in its form identical to the case of glacier ice (Cuffey and Paterson 2010), the flow exponent n and the rate factor A (referring to the material softness) are, due to the presence of debris and water within the ice, not necessarily the same. From boreholes and laboratory experiment flow law exponents of rockglaciers have been found between n=1.9 and 4.5 (mean n=2.72) and increase linearly with volumetric ice content c_{ice} of the sediment (Arenson and Springman, 2005). For our relatively high ice contents (60%) a value of n=3 equivalent to the case of ice seems justified and has been used in earlier studies of Leysinger Vieli and Gudmundsson (2003) and Frauenfelder et al. (2008).

The rate factor A is estimated from observed surface flow speeds by inverting Eq. (3) for A but is known to be influenced by the material temperature. Thus, for the purpose of our temperature forcing experiments and in agreement with known rheological investigations (Paterson and Budd, 1982, Arenson and Springman, 2005) we write the rate factor of the rockglacier material as a product of the temperature dependent part $A^*(T)$ and a scaling factor f_A accounting for the influence of the debris:

$$A = A^*(T) \cdot f_A \tag{6}$$

For the temperature dependent part we use two approaches. Firstly, as done in Kääb et al. (2007) we use the dependence to temperature of pure ice, for which $A^*(T)$ increases exponentially with temperature (see Figure 25; Paterson and Budd, 1982).

Secondly, and probably more realistic for rockglaciers, we follow the description based on shearing experiments of frozen debris material of Arenson (2005) which is given by

$$A^*(T) \propto \frac{2}{T+1} \qquad (7)$$

for temperatures between -1 and -4oC. Note that this second version is at warm temperatures above -2oC, as expected for our two cases, more sensitive to temperature warming (Figure 25). For both approaches the temperature dependence is applied at a reference temperature which refers approximately to the real mean annual temperature within the rockglacier body.
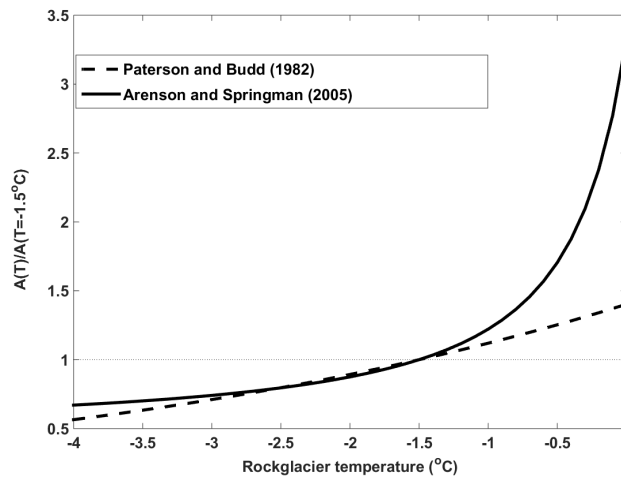

Figure 25: Temperature dependence of the rate factor relative to the rate factor at a reference temperature of -1.5°C as derived for pure ice (Paterson and Budd, 1982) and for rockglacier material (Arenson and Springman 2005).

Thickness evolution

The evolution of rockglacier thickness h and surface s is calculated from the principle of mass conservation which takes for the 1-dimensional representation along the central flowline the following form (Oerlemans, 2001)

$$\frac{\partial h}{\partial t} = a_r - \frac{1}{w} \cdot \frac{\partial \bar{u}hw}{\partial x} \qquad (8)$$

where t is the time, a_r is the rate of rockglacier material accumulation or removal at the surface (>0 for accumulation; in m a^{-1}), w the rockglacier width and $\bar{u}$ the horizontal and vertically averaged flow speed. The geometry of the rockglacier bed transverse to flow is accounted for by assuming a parabolic shaped valley that is prescribed and here assumed to be uniform along the flow.

The evolution of the rockglacier thickness and surface is calculated numerically on a regular grid with 10 m spacing along the central flowline. Using a standard implicit finite-difference scheme (Oerlemans, 2001) the surface evolution equation (8) is solved at each time step and for all grid points from the depth averaged material flux $\bar{q} = \bar{u} \cdot h \cdot w$ and the material input a_r at the rockglacier surface.

9.4.3 Model input and calibration

Model geometry

Approximate bedrock topographies are derived for both rockglaciers from the DEMs and geomorphic mapping (Sect. 9.4.1) and assuming the bedrock being roughly parallel to the rockglacier surface. The shapes of the rockglacier beds are approximated to two sections of constant slope which are representative of the two respective rockglaciers. For both rockglaciers we mapped the first 150m of the distance along flow as deposition area and apply there a spatially uniform material accumulation rate at the specified sedimentation rate and ice content whereas further downstream no mass is added or lost at the surface. In the talus slope, where the material is accumulated, we use a slope of 37° (which is slightly below the critical angle of talus slopes) and which is steeper than on the rockglacier part (12° for Murtèl and 27° for Huhh1, see Tab. 18). The respective dimensions and slopes for the two rockglaciers are presented in detail in Tab. 16 and visualized in Fig. 26.

Material input

This rockglacier material input rate a_r at the surface is assumed to be positive and uniform on the talus slope and if not mentioned otherwise set to zero on the surface of the main rockglacier body. The latter means that in general no sediment or ice is lost at the surface of the main rockglacier. The rockglacier material input at the surface is estimated from the sediment input from the headwall to the talus slope and its respective ice content which is assumed to be constant in time. The total amount of sediment produced at the headwall is

calculated from backweathering rate and headwall area and is distributed equally over the deposition area (talus slope/accumulation area). Based on insitu measurements (Müller et al., 2014a) and literature review (Glade, 2005, Krautblatter, 2012), a backweathering rate of 2 mm a^{-1} is used resulting in an annual sediment input over the entire talus slope of 0.006 m^3 m^{-2} for Murtèl and 0.022 m^3 m^{-2} for Huhh1 These backweathering rates are consistent with values presented in Glade (2005) and Krautblatter et al. (2012). Together with the ice content of the material the accumulation rate of rockglacier material (sediment-ice mixture) is then calculated

$$a_r = \frac{a_s}{(1-c_i)} \qquad (9)$$

Based on field studies (Hoelzle et al. 2002) and literature assumptions (Gärtner-Roer, 2012) we use an estimated ice content c_i of 60% for both rockglaciers which results in a rockglacier material input rate that is 2.5 times higher than the pure sediment input rate.

Rockglacier density

We estimate the density of the rockglacier material ρ_r from the percentage ice content c_i and from the respective densities of ice $\rho_i = 910$ kg m^{-3} and the debris material $\rho_d = 2700$ kg m^{-3}

$$\rho_r = (1 - c_i) \cdot \rho_d - c_i \cdot \rho_i \qquad (10)$$

Estimating the rate factor A

Solving the equation describing surface ice flow from creep of a viscous material (Eq.4) for the rate factor *A*, we obtain

$$A = A^*(T) \cdot f_A = \frac{(n+1)u_s}{2h^n\tau_d} = \frac{(n+1)u_s}{2h^{n+1}\rho_r g\frac{\partial s}{\partial x}} \qquad (11)$$

Using observed surface flow speed data (u_s) we can then estimate the corresponding rate factor *A* (respective f_A for a given reference temperature and temperture dependence model) for both rockglaciers. These rate factor values are both substantially lower than the values known for pure ice at similar temperatures (Paterson and Budd, 1982; (-1.5°oC)) which probably reflects enhanced mechanical resistance from the sediment within the ice (Arenson and Springman, 2005).

9.5 Model experiments

9.5.1 Rockglacier build-up

The model is applied to the two selected rockglacier systems using the landform specific input parameters in Table 18 and the simplified geometries described in Sect. 9.4.

Table 18: Specific model input parameters for the rockglaciers. The sediment/ice input describes the volume of debris deposited on the accumulation area per year. The rate factor A is derived from Eq. 11 and the runtime of each rockglacier model is selected due to their approximated age (see Sect. 9.3).

Input Parameter	Murtèl	Huhh1
Material input rate	$0.006 \text{ m}^3\text{ m}^{-2}\text{ a}^{-1}$	$0.022 \text{ m}^3\text{ m}^{-2}\text{ a}^{-1}$
Rate Factor A	$4.5*10^{-18}\text{ Pa}^{-3}\text{ a}^{-1}$	$7*10^{-17}\text{ Pa}^{-3}\text{ a}^{-1}$
Runtime	6000a	600a
Rockglacier Slope	$12°o$	$27°o$

The build up experiment is documented for Murtèl in Fig. 27 (first 6000 years) and is qualitatively very similar for Huhh1. The model starts with an 'empty' topography of bedrock (bedrock topographies in Fig. 25). Initially, it builds up a homogenous sediment-ice body in the talus slope which starts to creep and therefore advance once it reaches a critical thickness and shear stress which occurs roughly after 600 years for Murtèl and 150 years for Huhh1. A rockglacier body is then generated to a characteristic thickness while the front keeps advancing at a roughly constant rate. Further, the growth and geometry change of the rockglacier landform mainly occurs through moving the rockglacier forward at the front. The modeled advance rate is slightly below the surface speed of the main rockglacier body. After a run time of 6000 years for the Murtèl rockglacier and 600 years for Huhh1 which correspond to the ages of the landforms estimated earlier, we obtain geometries (lengths and thicknesses) that are very close to ones currently observed (Fig. 25 and Tab. 19). The actual furrow-ridge structure of the landform cannot be replicated (Fig. 25) due to model design but the overall geometry is well reproduced.

The modeled surface velocities on the main rockglacier lobes range between 0.06 m a^{-1} and 0.09 m a^{-1} for Murtèl and between 0.63 m a^{-1} and 0.79 m a^{-1} at Huhh1 which is in good agreement with the observed values from long term kinematic monitoring (see Tab. 16).

Table 19: Comparison of the observed (obs.) and modeled (mod.) rockglacier thickness and velocity for Murtèl and Huhh1 after 6000 years and 600 years respectively.

	Murtèl obs.	Murtèl mod.	Huhh1 obs.	Huhh1 mod.
Length	280m	300m	310m	240m
Thickness	30m	28m	12m	16m
Hor. velocity	0.06-0.13 ma^{-1}	0.06-0.09 ma^{-1}	0.75 - 1.55 ma^{-1}	0.63-0.79 ma^{-1}

Note that the observed rockglacier front shapes and positions differ slightly from the modeled ones as the real bedrock geometries of the rockglaciers are more complex than the assumed uniform mountain slopes.
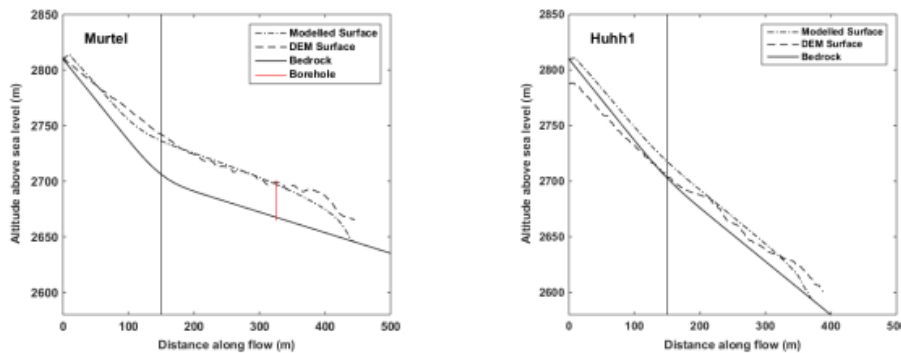

Figure 26: Observed and modeled rockglacier geometry after build-up. The along flow bed topography used in the model and the modeled and observed (from the most recent DEMs) rockglacier surfaces are shown. The vertical fine black line marks the boundary between the deposition area (talus slope) and the main rockglacier lobe.

9.5.2 Perturbation modeling experiments

Starting with the rockglacier geometries from the build-up experiments (see Sect. 9.5.1) we investigate the impact of variations in temperature and material input on rockglacier dynamics. In a first phase we perform two distinctly different perturbation experiments in which we increase the temperature of the rockglacier body by 1°C (Sect. 9.5.2.1) and in a second independent experiment we completely switch off the material supply to the talus slope (Sect. 9.5.2.2). In a second step, we then combine these perturbations in temperature and sediment supply.

Atmospheric warming is expected to influence both rockglacier temperatures and consequently creep, as well as the production of sediment and incorporation of subsurface ice but quantification of the latter is highly uncertain (Gruber, 2004, Fischer et al., 2010,

143

Ravanel and Deline, 2011, Schneider et al., 2012). We therefore run varying scenarios for the sediment and ice input with the zero sediment supply being at the extreme end of the spectrum.

For the temperature experiments the chosen step temperature increase of 1°C in the rockglacier depicts a potential warming scenario which roughly refers to a 2°C warming in ground surface temperature (GST) for a fixed position at the permafrost base. The 1°C subsurface warming is also consistent with current and expected future subsurface warming trends based on borehole observations (PERMOS, 2013).

Table 20: Multiplicative increase in rate factor A from a 1°C rockglacier warming for the different temperature relations of Arenson and Springman (2005) and Paterson and Budd (1982) and varying rockglacier reference temperatures

Rockglacier reference temperature	Change in rate factor A for Arenson and Springman (2005) for a 1°C warming	Change in rate factor A for Paterson (1982) for a 1°C warming
-2°C	1.396*A	1.254*A
-1.5°C	1.705*A	1.253*A
-1°C	2.718*A	1.252*A

Increases in material temperature are applied by changing the flow rate factor *A* according to its temperature dependence and for a given reference temperature (Eq. (6) & (7)). For relatively warm rockglaciers between -1 and -2°C as typically observed in the Swiss Alps, a 1°C warming would for the Arenson and Springman (2005) temperature dependence result in an increase of the rate factor by a factor 1.4 to 2.7 respectively (Tab. 20) . For the Paterson and Budd (1982) temperature relation the increase is with a factor 1.25 smaller but also insensitive to the reference temperature (Tab. 20). If not indicated otherwise, we use in the temperature warming experiments a rate factor increase according to the Arenson and Springman (2005) relation rather than the Paterson relation based on pure ice.

The results for the singular temperature and sediment experiments are in the section below only presented for the Murtèl rockglacier but the qualitative results are similar for Huhh1 rockglacier although of higher absolute magnitude. The more realistic experiments combining variations in temperature and sediment supply are presented for both rockglaciers later (section 9.5.2.3).

9.5.2.1 Temperature experiment

In a first experiment, a step temperature increase of the entire rockglacier body of 1°C is applied after rockglacier build-up (at 6000a), while the sediment supply is held constant. The reference temperature of the rockglacier is set at -1.5°C which results in a rate factor increase

by a factor 1.7.

Figure 27 shows the modeled response of the surface geometry, landform thickness and horizontal surface velocity of the Murtèl rockglacier along the central flowline. For reference, the black line in Fig. 27 shows the state of the rockglacier just after build-up (6000 a), immediately before the temperature step change is introduced. The increase in the rate factor causes an immediate speed-up in horizontal flow of the entire landform by roughly a factor of two (Fig. 27c, yellow lines) which then decays with time (orange to red lines). As a result of the enhanced mass transport, the landform also shows a distinct thinning of up to 0.02 m a^{-1} in the upper part of the rockglacier and on the talus slope (Fig. 27b). At the front the rockglacier continues to thicken and consequently advance, but at accelerated rates as a consequence of enhanced flow speeds (Fig. 27d). With time, both the creep velocity, advance rate and thinning reduce and approach stable values again after about 1000a for Murtèl. This state is, apart from the advancing front, stable and characterised by a slightly faster flowing and a slightly thinner main rockglacier body in order to transport through the constant material supply from upstream. Consistent with the creep velocity, the advance rate is also slightly enhanced (Fig. 27d) whereas the volume grows at a constant rate throughout the simulation, reflecting again the constant material supply and mass conservation (Fig. 27e).

Additional model simulations for other reference temperatures of the rockglacier of -1°C and -2°C, show qualitatively very similar results but the absolute rates of changes differ roughly proportional to the enhancement factors in the rate factor given in Tab. 20. The same experiments for the Huhh1 rockglacier show quantitatively very similar responses which are of higher absolute magnitude. The adjustment to a new quasi stable state is with 100 years also much faster.
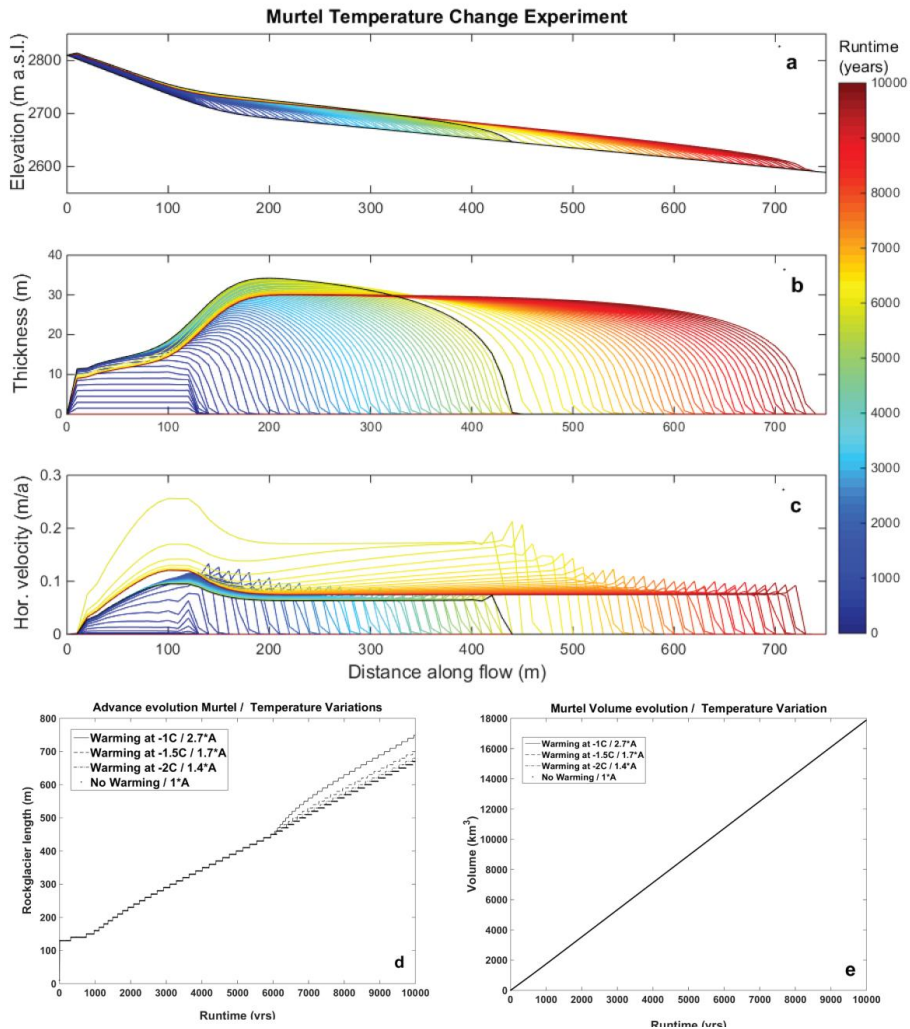
Figure 27: Modeled evolution of surface geometry (a), absolute thickness (b) horizontal velocity (c) along the central flow line, terminus advance (d) and volume evolution (e) for the rockglacier build-up (first 6000a runtime) and for the successive temperature perturbation experiment (temperature increase of 1°C, with -1.5°C reference temperature). The black line shows the state of the system before the temperature step-change at 6000a. The lines are plotted at 100a time intervals.

9.5.2.2 Sediment experiment

In a second set of experiments, the influence of variations in sediment and ice supply is investigated by varying the material input a_r but keeping the rockglacier temperature constant. Since there is no empirical data on the impact of temperature increase on sedimentation rates and ice, a range of changes in material supply rates has been explored.
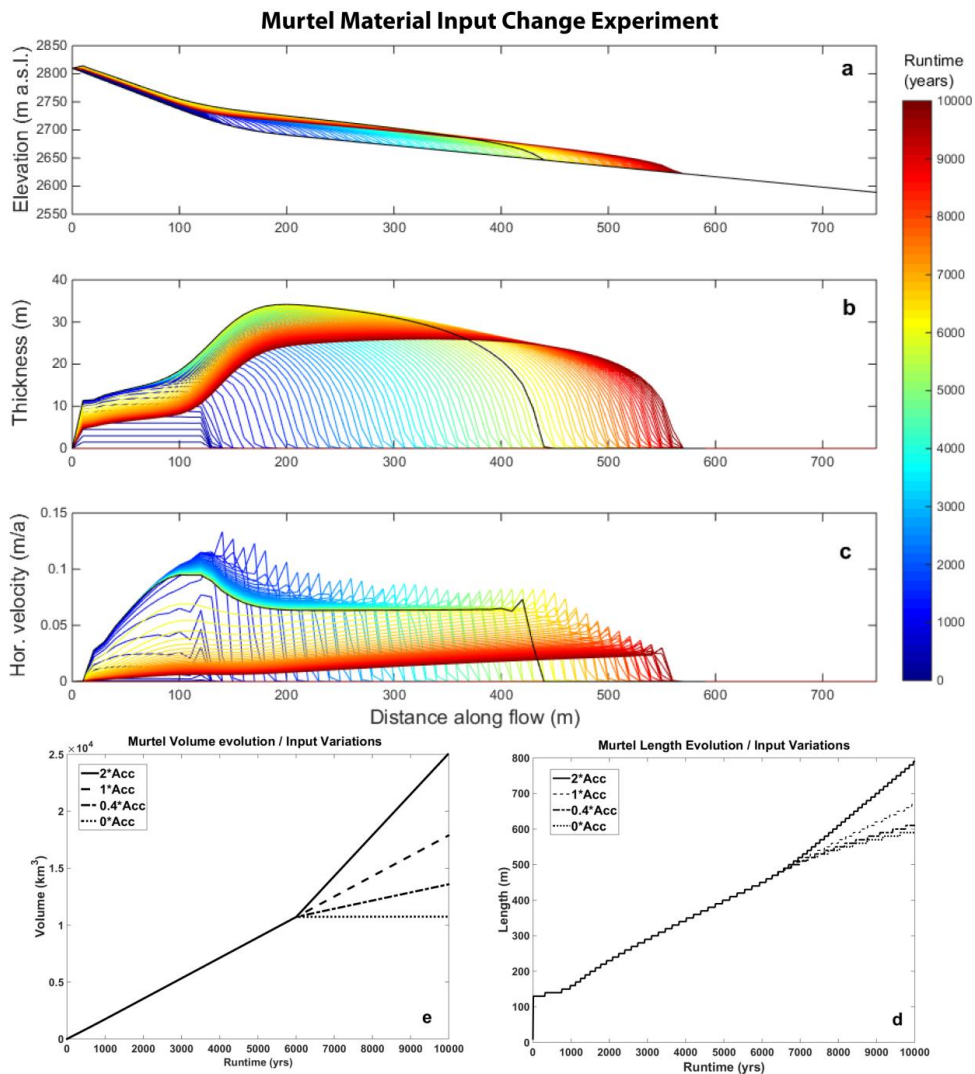
Figure 28: Modeled evolution of surface geometry (a), absolute thickness (b) horizontal velocity (c) along the central flow line, terminus advance (d) and volume evolution (e) for Murtèl rockglacier when the material input is switched off at 6000a, after the rockglacier build-up (-1.5 C rockglacier temperature). The black line shows the state of the system before the switch-off of material supply at 6000 years. The lines are plotted at 100a time intervals.

Figure 28 shows the modelled response for an extreme example in which the ice and sediment input is completely switched off after rockglacier build-up (at 6000a). The results show that the rockglacier continues to creep downslope and advance but with reduced velocities that start to decrease from upstream. This slow-down is related to a thinning, reduced slope and driving stresses in the upper part of the rockglacier as the downstream flowing mass is no longer fully replaced by accumulation of material on the talus slope. The rockglacier body essentially creeps downstream without any mass added or removed which

is well reflected in the constant volume with time (dotted line in Fig. 28e). The advance rates thereby decrease at relatively low rates. The upper parts of the rockglacier react immediately to the change of material input as this is where the sedimentation is taking place. Note that the maximal thinning rates are only as high as the former material accumulation rate (in case of Murtèl 0.006 ma^{-1}, for Huhh1 0.022 ma^{-1}).

Experiments with different perturbations in material input rates show qualitatively similar changes but of reduced magnitude (Appendix Tab. A1 and A2) and are also evident in differing advance and volume growth rates (Fig. 28 d and e).

9.5.2.3 Combined experiment

As atmospheric warming is expected to influence both rockglacier temperatures as well as ice and sediment production, thus we perform a third set of experiments in which we combine the above perturbations.

12 scenarios were run for each rockglacier assuming three different initial thermal states of each rockglacier (see Tab. 20), a potential warming of 1°C and four different scenarios concerning the material input (see Tab. 21) and the main results of all perturbation experiments are shown in the Appendix (Tab A1 and A2).

Table 21: All combined experiments. A is the flow rate factor (see Eq. 11) and Acc describes the entire material input.

Model run	Creep Rate change	Accumulation change
1.4*A and 0*Acc	1.4*A	$0*a_r$
1.4*A and 0.4*Acc	1.4*A	$0.4*a_r$
1.4*A and 1*Acc	1.4*A	$1*a_r$
1.4*A and 2*Acc	1.4*A	$2*a_r$
1.7*A and 0*Acc	1.7*A	$0*a_r$
1.7*A and 0.4*Acc	1.7*A	$0.4*a_r$
1.7*A and 1*Acc	1.7*A	$1*a_r$
1.7*A and 2*Acc	1.7*A	$2*a_r$
2.7*A and 0*Acc	2.7*A	$0*a_r$
2.7*A and 0.4*Acc	2.7*A	$0.4*a_r$
2.7*A and 1*Acc	2.7*A	$1*a_r$
2.7*A and 2*Acc	2.7*A	$2*a_r$

In Fig. 29 and 30 we show detailed results for both Murtèl and Huhh1 rockglacier for one representative perturbation experiment in which we used a reference rockglacier temperature of -1.5°C, an increase in temperature of 1°C (corresponding to a rate factor increase by factor 1.7, Tab. 20) and a decrease of material input to 40% of the original value is applied.
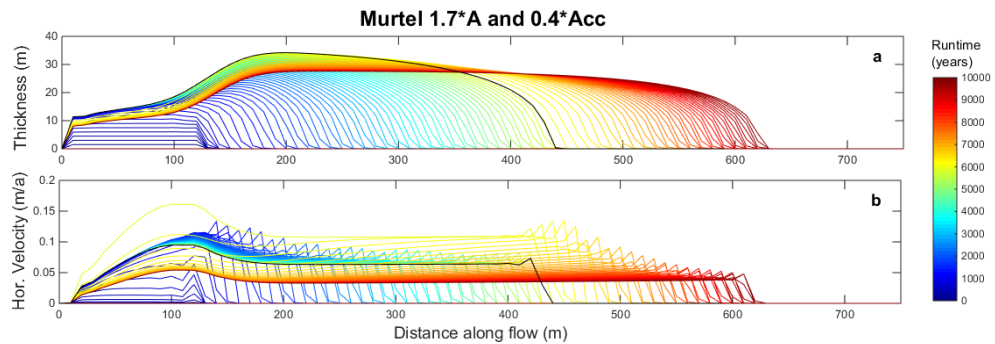
Figure 29: Modeled evolution of absolute thickness (a) and horizontal velocities (b) of the Murtèl rockglacier introducing a 1°C temperature increase (1.7 times increase in rate factor) and a reduction in material input to 40% after the rockglacier build-up (6000a, black line). The black lines in all plots depict the state of the rockglacier as shown in Fig. 27 before the perturbations were introduced The lines are plotted at 100a time steps.

Figure 29 and 30 illustrate the evolution of surface geometry and horizontal velocities along the central flow line of Murtèl and Huhh1 rockglacier, respectively. This combined experiment shows an upstream thinning of the "initial" landform in the subsequent years (Fig. 29a and 30a) and a substantial increase in horizontal velocities (Fig. 29b and 30b). The maximum thinning rates occur within the first few decades of the experiment and amount to 1.6 cm a^{-1} for Murtèl and 6 cm a^{-1} for Huhh1 (see Fig. 31). A new stable geometry with advancing front is successively approached, again within roughly 1000a and 100a for Murtèl and Huhh1, respectively. The final thickness and velocities of the main rockglacier body are, however, very close to the initial values.

Figure 31 shows the more detailed temporal evolution of geometry and creep velocity at three distinct positions on both rockglaciers. The rockglaciers keep advancing throughout the simulation, with initially slightly enhanced rates caused by the temperature increase and a successive slight slowdown caused by the reduced material accumulation rates. As found before, the adjustment times-scales of the Murtèl rockglacier are compared to the Huhh1 much lower.
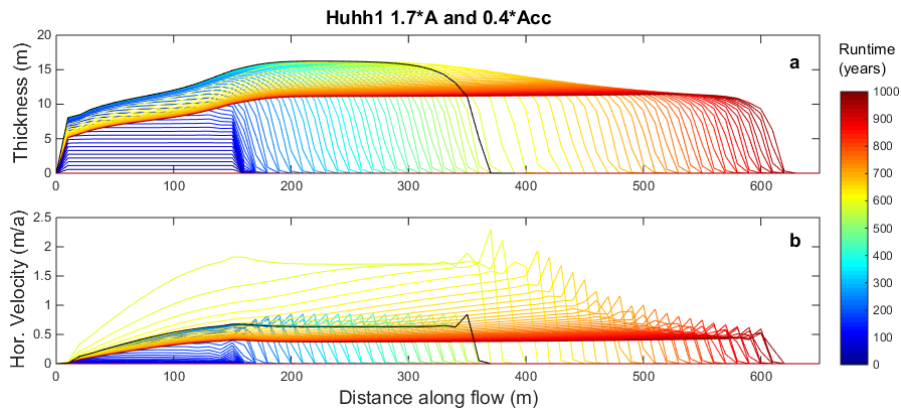
Figure 30: The evolution of absolute thickness (a) and horizontal velocities (b) of the Huhh1 rockglacier introducing a 1°C temperature increase (1.7 times increase in rate factor) and 40% of the initial material input after rockglacier build-up (600a, black line). The black lines in all plots depict the state of the rockglacier as shown in Fig. 27 before the perturbations were introduced. The lines are plotted in 10a steps.
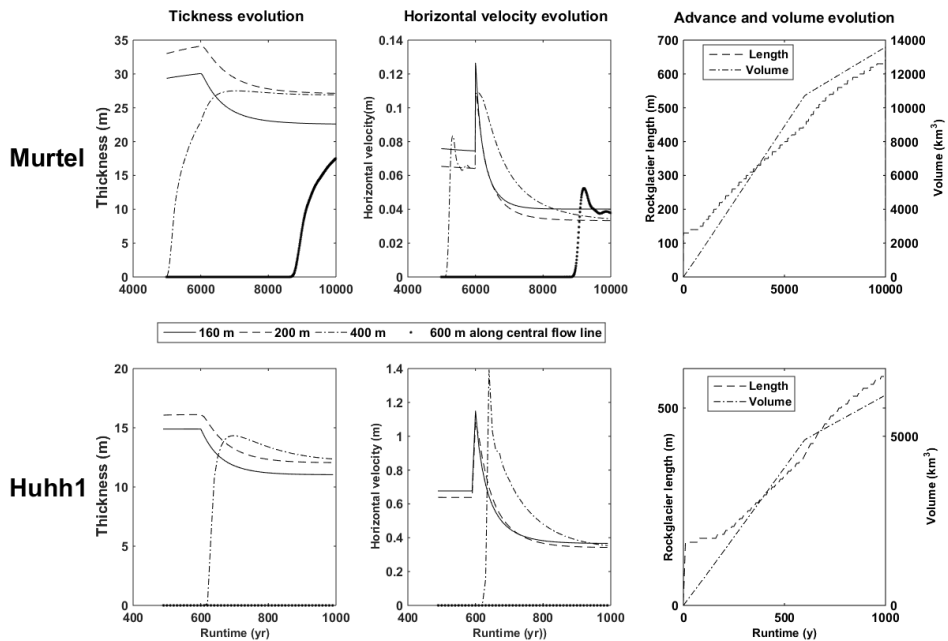

Figure 31: Rockglacier evolution of thickness, horizontal velocity, advance and velocity after a 1°C temperature increase and 40% decrease in material input after rockglacier build-up. The dynamic evolution is shown for three points along the central flow line at 160m, 200m and 400m. The rockglacier is assumed to have an initial temperature of -1.5°C

The additional combined experiments with a 1°C temperature increase but variable reference temperatures and varying sediment supply rates show qualitatively similar geometric and kinematic responses (see Appendix Tab. A1 und A2).

Subsidence

The sensitivity of the dynamic response to the initial temperature and to the temperature dependent model has been further analysed for the combined perturbation (1°C warming, 60% reduction in material input) in a sensitivity modeling study (for detailed results see Supplement). As subsidence is one of the observable quantities from repeated DEM-analysis on real rockglaciers, we summarized the results in terms of maximum thinning rates in Fig. 32.

For the Paterson and Budd (1982) temperature relation, thinning rates are almost independent to the reference rockglacier temperature, but increase with a reduction in material supply and reach maximum thinning rates of 1.8 cm a^{-1} and 6.5 cm a^{-1} for Murtèl and Huhh1, respectively. When using the Arenson and Springman (2005) temperature model, thinning rates strongly increase towards warmer rockglacier reference temperatures, reaching maximum values of 3.4 cm a^{-1} and 12.5 cm a^{-1} for Murtèl and Huhh1, respectively.
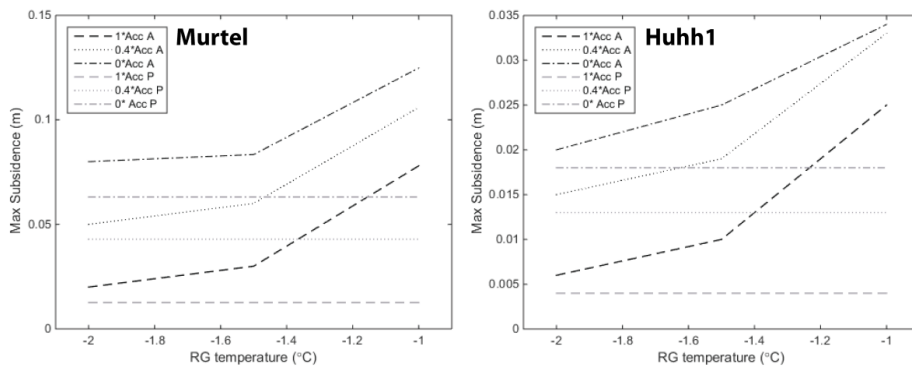

Figure 32: Modeled maximum annual subsidence rates in the deposition area of the rockglacier in relation to the reference temperature and change in material input and for the two temperature models of Arenson and Springman (2005; black lines) and Paterson and Budd (1982; grey lines) after a 1°C temperature increase. Note the different scales for subsidence for the two rockglaciers.

9.6 Discussion

9.6.1 Modeling approach and rockglacier build-up

Based on a continuum approach, our numerical model couples observed sediment input rates and the rockglacier creep process in order to simulate the evolution of creep velocities and surface geometry as well as their dynamical interactions. This quantitative approach of coupling the relevant subsystems (headwall, deposition area and rockglacier), although highly simplified, was successful in building-up the observed rockglacier geometries and related kinematics (horizontal velocities) within the expected timescales (Tab. 16). Further after build-up, the basic dynamical behaviour of a continuously advancing rockglacier body, while the thickness of the main body remains roughly constant, is well reproduced.

From our modeling of rockglacier build-up we find that besides topographical factors such as slope, the long-term advance rates and horizontal velocity are dominantly controlled by the rates of material accumulation and the rockglacier rheology, whereas the thickness of the main landform seems not that sensitive to material supply rates (but rather to surface slope and rheology).

The match of observed to modeled velocities and thicknesses should by model construction be expected (for similar surface slopes), as the rate factor A and therefore the viscosity of the rockglacier material has been derived from such observed quantities (Eq. 11), but the agreement supports our modeling approach. Importantly, the material input rates and build-up times are fully independent estimates and it is therefore not necessarily obvious to get the right rockglacier geometry at the prescribed time.

Our modeled constant advance rates and consistency between modeled and previously estimated rockglacier build-up times further supports the method of back-calculating rockglacier age from current surface velocities (Frauenfelder and Kääb, 2000, Kääb und Vollmer, 2000, Haeberli et al., 2003). Even for the case of temperature perturbations, advance rates of the front do not substantially change in the long-term and thus this 'dating' method seems still appropriate for alpine rockglaciers. Advance rates are in the long-term however affected by changes in material supply rates. It remains to note that it is actually the vertically averaged velocity, and not the surface velocity, that should match the advance rates. For our rheology with n=3 this corresponds according to Eq. (5) to 4/5 of the surface velocity which is consistent with our modeling of Murtèl rockglacier (modeled surface velocity on the main body of 0.065 m a^{-1} and an advance rate of 0,054 m a^{-1}). Consequently,

using surface velocities in back-calculations of rockglacier age may overestimate the age. For many real-world rockglaciers (including Murtèl), rockglacier movement is dominated by deformation in a shear zone near the base and thus surface and vertically averaged creep are almost identical.

Strong simplifications have been made for our modeling approach such as using a homogenous sediment-ice body of uniform temperature and rheology and a spatially uniform and temporally constant material input. The successful rockglacier build-up, therefore supports the idea that despite such simplifications rockglacier dynamics and evolution can be reduced to our simple model approach which is based on the historic concept of Wahrhaftig and Cox (1959) and confirms earlier numerical modeling approaches of Olyphant (1983) and Frauenfelder et al. (2008).

The non-linear viscous Glen-type flow-law used here is also supported by laboratory experiments (Arenson and Springman, 2005) and field observations from boreholes (Arenson et al., 2002). However, in reality the involved flow law parameters are, unlike assumed in our model, rarely constant in space and time. The flow-law exponent n has been found to increase with ice content (Arenson and Springman, 2005) and relatively thin shear layers with strongly reduced viscosity often dominate rockglacier creep (Hoelzle et al., 2002, Haeberli et al., 2006, Buchli et al., 2013). Such more complex ice rheology could in theory and should in the future be included in rockglacier creep models, but currently there is very limited quantitative information available to constrain such more complex constitutive relationships. Due to the fact that the creep deformation is also dominated near the base within our model and that we have calibrated our model parameters to observed geometry and velocities, we do not expect the general dynamical behaviour and involved time-scales to be substantially different for other rheological parameters choices. We see our highly reduced approach also as an advantage for identifying the most essential controls and processes in rockglacier evolution.

In our approach the geomorphological mapping of the different subsystems, the quantification of sediment input rates, the ice content and the horizontal velocities are the crucial observational constraints and sufficient to set up a model of rockglacier evolution. The simplicity of the model design does by construction, however, not allow to produce the exact small scale features such as ridges and furrows of the two chosen real-world rockglaciers (Frehner et al., 2015).

9.6.2   Dynamical adjustment to external forcing

The perturbation modeling experiments of applying a sudden change in sediment input, material temperature or a combination of the two provide useful insights into the dynamic and geometrical adjustment of rockglaciers to changes in external forcing and therefore also into potential mechanisms that explain observed rockglacier degradation.

The two types of perturbation experiments show similarities but also clear differences in their dynamical response. Both, an increase in the rockglacier temperature as well as a reduction in material input lead to a thinning of the rockglacier and the talus slope whereas the front keeps advancing through thickening. Although the thinning is caused by different mechanisms (lack of material supply from the front or a runaway of mass through creep acceleration) from an observational point of view, the two forcing mechanisms would be difficult to be kept apart. Importantly, the thinning also occurs for both in the deposition area (talus slope).

Regarding changes in horizontal velocities, their response are for the two types of perturbations distinctly different. For a reduction in material supply the velocities slow down from the top, whereas the temperature increase results in an immediate acceleration everywhere that relaxes in the long-term to almost pre-perturbation conditions (see Fig. 27c and 28c). Further, for the temperature experiments advance rates of the rockglaciers increase briefly but in the longer-term return to similar rates as before the perturbation which is in contrast to a continuous reduction of the advance rate at the decreased sediment supply experiment. Therefore, temperature changes within the rockglacier show a strong impact on short term velocity variations whereas changes in the material input determine the long term advance rates and geometry. Similar experiments by Olyphant (1983) and Frauenfelder et al. (2008) focused only on combined experiments and could therefore not address the impact of the individual forcings.

9.6.2.1   Dependence on rockglacier properties

Irrespective of the type of experiments, the absolute magnitude in response (in velocity change, thickness change or advance rate) is for the two rockglaciers very different. Relative to the initial quantities (pre-perturbation velocity, thickness or advance rates) the changes and temporal evolution for both rockglaciers are very similar (Fig. 29 and 30). This means that we should expect dynamic changes of rockglaciers to be scalable by their geometric and kinematic characteristics. This is for the temperature increase experiment not surprising, as the applied increase in rate factor scales linearly with velocity in our model (Eq. 4). This

scalability is also in good agreement with the observational dataset of multiannual creep variations of rockglaciers in the Swiss Alps (PERMOS, 2013). These show very similar normalized horizontal velocity variations as a potential response to air temperature changes despite their distinctly different characteristics (Delaloye et al., 2010a and PERMOS, 2013). Recent continuous observations of creep velocities on rockglaciers in the Matter Valley confirm this finding even for seasonal timescales (Wirz et al. 2015).

The modeled short-term increase in horizontal velocity for a 1°C warming in rockglacier body is also consistent with the observed speed-up in rockglacier creep of about 300% in the year 2003/2004 with exceptional snow conditions and a very warm summer (Delaloye 2010a).

9.6.2.2 Temperature dependence

Unlike in our temperature perturbation experiment, in reality any increase in air temperature and consequently GST does not immediately warm up the entire rockglacier body. The vertical heat transfer depends on the energy balance at the surface and heat transport processes and properties within the rockglacier material (Hoelzle and Hanson 2004) and could potentially be implemented in future studies (Kääb et al 2007, Scherler, 2014). Hence we consider our modeled warming rather as a simple way to investigate the sensitivity to temperature increase.

For relatively thin rockglaciers such as Huhh1, a climatic warming could affect the whole rockglacier thickness in time scales of a few years. For thicker rockglaciers such as Murtèl, it could take several decades for the temperature change to reach the base where most of the deformation actually occurs. This implies that thin, and consequently steep and fast rockglaciers, should be more sensitive to warming from the surface.

The sensitivity to temperature warming is also enhanced for relatively warm rockglacier (with temperatures only a few degrees below freezing) when we consider the most realistic model for temperature dependence of rockglacier rheology by Arenson and Springman (2005). At -1.0°C rockglacier temperature, a warming of 1°C results in a 2.7 times increase in the rate factor (and hence creep velocity) whereas the same warming at -2°C results only in a 1.4 times higher rate factor. Observed rockglacier temperatures in the Swiss Alps indicate already relatively 'warm' temperatures (close to zero degrees) and show a tendency for further warming (PERMOS, 2013). Such a warming would further amplify the response in acceleration. In contrast, when using a temperature dependence of pure ice (Paterson and

Budd, 1982), as done in an earlier attempt of modeling the impact of temperature change on rockglacier creep (Kääb et al., 2007), the sensitivity of creep to temperature warming is smaller (a 1oC warming results in only a 1.25 times increase in rate factor) and does not additionally increase towards warmer rockglacier temperatures (Fig. 25). Thus, the impact of warming on creep acceleration could be bigger than previously expected.

9.6.2.3   Adjustment timescales

Regarding the time-scales for the rockglaciers to adjust their thickness and advance rates to step perturbations, the modeling shows for the faster and steeper Huhh1 rockglacier with about 100a an order of magnitude faster *adjustment times* of thickness and advance rates as compared to the 1000a of Murtèl rockglacier (26d and 27e). While in the literature such differences in adjustment times have qualitatively been linked to the general rheology and mass turnover, the controlling factors remain unquantified. At least for the case of the sediment supply experiment, a comparison to theoretical considerations based on the kinematic wave theory developed by Nye (1963) can be made. The travelling wave speed v_0 of thickness changes is thereby given by

$$v_0 = (n + 2) \cdot u_s \hspace{4cm} \text{(Eq 12)}$$

which results in a typical adjustment timescale of this thickness change to reach the terminus of

$$T_k = \frac{L_0}{v_0} = \frac{L_0}{(n+2) \cdot u_s} \hspace{4cm} \text{(Eq. 13)}$$

where L_0 is the length-scale of the rockglacier lobe. Thus, the time scale is inversely proportional to the horizontal velocity and consistent with our modeling means that a factor 10 difference in creep velocity between Huhh1 and Murtèl rockglacier translates into a factor 10 difference in adjustment time. For n=3, lengths of 300m and 250m and creep velocities of 0.07 m a^{-1} and 0.6 m a^{-1} for Murtèl and Huhh1, we obtain adjustment timescales of 860a and 83a respectively. These adjustment timescales agree in absolute magnitude and relative to each other well with our modeled estimates. This implies that the kinematic wave speed, obtained from observed horizontal velocity, is a simple and meaningful measure for rockglacier adjustment times.

Based on the same theory (Nye, 1963), the diffusion of the thickness perturbation is proportional to the diffusivity which is given by

Publication III

$$D_0 = \frac{n \cdot q}{\alpha} = \frac{n \cdot \bar{u} h}{\alpha}$$ (Eq. 14)

where q is the ice flux and α the surface slope. For Murtèl and Huhh1 this gives diffusivities of 30 m² a⁻¹ and 53 m² a⁻¹, which are as a result of very small creep velocities much lower than obtained from a similar analysis on pure-ice glaciers. Thickness perturbations spreading over length scales of L_0 result in diffusion timescales of $T_d = \frac{L_0^2}{D_0}$. This results in 3000a and 1200a for the perturbation to spread over the whole landform for Murtèl and Huhh1, respectively, which is substantially longer than the timescales derived above for kinematic wave propagation. These diffusion timescales are also much longer compared to pure-ice glaciers and are consistent with the existence of the characteristic morphological features of ridges and furrows on the surface of rockglaciers. The very similar adjustment timescales obtained for all perturbation experiments support the notion that the kinematic wave propagation timescale T_k can be used as a general measure of adjustment in creep dynamics to a step change in external forcing. Note that the introduced adjustment timescale is as a concept similar to the *volume response time* for pure-ice glaciers for adjusting to a new climate (Johannesson, 1989) and should not be confused with a reaction time (time it takes for a rockglacier to show a detectable reaction on an external forcing).

9.6.2.4 Geometry change and subsidence

Regarding geometry, the modeled rockglaciers respond to both warming and reduction in material input by a thinning of the landform that is fastest and most pronounced in the deposition area and in the upper parts of the rockglacier (Fig. 29, 30 and 31). The front and therefore the landform as a whole remains advancing, although at slightly differing speeds depending on the applied perturbations (see Fig. 27 and 28); even if the material input is completely stopped. The perturbation experiments can also be compared with the observed subsidence data presented in Sect. 9.3, in order to investigate the potentially controlling mechanisms of such geometry change. The observations in Fig. 23 and 24 show a pronounced subsidence in the lower deposition area and upper parts of the rockglacier of roughly -0.05 m a⁻¹ for the Murtèl rockglacier and -0.16 m a⁻¹ for Huhh1 rockglacier while the lower rockglacier lobe shows relatively small or unchanging thicknesses and an advancing front. Thus, the spatial patterns in modeled geometry changes agree well with the observations. The absolute maximum rates of modeled subsidence are for both rockglaciers between 2 to 10 times smaller than the observed rates depending on the perturbation. These modeled rates are also for an immediate warming of 1ºC which is rather extreme. Further,

158

the possible maximum rates of thinning from a total switch off in material input rates are limited to their pre-perturbation absolute values (0.006 m a^{-1} for Murtèl and 0.022 m a^{-1} for Huhh1) which are also almost an order of magnitude smaller than the observed subsidence rates, even for extreme scenarios (Fig. 32).

Thus, we conclude that although the two processes of acceleration through rockglacier warming and a reduction in material input could substantially contribute to the observed subsidence patterns at Murtèl and Huhh1, they are not sufficient in explaining the observations. Instead melt of subsurface ice is likely required as an additional process of rockglacier volume loss. The process of landform thinning, especially in the upper parts of the rockglacier, has been described as a sign of degradation by Ikeda and Matsuoka, (2002b), Roer et al. (2008b) and Springman et al. (2013). However, subsidence through melt of subsurface ice remains poorly constrained through observations and our process understanding and models linking them to external forcing are still limited (Scherler, 2014).

9.7   Conclusions

This study uses a numerical flow model based on the conservation of mass within the cascading transport system of coarse debris to simulate the long-term and current evolution of rockglacier surface and velocity. For a given sediment/ice input and rockglacier rheology, the model is able to generate observed rockglacier geometries and creep velocities in realistic time scales for two distinctly different rockglaciers. It is also capable of reproducing the continuing advancing front through creep which is often observed for rockglaciers (Barsch, 1996).

Climatic changes, especially increasing temperatures are expected to influence rockglacier dynamics in a profound way. Our modeling approach allows not only for investigation of the impact of a direct warming of the rockglacier material by adjusting the rheology (rate factor) but also for including the influence of changes in material input consisting of sediment and ice. Changes in geometry and related kinematics in response to such external perturbations can thereby be modeled and contribute towards a better understanding of the evolution of rockglaciers. Our detailed analysis of such perturbation experiments and modeling sensitivity study give the following insights on rockglacier dynamics:

- Short-term changes in velocities and advance rates result from temperature variations whereas long-term geometrical adaptations (thickness and advance rates) are mainly influenced by material supply. We show that a 1°C temperature increase in

rockglacier temperature can result in a 1.5-3 time (150%-300%) acceleration of horizontal velocity depending on the initial thermal state of the rockglacier.

- Both, rockglacier temperature increase and reduction in material supply lead to thinning, while for the later the maximum thinning rates are limited by the pre-perturbation material supply rate.

- Irrespective of the perturbation, the rockglaciers keep advancing and remain active although the thermal and sediment input conditions are not favorable for their sustenance which is consistent with field observations.

- Rockglaciers react spatially diverse to changes in environmental factors. Changes in temperature affect immediately the entire landform but the impact of material input variations are most pronounced in the sedimentation area and upper parts of the rockglacier. Comparing the model scenarios for localized geometrical adaptations (subsidence) introduced by warming and variations in sediment/ice supply to observed subsidence features shows that these controlling factors are not sufficient to explain the magnitudes observed for our two examples. This implies that other processes such as the melting of subsurface ice are responsible for subsidence and need further investigations.

- Although the absolute magnitudes in thinning and creep acceleration differ between the two rockglaciers, the changes relative to the initial thickness and creep velocity respectively are very similar thus indicating that changes scale with their geometric and dynamic characteristics.

- Based on most recent models of rockglacier rheology (Arenson and Springman, 2005) rockglaciers close to $0^{\circ}C$ likely show much stronger reactions to thermal forcing than colder ones.

- On the basis of our modeling and kinematic wave theory, we propose a typical *timescale of dynamic adjustment* to external perturbations that is given by the inverse of a few times the horizontal velocity of a rockglacier. This timescale explains the order of magnitude difference in dynamic adjustment of our two chosen rockglacier examples which amount to 1000a for Murtèl and 100a for Huhh1.

The modeling approach presented here and with further development might serve as a useful tool to determine the dynamic state of alpine rockglaciers, their potential state of degradation and related forcing mechanisms. The growing amount of observations on geometric changes and rockglacier movements may thereby serve as important constraints for such model assessments and serve as indicators for the recent changes affecting

periglacial high mountain systems. Therefore, future monitoring strategies should specifically be designed to detect spatially heterogeneous geometry changes and aim at observing entire slope systems, instead of focusing on single landforms.

9.8 Acknowledgements

9.9 Appendix

Table A1: 12 scenarios for Murtèl rockglacier were developed assuming three different initial thermal states of each rockglacier (-2°C, -1.5°C and -1°C). A potential warming of 1°C was combined with four different scenarios concerning the material input resulting from the suggested temperature increase. The values present the results after the perturbation (6000a-10000a).

Murtèl

Reference Temp. [°]	Model Run	Creep Rate change	Accumulation change	Length [m]	Thickness [m]	Max. Hor. Vel. [m a⁻¹]	Average Hor. Vel. [m a⁻¹]	Max. Subsidence [m a⁻¹]
-2	1.4*A and 0*Acc	1.4*A	0*aᵣ	590	24.5	0.14	0.03	0.02
-2	1.4*A and 0.4*Acc	1.4*A	0.4*ar	610	28.05	0.14	0.052	0.015
-2	1.4*A and 1*Acc	1.4*A	1*ar	670	34.01	0.14	0.1	0.005
-2	1.4*A and 2*Acc	1.4*A	2*ar	800	39.23	0.17	0.16	0
-1.5	1.7*A and 0*Acc	1.7*A	0*ar	610	23.9	0.16	0.033	0.024
-1.5	1.7*A and 0.4*Acc	1.7*A	0.4*ar	630	27.5	0.16	0.05	0.19
-1.5	1.7*A and 1*Acc	1.7*A	1*ar	700	32.8	0.16	0.1	0.01
-1.5	1.7*A and 2*Acc	1.7*A	2*ar	820	37.8	0.18	0.17	0
-1	2.7*A and 0*Acc	2.7*A	0*ar	660	22.24	0.25	0.0405	0.04
-1	2.7*A and 0.4*Acc	2.7*A	0.4*ar	680	25.62	0.26	0.04	0.0388
-1	2.7*A and 1*Acc	2.7*A	1*ar	750	30.06	0.26	0.12	0.02
-1	2.7*A and 2*Acc	2.7*A	2*ar	880	34.6	0.026	0.2	0.01

Table A2: 12 scenarios for Huhh1 rockglacier were developed assuming three different initial thermal states of each rockglacier (-2°C, -1.5°C and -1°C). A potential warming of 1°C was combined with four different scenarios concerning the material input resulting from the suggested temperature increase. The values present the results after the perturbation (600a-1000a).

Reference Temp. [°]	Model Run	Creep Rate change	Accumulation change	Length [m]	Thickness [m]	Max. Hor. Vel. [m a^{-1}]	Average Hor. Vel. [m a^{-1}]	Annual m.ax Subsidence [m a^{-1}]
-2	1.4*A and 0*Acc	1.4*A	0*a$_r$	540	12.03	1.18	0.37	0.07
-2	1.4*A and 0.4*Acc	1.4*A	0.4*ar	560	12.98	1.18	0.47	0.05
-2	1.4*A and 1*Acc	1.4*A	1*ar	610	15.21	1.18	0.9	0.02
-2	1.4*A and 2*Acc	1.4*A	2*ar	730	17.74	1.58	1.4	0.02
-1.5	1.7*A and 0*Acc	1.7*A	0*ar	560	11.62	1.39	0.43	0.083
-1.5	1.7*A and 0.4*Acc	1.7*A	0.4*ar	580	12.51	1.4	0.045	0.06
-1.5	1.7*A and 1*Acc	1.7*A	1*ar	630	14.63	1.41	0.94	0.03
-1.5	1.7*A and 2*Acc	1.7*A	2*ar	750	16.81	1.64	1.56	0
-1	2.7*A and 0*Acc	2.7*A	0*ar	610	10.69	2.29	0.46	0.12
-1	2.7*A and 0.4*Acc	2.7*A	0.4*ar	630	11.43	2.29	0.56	0.1
-1	2.7*A and 1*Acc	2.7*A	1*ar	690	13.16	2.29	0.98	0.08
-1	2.7*A and 2*Acc	2.7*A	2*ar	820	15.32	2.29	1.81	0.03

Huhh 1

9.10 References

Arenson, L., Hoelzle, M., and Springman, S.: Borehole deformation measurements and internal structure of some rock glaciers in Switzerland, Permafrost and Periglacial Processes, 13, 117–135, 2002.

Arenson, L. U., Johansen, M. M., and Springman, S. M.: Effects of volumetric ice content and strain rate on shear strength under triaxial conditions for frozen soil samples, Permafrost and Periglacial Processes, 15, 261–271, doi:10.1002/ppp.498, 2004.

Arenson, L. U. and Springman, S. M.: Mathematical descriptions for the behaviour of ice-rich frozen soils at temperatures close to 0 °C, Canadian Geotechnical Journal, 42, 431–442, doi:10.1139/t04-109, 2005.

Barsch, D.: Permafrost creep and rockglaciers, Permafrost Periglac. Process., 3, 175–188, doi:10.1002/ppp.3430030303, 1992.

Barsch, D.: Rockglaciers: Permafrost Creep and Rockglaciers., Springer, Berlin, 331 pp., 1996.

Barsch, D. and Caine, N.: The Nature of Mountain Geomorphology, Mountain research and development, 4, 287–298, 1984.

Bishop, M. P., Shroder, J. F., and Colby, J. D.: Remote sensing and geomorphometry for studying relief production in high mountains, Geomorphology, 55, 345–361, doi:10.1016/S0169-555X(03)00149-1, 2003.

Bodin, X., Rojas, F., and Brenning, A.: Status and evolution of the cryosphere in the Andes of Santiago (Chile, 33.5°S.), Geomorphology, 118, 453–464, doi:10.1016/j.geomorph.2010.02.016, 2010.

Bodin, X., Schoeneich, P., Deline, P., Ravanel, L., Magnin, F., Krysiecki, J.-M., and Echelard, T.: Mountain permafrost and associated geomorphological processes: Recent changes in the French Alps, rga, doi:10.4000/rga.2885, 2015.

Buchli, T., Merz, K., Zhou, X., Kinzelbach, W., and Springman, S. M.: Characterization and Monitoring of the Furggwanghorn Rock Glacier, Turtmann Valley, Switzerland: Results from 2010 to 2012, Vadose Zone Journal, 12, doi:10.2136/vzj2012.0067, 2013.

Cuffey, K. M. and Paterson, W.: The physics of glaciers, 4th ed., Elsevier, Amsterdam, 693 S, 2010.

Chorley, R. J. and Kennedy, B. A.: Physical geography: A systems approach, Prentice-Hall, Hemel Hempstead, 1971.

Delaloye, R., Lambiel, C., and Gärtner-Roer, I.: Overview of rock glacier kinematics research in the Swiss Alps, Geogr. Helv, 65, 135–145, 2010a.

Delaloye, R., Lambiel, C., and Gärtner-Roer, I.: Overview of rock glacier kinematics research in the Swiss Alps: seasonal rhythm, interannual variations and trends over several decades., Geographica Helvetica, 65, 135–145, 2010b.

Delaloye, R., Morard, S., Barboux, C., Abbet, D., Gruber, V., Riedo, K., and Gachet, S.: Rapidly moving rock glaciers in Mattertal., in: Mattertal - ein Tal in Bewegung, Graf, C. (Ed.), Jahrestagung der Schweizerischen Geomorphologischen Gesellschaft, St. Niklaus, 29. June-1. July, WSL, Birmensdorf, 2011.

Fischer, L., Amann, F., Moore, J. R., and Huggel, C.: Assessment of periglacial slope stability for the 1988 Tschierva rock avalanche (Piz Morteratsch, Switzerland), Engineering Geology, 116, 32–43, doi:10.1016/j.enggeo.2010.07.005, 2010.

Frauenfelder, R. and Kääb, A.: Towards a palaeoclimatic model of rock-glacier formation in the Swiss Alps, Annals of Glaciology, 31, 281–286, doi:10.3189/172756400781820264, 2000.

Frauenfelder, R., Schneider, B., and Kaeaeb, A.: Using dynamic modeling to simulate the distribution of rockglaciers, Geomorphology, 93, 130–143, doi:10.1016/j.geomorph.2006.12.023, 2008.

Frehner, M., Ling, A., and Gärtner-Roer, I.: Furrow-and-Ridge Morphology on Rockglaciers Explained by Gravity-Driven Buckle Folding: A Case Study From the Murtèl Rockglacier (Switzerland), Permafrost and Periglac. Process., 26, 57–66, doi:10.1002/ppp.1831, 2015.

Gärtner-Roer, I.: Sediment transfer rates of two active rockglaciers in the Swiss Alps, Geomorphology, 167–168, 45–50, doi:10.1016/j.geomorph.2012.04.013, 2012.

Gärtner-Roer, I. and Nyenhuis, M.: Volume estimation, kinematics and sediment transfer rates of active rockglaciers in the Turtmann Valley, Switzerland, in: Landform - structure, evolution, process control: Proceedings of the International Symposium on Landform organised by the Research Training Group 437, Otto, J.-C., and Dikau, R. (Eds.), Lecture notes in earth sciences, 115, Springer, Berlin, 185–198, 2010.

Glade, T.: Linking debris-flow hazard assessments with geomorphology, Geomorphology, 66, 189–213, doi:10.1016/j.geomorph.2004.09.023, 2005.

Glen, J. W.: The creep of polycristalline ice, Proceedings of the Royal Society of London Series A- Mathematical and Physical Sciences, 228, 519–538, doi:10.1098/rspa.1955.0066, 1955.

Gruber, S.: Permafrost thaw and destabilization of Alpine rock walls in the hot summer of 2003, Geophys. Res. Lett., 31, doi:10.1029/2004GL020051, 2004.

Haeberli, W., Brandova, D., B. C., Egli, M., Frauenfelder, R., Kääb, A., Maisch, M., Mauz, B., and Dikau, R.: Methods for the absolute and relative dating of rock-glacier surfaces in alpine permafrost, in: Permafrost: Proceedings of the Eighth International Conference on Permafrost, 21-25 July 2003, Zurich, Switzerland, Phillips, M., Springman, S., and Arenson, L. U. (Eds.), Lisse, Abingdon, 2003.

Haeberli, W., Hallet, B., Arenson, L., Elconin, R., Humlun, O., Kaab, A., Kaufmann, V., Ladanyi, B., Matsuoka, N., Springman, S., and Vonder Muhll, D.: Permafrost creep and rock glacier dynamics, Permafrost and Periglacial Processes, 17, 189–214, doi:10.1002/ppp.561, 2006.

Haeberli, W., Hoelzle, M., Kääb, A., Keller, F., Vonder Mühll, D., and Wagner, S.: Ten years after drilling through the permafrost of the active rock glacier Murtèl , Eastern Swiss Alps: answered questions and new perspectives., in: Proceedings of 7th Interntional Permafrost Conference, Yellowknife, Nordicana 57, 1998.

Hanson, S. and Hoelzle, M.: The thermal regime of the active layer at the Murtèl rock glacier based on data from 2002, Permafrost and Periglacial Processes, 15, 273–282, doi:10.1002/ppp.499, 2004.

Hasler, A., Gruber, S., and Beutel, J.: Kinematics of steep bedrock permafrost, Journal of geophysical research, 117, doi:10.1029/2011JF001981, 2012.

Heckmann, T. and Schwanghart, W.: Geomorphic coupling and sediment connectivity in an alpine catchment — Exploring sediment cascades using graph theory, Geomorphology, 182, 89–103, doi:10.1016/j.geomorph.2012.10.033, 2013.

Hoelzle, M., Mühll, D. V., and Haeberli, W.: Thirty years of permafrost research in the Corvatsch- Furtschellas area, Eastern Swiss Alps: A review, Norsk Geografisk Tidsskrift - Norwegian Journal of Geography, 56, 137–145, doi:10.1080/002919502760056468, 2002.

Ikeda, A. and Matsuoka, N.: Degradation of talus-derived rock glaciers in the Upper Engadin, Swiss Alps, Permafrost and Periglacial Processes, 13, 145–161, doi:10.1002/ppp.413, 2002a.

Ikeda, A. and Matsuoka, N.: Degradation of talus-derived rock glaciers in the Upper Engadin, Swiss Alps, Permafrost and Periglacial Processes, 13, 145–161, doi:10.1002/ppp.413, 2002b.

IPCC - Intergovernmental Panel on Climate Change: Climate Change 2013 - The Physical Science Basis, Cambridge University Press, Cambridge, 2014.

Jansen, F. and Hergarten, S.: Rock glacier dynamics: Stick-slip motion coupled to hydrology, Geophysical research letters, 33, n/a, doi:10.1029/2006GL026134, 2006.

Johannesson, T., Raymond, T. C., and Waddington, E. D.: Time-scale for adjustment of glaciers to change in mass balance., Journal of Glaciology, 35 (121), 355–369, 1989.

Kääb, A.: Remote sensing of permafrost-related problems and hazards, Permafrost and Periglacial Processes, 19, 107–136, doi:10.1002/ppp.619, 2008.

Kääb, A., Frauenfelder, R., and Roer, I.: On the response of rockglacier creep to surface temperature increase: Climate Change Impacts on Mountain Glaciers and Permafrost, Global and Planetary Change, 56, 172–187, doi:10.1016/j.gloplacha.2006.07.005, 2007.

Kääb, A., Kaufmann, V., Ladstädter, R., and Eiken, T.: Rock glacier dynamics: implications from high-resolution measurements of surface velocity fields, in: 8th International Conference on Permafrost, Zurich, Swets & Zeitlinger, 501–506, 2003.

Kääb, A. and Vollmer, M.: Surface Geometry, Thickness Changes and Flow Fields on Creeping Mountain Permafrost: Automatic Extraction by Digital Image Analysis, Permafrost and Periglacial Processes, 11, 315–326, doi:10.1002/1099-1530(200012)11:4<315:AID-PPP365>3.0.CO;2-J, 2000.

Kääb, A. and Weber, M.: Development of transverse ridges on rock glaciers: field measurements and laboratory experiments, Permafrost and Periglacial Processes, 15, 379–391, doi:10.1002/ppp.506, 2004.

Kenner, R., Bühler, Y., Delaloye, R., Ginzler, C., and Phillips, M.: Monitoring of high alpine mass movements combining laser scanning with digital airborne photogrammetry, Geomorphology, 206, 492–504, doi:10.1016/j.geomorph.2013.10.020, 2014.

Krautblatter, M., Moser, M., Schrott, L., Wolf, J., and Morche, D.: Significance of rockfall magnitude and carbonate dissolution for rock slope erosion and geomorphic work on Alpine limestone cliffs (Reintal, German Alps), Geomorphology, 167–168, 21–34, doi:10.1016/j.geomorph.2012.04.007, 2012b.

Lambiel, C.: Le glacier rocheux déstabilisé de Tsaté-Moiry (VS) caractéristiques morphologiques et vitesses de déplacement., in: La géomorphologie alpine: Entre patrimoine et contrainte / actes du colloque de la Société suisse de géomorphologie, 3-5 septembre 2009, Olivone, Lambiel, C., Reynard, E., and Scappozza, C. (Eds.), Géovisions, 36, Institut de géographie de l'Univ. de Lausanne, Lausanne, 2011.

Leysinger Vieli, G.-M. and Gudmundsson, G. H.: Evolution of rock glaciers and alpine glaciers: A model - model approach, in: Permafrost: Proceedings of the Eighth International Conference on Permafrost, 21-25 July 2003, Zurich, Switzerland, Phillips, M., Springman, S., and Arenson, L. U. (Eds.), Lisse, Abingdon, 2003.

Leysinger Vieli, G. J.-M. C. and Gudmundsson, G. H.: On estimating length fluctuations of glaciers caused by changes in climatic forcing, J. Geophys. Res., 109, n/a, doi:10.1029/2003JF000027, 2004.

Micheletti, N., Lambiel, C., and Lane, S. N.: Investigating decadal-scale geomorphic dynamics in an alpine mountain setting, J. Geophys. Res. Earth Surf., 120, 2155–2175, doi:10.1002/2015JF003656, 2015.

Müller, J., Gärtner-Roer, I., Kenner, R., Thee, P., and Morche, D.: Sediment storage and transfer on a periglacial mountain slope (Corvatsch, Switzerland), Geomorphology, 218, 35–44, doi:10.1016/j.geomorph.2013.12.002, 2014a.

Müller, J., Gärtner-Roer, I., Thee, P., and Ginzler, C.: Accuracy assessment of airborne photogrammetrically derived high-resolution digital elevation models in a high mountain environment, ISPRS Journal of Photogrammetry and Remote Sensing, 98, 58–69, doi:10.1016/j.isprsjprs.2014.09.015, 2014b.

Nye, J. F. The response of a glacier to changes in the rate of nourishment and wastage. Proc. R. Soc. London, Ser. A 275, 87{112 (1963).

Oerlemans, J.: Glaciers and climate change, A.A. Balkema Publishers, Lisse, 148 S, 2001.

Olyphant, G.: Computer simulation of rock-glacier development under viscous and pseudoplastic flow, Geol Soc America Bull, 94, 499, doi:10.1130/0016-7606(1983)94<499:CSORDU>2.0.CO;2, 1983.

Paterson, W. and Budd, W. F.: Flow parameters for ice sheet modeling, Cold Regions Science and Technology, 6, 175–177, doi:10.1016/0165-232X(82)90010-6, 1982.

PERMOS: Glaciological Report Permafrost No. 10/11 of the Cryospheric Commission of the Swiss Academy of Sciences., 2013.

Phillips, M., Mutter, E. Z., Kern-Luetschg, M., and Lehning, M.: Rapid degradation of ground ice in a ventilated talus slope: Flüela Pass, Swiss Alps, Permafrost Periglac. Process., 20, 1–14, doi:10.1002/ppp.638, 2009.

Ravanel, L. and Deline, P.: Climate influence on rockfalls in high-Alpine steep rockwalls: The north side of the Aiguilles de Chamonix (Mont Blanc massif) since the end of the 'Little Ice Age', The Holocene, 21, 357–365, doi:10.1177/0959683610374887, 2011.

Roer, I.: Rockglacier kinematics in a high mountain geosystem, Dissertation, Geographie, Rheinische Freidrich Wilhelms Universität, Bonn, 2005.

Roer, I., Avian, W., Kaufmann, V., Delaloye, R., Lambiel, C., and Kääb, A.: Observations and considerations on destabilizing active rock glaciers in the European Alps., in: Proceedings of the 9th International Conference on Permafrost, University of Alaska, Fairbanks, Alaska, June 29 - July 3, 2008, Kane, D. L., and Hinkel, K. M. (Eds.), Institute of Northern Engineering, University of Alaska, Fairbanks, Fairbanks, Alaska, 1505–1510, 2008a.

Roer, I., Haeberli, W., Avian, M., Kaufmann, V., Delaloye, R., Lambiel, C., and Kääb, A.: Observations and considerations on destabilizing active rock glaciers in the European Alps, in: Ninth International Conference on Permafrost, 1505–1510, 2008b.

Roer, I., Kääb, A., and Dikau, R.: Rockglacier acceleration in the Turtmann valley (Swiss Alps): Probable controls, Norwegion Journal of Geography, 59, 157–163, 2005a.

Roer, I., Kääb, A., and Dikau, R.: Rockglacier acceleration in the Turtmann valley (Swiss Alps): Probable controls, Norsk Geografisk Tidsskrift - Norwegian Journal of Geography, 59, 157–163, doi:10.1080/00291950510020655, 2005b.

Roer, I., Kääb, A., and Dikau, R.: Rockglacier kinematics derived from small-scale aerial photography and digital airborne pushbroom imagery, Zeitschrift für Geomorphologie, 49, 73–87, 2005c.

Roer, I. and Nyenhuis, M.: Rockglacier activity studies on a regional scale: comparison of geomorphological mapping and photogrammetric monitoring, Earth Surf. Process. Landforms, 32, 1747–1758, doi:10.1002/esp.1496, 2007.

Scherler, M., Schneider, S., Hoelzle, M., and Hauck, C.: A two-sided approach to estimate heat transfer processes within the active layer of the Murtèl–Corvatsch rock glacier, Earth Surf. Dynam., 2, 141–154, doi:10.5194/esurf-2-141-2014, 2014.

Schneider, S., Hoelzle, M., and Hauck, C.: Influence of surface and subsurface heterogeneity on observed borehole temperatures at a mountain permafrost site in the Upper Engadine, Swiss Alps, The Cryosphere, 6, 517–531, doi:10.5194/tc-6-517-2012, 2012.

Springman, S. M., Arenson, L. U., Yamamoto, Y., Mayer, H., Kos, A., Buchli, T., and Derungs, G.: Multidisciplinary investigations on three rockglaciers in the Swiss alps: Legacies and future perspectives, Geografiska Annaler: Series A, Physical Geography, 94, 215–243, doi:10.1111/j.1468-0459.2012.00464.x, 2012.

Springman, S. M., Yamamoto, Y., Buchli, T., Hertrich, M., Maurer, H., Merz, K., Gärtner-Roer, I., and Seward, L.: Rock Glacier Degradation and Instabilities in the European Alps: A Characterisation and Monitoring Experiment in the Turtmanntal, CH, in: Landslide Science and Practice, Margottini, C., Canuti, P., and Sassa, K. (Eds.), Springer Berlin Heidelberg, Berlin, Heidelberg, 5–13, 2013.

Vonder Mühll, D., Noetzli, J., and Roer, I.: PERMOS – a comprehensive monitoring network of mountain permafrost in the Swiss Alps., in: Proceedings of the 9th International Conference on Permafrost, University of Alaska, Fairbanks, Alaska, June 29 - July 3, 2008, Kane, D. L., and Hinkel, K. M. (Eds.), Institute of Northern Engineering, University of Alaska, Fairbanks, Fairbanks, Alaska, 2008.

Wagner, S.: Creep of alpine permafrost, investigated on the Murtèl rock glacier, Permafrost Periglac. Process., 3, 157–162, doi:10.1002/ppp.3430030214, 1992.

Wahrhaftig, C. and COX, A.: Rock Glaciers in the Alaska Range, Geological Society of America Bulletin, 70, 383, doi:10.1130/0016-7606(1959)70[383:RGITAR]2.0.CO;2, 1959.

Whalley, W. B. and Martin, H. E.: Rock glaciers: II models and mechanisms, Progress in Physical Geography, 16, 127–186, doi:10.1177/030913339201600201, 1992.

Wirz, V., Gruber, S., Purves, R. S., Beutel, J., Gärtner-Roer, I., Gubler, S., and Vieli, A.: Short-term velocity variations of three rock glaciers and their relationship with meteorological conditions, Earth Surf. Dynam. Discuss., 3, 459–514, doi:10.5194/esurfd-3-459-2015, 2015.

Part III Appendix

10 Personal Bibliography

10.1 Peer Reviewed Publications

Müller, J., Gärtner-Roer, I., Thee, P., Ginzler, C., 2014. Accuracy assessment of airborne photogrammetrically derived high-resolution digital elevation models in a high mountain environment. ISPRS Journal of Photogrammetry and Remote Sensing 98, 58–69.

Müller, J., Gärtner-Roer, I., Kenner R., Thee P., Morche, D., 2014. Sediment storage and transfer on a periglacial mountain slope (Corvatsch, Switzerland). Geomorphology 218 (0), 35–44.

Müller, J., Vieli, A., Gärtner-Roer, I., 2016. Rockglaciers on the run - Understanding rockglacier landform evolution and recent changes from numerical flow modeling. The Cryosphere Discussions, (in review).

10.2 Conference Contributions

Gärtner-Roer, I. & J. Müller (2013). Identification of geomorphic and climatic controls on degradation of Alpine rockglaciers. 8th IAG International Conference on Geomorphology, Paris, 2013.

Gärtner-Roer, I. & J. Müller (2014). Fast Degradation of subsurface ice at Corvatsch, Eastern Switzerland. *4th European Conference on Permafrost*, Evora, Portugal.

Hauck, C., Delaloye, R., Gärtner-Roer,I., Hilbich, C., Hoelzle, M., Kenner, R., Kotlarski, S., Lambiel, C., Marmy, A., Müller, J., Noetzli, J., Phillips, K., Rajczak, J., Salzmann, N., Schaepman, M., Schär, C., Staub, Völksch I., (2013): The TEMPS Project – The evolution of mountain permaforst in Switzerland. *Davos Atmosphere and Cryosphere Assembly DACA-13*, Davos, Switzerland

Heim, L., Müller, J., Gärtner-Roer, I., Purves, R., (2014): plication and analysis of terrestrial laser scanning in a periglacial high mountain area. *Swiss Geosciense Meeting 2014*, Bern, Switzerland.

Müller, J., Gärtner-Roer, I., Ginzler, C. (2012): On the performance of digital elevation models in a high mountain environment. *7th Working Group on Sediment Budgets in Cold Environments (SEDIBUD)*. Trondheim, Norway.

Müller, J., Gärtner-Roer, I., Thee, P., Ginzler, C., Menz, G. (2012): How accurate can we be? – An evaluation of airborne digital elevation models in a high mountain environment. Geophysical Research Abstracts, Vol. 14, EGU2012-3775, EGU General Assembly 2012

Müller, J., Gärtner-Roer, I., Thee, P., Ginzler, C. (2013): Permafrost kinematics from high resolution stereophotogrammetry – Application and Restrictions. Geophysical Research Abstracts. Vol. 15, EGU2013-4375, EGU General Assembly 2013.

Müller, J., Gärtner-Roer, I., Kenner, R., Thee, P., Morche, D. (2013): Sediment transfer and geomorphic work on a periglacial slope. *8th IAG/AIG International Conference on Geomorphology*, Paris.

Müller, J., Gärtner-Roer, I. (2014): Rockglacier Rheology – Recent developments in modeling approaches. *4th European Conference on Permafrost,* Evora, Portugal.

Müller, J., Gärtner-Roer, I., Thee, P., Ginzler, C. (2013): Permafrost kinematics from high resolution stereophotogrammetry – Application and Restrictions. *CH-AT Mountain Days*, Mittersill.

Müller, J., Gärtner-Roer, I. (2013): Transferraten und Energiebilanzen eines periglazialen Sedimentsystems im Hochgebirge. *Deutscher Geographentag 2013*, Passau.

Stamm, D. & Müller, J., (2015): Auswertung UAS generierter Hoiehenmodelle in periglazialer Umgebung. Am Beispiel Blockgletscher Muragl, Oberengadin. *Jahrestagung Schweizer Geomorphologische Gesellschaft 2015*, Innertkirchen, Switzerland.

11 Curriculum Vitae

Personal Information

Name	Johann Müller
Date of Birth	October 9, 1984
Place of Birth	Pforzheim / Germany

Education

02/2012 - present	**University of Zürich / Department of Geography** PhD candidate at the Remote Sensing Laboratories and 3G-Group within the **TEMPS project** (The evolution of mountain permafrost in Switzerland). **Subproject C**: From kinematics to dynamics: geomorphic and physical controls of permafrost creep derived from airborne digital sensors and terrestrial surveys.
04/2005 – 01/2012	**Rheinische Friedrich Wilhelms University Bonn** Diploma degree in geography Minors: Geology, Political Science Specialization in Remote Sensing, glacial and periglacial systems, alpine hazard and risk assessment and management, GIS
06/2004	**Abitur** Ludwig Georgs Gymnasium Darmstadt

Signature

Zürich, 11 January 2016

12 Acknowledgements

Science is the belief in the ignorance of experts.

R. Feynman (1966)

All good things come to an end. And so does this thesis and the time associated with it. There were stressful days, broken equipment, bad weather, cold nights and so many pages to write but in hindsight –and even more importantly – what I will remember are the good and exciting times: remote and special places, challenging fieldwork, motivating (and challenging) colleagues and interesting questions to be discussed and maybe answered. If I had the chance, I would do it all over again. Besides the scientific insights that I feel thankful to have experienced, it's the people to whom I would like to express my gratitude:

First and foremost, Isabelle Gärtner-Roer for giving me the opportunity to come to Zurich, for supporting me academically and as a friend and fostering my scientific (maybe sometimes a bit too egoistic) adolescence in an exceptional way. Her openness towards new ideas, her enthusiasm and expertise culminated in a fruitful work and research environment for me and I hope the feeling is mutual.

Michael Schaepman, who took me on as a PhD Student and was always very supportive to all my ideas and ambitions and who made sure that I set the academic bar high – but not insurmountable.

Ross Purves, with his outstanding skill to ask the necessary questions. Even though I tried my hardest to deviate and avoid these questions.

Andreas Vieli, who supported me without any hesitations, although he had almost no reason to do so. His fresh sight on permafrost and his expertise in modeling contributed significantly to the successful completion of this work.

Since the early beginnings of my remote sensing and surveying career, I had the great pleasure to work with Christian Ginzler and Patrick Thee of the Federal Research Institute WSL in Birmensdorf. I have to thank both of them sincerely for all the time they sacrificed to teach me the most basic things indoors and outdoors.

My position within/between two research groups came with the benefit that I got to live the geographical interdisciplinarity. Therefore I want to thank all my RSL and 3G colleagues who shared their knowledge, field expertise and equipment. Special thanks go to my office mates Reik, Philip and Jörg for welcoming me so heartily and the "Newbies" Irene and Gilian for supplying me with chocolate and gossip.

A very warm thank you is extended to my 3G colleagues Ingo, Nico, Phil and Saemi who turned from work colleagues into good friends, and the 3G group altogether for providing

the stimulating and creative work atmosphere I had the pleasure to experience. I want to especially acknowledge the constructive and motivating feedback of Gwendolyn and her supply of and elaboration on hipster coffee.

In the context of the completion if this thesis and living life in general I want to thank Barbara, Elisabeth, Frank, Henning, Ingo, Irene, Jeannette, Kathrin, Nico, Raimund, Sämi and Valerie for proofreading and/or systemically having a good time.

I am greatly thankful towards my parents and families whose support and enthusiasm is endless and in the end, I have to thank Jana for ALL the things.